The Identification of the Tao-1 Kinase as a Key Regulator of Microtubule Dynamics

A dissertation submitted to University College London

for the degree of Doctor of Philosophy

By

Tao Liu

Department of Cell and Developmental Biology

and

MRC Laboratory for Molecular Cell Biology

University College London

Feb, 2009

Abstract

In a multicellular animal, the different functions of cells are dependent on their diversity of shapes. Protein phosphorylation and dephosphorylation play an important role in altering the cell shape in response to internal and external signals. In this study I focused on all kinases to explore the gene functions and mechanisms underlying the regulation of cell morphology.

Using genomic information I have constructed a *Drosophila* kinase RNAi library, which was then used to screen six different cell lines from two different tissues of origin for novel genes involved in the generation of cell form. In doing so, I identified a group of common regulators of cell behaviour and morphology together with a set of cell-type specific kinases. Importantly, this analysis also revealed that, when considering the kinome, gene expression signatures are a poor measure of cell type specific differences in gene function, measured by comparing with the microarray data available in our lab. Most significantly, these screens identified a novel role for Mnb/DYRK1A, a kinase associated with Down's Syndrome, in the regulation of actin-based protrusions in cell lines derived from neuronal lineages.

Furthermore, I identified a single STE20 kinase *Drosophila* Tao-1 in the core set which was required for the normal morphology of all cell lines

examined. The RNAi-mediated depletion of Tao-1 or expression of the kinase-dead protein leads to the stabilisation of microtubules and to the formation of long microtubule-based protrusions, whereas the overexpression of Tao-1 destabilizes microtubules. I also showed in this study that Tao-1 acts independently of Par-1 and Tau in this process. Instead, Tao-1 appears to function together with EB1 in the regulation of microtubule plus end instability at the cell cortex. Two microtubule motor proteins, Khc and Khc-73, interact with Tao-1 in a yeast two hybrid screen, which hints at a possible role for the transport of Tao-1 along filaments to microtubule plus ends and the cell cortex. Although evidence for a direct role for Tao-1 in the phosphorylation and/or regulation of EB1 has yet to be established, this is to my knowledge first time a kinase has been found acting at the cell cortex to regulate microtubule plus end stability.

Statement

I, Tao Liu, confirm that this thesis is based on the research work at the Ludwig Institute for Cancer Research (University College London Branch), between Feb, 2006 and Jun, 2007 and at the MRC Laboratory for Molecular Cell Biology (University College London), between July, 2007 and Dec 2008. Except where explicitly stated, this thesis contains my own original work. Contributions made by others are highlighted within the text. This work has not been accepted in a previous application for a degree.

Some of the work in this thesis was accepted for publication in ***Genome Biology*** at the time of submission:

Liu T, Sims D and Baum B. '**Parallel RNAi screens across different cell lines identify *minibrain* or DYRK1A as a cell-type specific regulator of actin organisation**'

Acknowledgements

Firstly, I would like to particularly thank my supervisor, Buzz Baum who has guided my entry into the world of cell biology, who has provided continuing advice and supervision that have been so vital in pushing me further in my work.

I am also indebted to all the members of the Baum lab at the Ludwig Institute for Cancer Research and MRC Laboratory for Molecular Cell Biology who have provided excellent scientific and technical input to my work. In particularly, I thank David Sims for contributions to the microarray data and bioinformatics information; Remigio Picone for contributions to the analysis of microtubule plus end dynamics; Jenny Rohn for help with Hela cell experiments; Pato Kunda for discussions throughout the three years of my PhD; Helen Matthews and Kate Van Hegan for their kind help in proofreading my thesis.

Finally, I would like to acknowledge the generous financial support from the Ludwig Institute for Cancer Research and the Faculty of Life Sciences at the University College London.

This thesis would have been impossible to complete without so much help from people behind me, especially my wife Junyan Pei and my parents who have given me their altruistic support, motivation and sense of

perspective over so many years.

Table of contents

List of Figures

List of Tables

List of additional files in attached DVD

Additional File 1:……Q-PCR primers

Additional File 2:……Cloning work primers

Additional File 3:……All sequencing results and maps

Additional File 4:……Primers of 265 *Drosophila* kinase dsRNA library

Additional File 5:……Screen hit clustering results across 6 cell lines

Additional File 6:..... The results from three RNAi experiments to estimate false positive rate

Additional File 7……Map of Tao-1 modified screen library

Additional File 8: ……Electronic version of the thesis

Additional File 9: ……Original movies used in the work

Additional File 10: …… The actual data for the analysis of MT dynamic

Abbreviations

+TIP	Microtubule (MT) plus-end tracking protein
Ab	Antibody
APC	Adenomatous polyosis coli
ATP	Adenosine triphosphate
bp	Base pair
BSA	Bovine serum albumin
CDK	Cyclin-dependent kinase
CLAPs	CLIP-associating protein
CLIPs	Cytoplasmic linker proteins
ConA	Concanavalin A
DGRC	Drosophila Genomics Resource Center
DMSO	Dimethyl Sulfoxide
dsRNA	Double-standed RNA
DYRK	Dual-specificity tyrosine-(Y)-phosphorylation
EB1	Plus-End Binding Protein 1
ERK	Extracellular-signal Regulated Kinase
FERM	Ezrin, Radixin, Moesin Domain
FITC	Fluorescein isothiocyanate
FL	Full length
GAP	GTPase Activating Protein
GCK	Germinal Center Kinases
GDP	Guanine-nucleotide diphosphate
GFP	Green Fluorescent Protein
GTP	Guanine-nucleotide triphosphate
IF	Immunofluorescence
JNK	Jun N-terminal Kinase
kDa	KiloDalton
KIFs	Kinesin super family proteins
LatB	Latrunculin B
LOF	Loss of function
MAPK	Mitogen Activated Protein Kinase
Maps	Microtubule associate proteins
mRNA	Messenger RNA
Msn	Misshapen
MT(s)	Microtubule(s)
MTOC	Microtubule organizing center
NEB	Nuclear envelop breakdown
NES	Nuclear export signal
NLS	Nuclear localisation signal
nt	Nucleotide
OTEs	Off-target effects

PAKs	P21-activated kinases
PBS	Phosphate Buffered Saline
PCR	Polymerase Chain Reaction
PH	Pleckstrin homology domain
PI3K	Phosphoinositol-3-Kinase
Q-PCR	Quantitative Polymerase Chain Reaction
RFP	Red Fluorescent Protein
RISC	RNA-induced silencing complex
RNAi	RNA-mediated interference
RT	Reserve transcriptase
shRNA	Short hairpin RNA
STE20	Sterile 20 protein
TAO-1	Thousand and one amino acid kinase -1
TBS	Tris-Buffered Saline
TIRF	Total internal reflection fluorescence microscope
TRITC	Tetramethylrhodamine isothiocyanate
WASP	Wiskott–Aldrich syndrome protein
WB	Westernblot
WT	Wild-type
YFP	Yellow Fluorescent Protein

Thesis Organisation

The work in this thesis has been organized into six chapters. Chapter 1 gives the necessary background to my research, with a general introduction to the cytoskeleton and to RNAi screening. Chapter 2 provides information on the materials and methods which have been used in my PhD project. Chapter 3 describes the results of parallel RNAi screens carried out in multiple *Drosophila* cell lines, and a comparison of this data with microarray gene expression data generated in the lab. Chapter 4 looks at the function of Mnb/DYRK1A which was identified as a cell type specific actin regulator in neuronal cell lines. Chapter 5 details my analysis of the Tao-1 kinase which was identified as a key regulator of microtubule dynamics in all 6 cell types studied. In the final part of this thesis, Chapter 6, I discuss these experimental results and hypothesis in the context of other work in the field, and based on this analysis discuss ideas for future research in this area.

Chapter 1

General Introduction

Here I introduce the background related to my research work. This introduction consists of two main sections which present, first, the dynamic regulation of the cytoskeleton and second, the background to the main methodology used in my study. In the first part, two kinds of cytoskeletal proteins, actin filaments and microtubules, will be introduced. Microtubule dynamic instability will be emphasized. Following the above, STE20 family kinases will be briefly discussed because Tao-1 kinase belongs to this family and its biological function should be seen in this light. RNAi and high-throughput RNAi screening are main methodologies in my study. The principles of these techniques will also be discussed in the second section. Finally, the aims of this study will be clarified in this chapter to help to make clear the significance of my work.

1.1 Cytoskeleton and Cell morphology

Cells have to maintain their shape, their internal structure and to interact mechanically with their environment. This can not be realized without a remarkable system of filaments which both support cellular structure and generate the forces required to move molecules, complexes and organelles to alter cell shape. There are three main types of filaments in eukaryotic cells, which together are named the cytoskeleton: actin filaments, microtubules and intermediate filaments. Each type of cytoskeletal filament is built from smaller protein subunits like actin monomers and α/β-tubulin subunits joined end to end. Their assembly and disassembly is tightly regulated, so that cytoskeletal organization can promptly respond to changing internal and external environments. The regulation of the dynamic behavior of these cytoskeletal proteins also contributes to each step in the eukaryotic cell cycle, for example, to the formation of the mitotic spindle and of the lamellipodium of a migrating interphase cell. Thus, the study of the dynamic regulation of cytoskeleton will allow us to better understand the mechanisms underlying diverse cell behaviors.

The term ‘morphology’ in biology refers to the outward appearance (shape, structure or pattern) of biological system. In this study, when I talk about cell morphology, my focus is cell shape, since cell shape is a key element

in development and differentiation. Multicellular organisms are composed of a variety of specialised tissues, each of which is made up of cells with very different shapes. Furthermore, diseases like cancer are characterised by defects in cell differentiation and altered cell shapes. In addition, the disruption of normal cell form is thought to be one of the causal pathological changes in cancer. So, identifying novel genes involved in the regulation of cell shape could contribute to the development of new cancer diagnostic markers and therapies.

1.2 Actin-based protrusions

Actin filaments are two-stranded helical polymers of the protein actin. They appear as flexible structures with a diameter of 5-9 nm, and they are organized into a variety of filament networks that underlie different macroscopic cellular structures. In a motile cell, actin filaments drive migration in three steps [6]. First, actin assembly drives the extension of a flat membrane extension at the cell leading edge, called a lamellipodium, then adhesions are formed within this structure that connect the extracellular substrate to the actin cytoskeleton to anchor the protrusion. The final step is to move the mass of the cell forward and to retract the trailing edge by combining actomyosin contraction and disassembly of adhesions at the cell rear [7].

1.2.1 The lamellipodium formation

The lamellipodium is the big flat membrane protrusion driven by the extension of actin assembly at cell's leading edge. A process called 'treadmilling' plays an important role in maintaining the form of the lamellipodium. It occurs when one end of an actin filament grows in length while the other end shrinks, as actin protein subunits are removed from one end of the filament and added at the other end [8], resulting in a filament seemingly "moving" across the substratum. This treadmilling of actin filaments in the lamellipodium, driven by ATP hydrolysis, is thought to be the source of forces moving the leading edge forwards [9]. It has been reported that WAVE/Scar are responsible for lamellipodium protrusion in response to Rac [10].

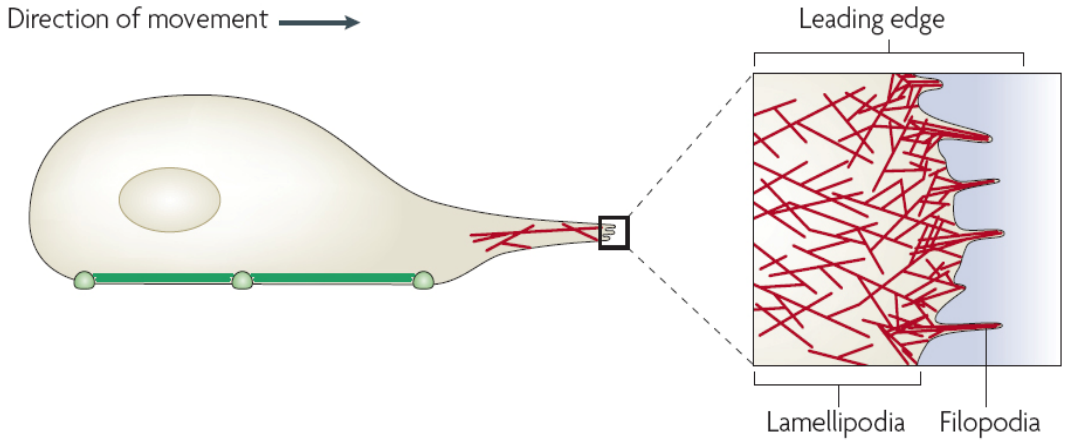

Figure 1-1 Cell migration is dependent on different actin filament structures
Cell migration is initiated by an actin-dependent protrusion of the leading edge, which is composed of lamellipodia and filopodia. (This picture was modified from Pieta Mattila's paper [2]).

1.2.2 The Filopodia formation

Filopodia are slim and finger-like cytoplasmic protrusions which extend from the leading edge of migrating cells [2]. In the process of cell migration, lamellipodia and filopodia are overlapping but their actin structures are differently organized and have distinct properties (see Figure 1-1). Filopodial protrusions contain 15-20 parallel filaments tightly packed into a bundle pushing the membrane [11]. These finger-like protrusions are highly dynamic and are controlled by actin monomer addition to filament ends at the protrusion tip [12]. Filopodia are also thought to have an important role in cell migration, probing their microenvironment and serving as “pioneers” during protrusion [13]. The elongation of filopodia depends on the precisely regulated polymerization of actin [14]. Nobes, Ridley and Hall have suggested that the Rho-GTPase Cdc42 controls the formation of filopodia via N-WASP [15]. It has since become clear that Formins may play a key role in this process. Formins are a group of proteins that can both nucleate new actin filaments and associate with the fast-growing end (barbed end) of existing actin filaments to form a dynamic cap and which catalyze the processive addition of profilin bound actin monomers to this end of the filament [16, 17]. They can also act as effectors for the Rho small GTPase, Cdc42 [17].

1.3 Microtubules and Microtubule dynamic instability

Microtubules are hollow cylindrical cytoskeletal filaments which cells use for many different purposes, such as intracellular trafficking, cell motility and division.

1.3.1 Microtubule structure

Microtubules were first observed in the 1950's in electron microscopy studies of cell sections [18]. They have a diameter of 25 nm and their length varies from 200 nanometers to 25 micrometer [19] as shown in Figure 1-2. They consist of polymers of α/β-tubulin dimers. These tubulin dimers polymerize end to end into protofilaments. The protofilaments are bundled to form hollow cylindrical filaments in which 13 dimers are arranged in a helical fashion so that each turn of the helix contains 13 tubulin dimers, each from a different protofilament.

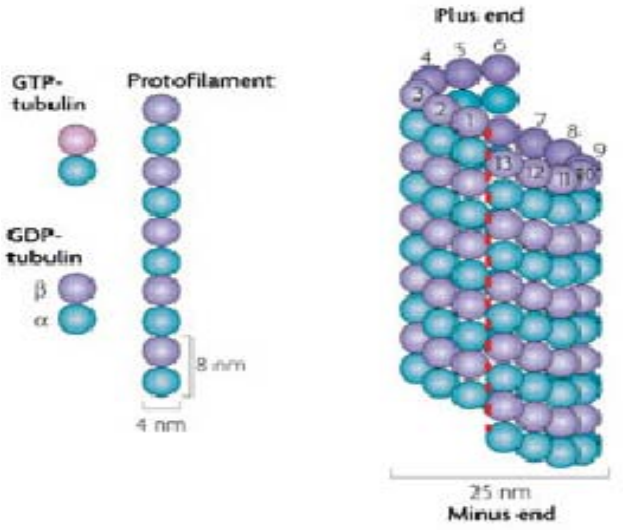

Figure 1-2 Microtubule structure and its dynamic instability (The picture was taken from Cheeseman's nature review [3])

Each individual microtubule filament has two ends. One end will have the α subunit exposed while the other end will have the β subunit exposed. The protofilaments bundle parallel to one another, so in a microtubule there is one end, called the plus end, with only β subunits exposed while the other end, called the minus end, only has α subunits exposed. The two distinct ends of microtubules have different growth rates.

1.3.2 Microtubule organization in animal cells

In animal cells, Microtubules are organized by microtubule organizing centers (MTOCs), such as centrosomes in the cytoplasm. This is because microtubule nucleation is rate limiting at cellular concentrations of monomeric tubulin. Contained within the MTOC is another type of tubulin, γ-tubulin, which is distinct from the α and β subunits that compose the microtubules themselves. γ-tubulin combines with several other proteins to

form a circular structure known as the 'γ-tubulin ring complex' [20, 21]. This complex acts as a scaffold for α/β tubulin dimers to begin polymerization, functioning as a minus-end nucleator of microtubules [21], while microtubule growth continues away from the MTOC, at its plus ends.

In animals, there are two important types of MTOC. One is the basal body associated with cilia and certain intercellular junctions in epithelial cells; the other is the centrosome associated with spindle formation. At its core, each centrosome has a pair of centrioles. Microtubules are anchored with their minus ends embedded in centrosomes, which are thought to function as microtubule-organizing centers throughout the cell cycle in animals. However, recent data from Jordan Raff's lab show that *Drosophila* presents an interesting paradox as centrosome-deficient mutant flies can develop into viable adults [22]. The Rogers' lab also found that many *Drosophila* cell types display an altered cycle, in which functional centrosomes are only present during cell division. On mitotic exit, centrosomes disassemble producing interphase cells containing centrioles that lack microtubule-nucleating activity [23]. Furthermore, steady-state interphase microtubule levels are not changed by depleting γ-tubulin [23]. These recent data suggest that there might be other redundant pathways catalysing microtubule nucleation, which are MTOC independent.

1.3.3 Microtubule kinetics and its dynamic instability

Each microtubule filament is a highly dynamic polymer. As mentioned above, it has two distinct ends, called plus ends and minus ends, with different growth rates. This is because a linear polymer of protein molecule assembles and disassembles by the addition and removal of subunits (called monomers) at its ends. The rate of addition of these subunits is given by the rate constant k_{on}. The number of monomers that are added to the microtubule per second will be proportional to the concentration of the free subunit, but the subunits will leave the polymer end at a constant rate k_{off} that does not depend on the concentration of free subunits. When the microtubule filament grows, subunits are used up, and the concentration of free subunits drops until it reaches a constant value, called the 'critical concentration'. At this concentration the rate of subunit addition equals the rate of subunit loss. A difference in the rates of growth at the two different ends is made possible by changes in the conformation of each subunit as it enters the polymer which affects the rates at which subunits add to the two ends. In microtubules this is achieved by the addition of tubulin dimers entering the microtubule in a GTP-bound state. The hydrolysis of GTP in the filament then induces a change in conformation so that in a growing microtubule, the plus end contains a GTP-tubulin while the minus end of the microtubule contains GDP-tubulin. As a result, the rate of elongation is the different at the two

ends.

So, when a microtubule filament grows in the plus end direction, the β subunits bound to a molecule of GTP act as a GTP cap. This GTP cap protects and stabilizes the plus end so that microtubules depolymerise about 100 times faster from an end containing GDP tubulin than from a GTP tubulin one [24]. So, when the GTP cap is hydrolized the plus end of microtubule undergoes rapid depolymerization and shrinkage [24]. This switch from growth to shrinking is called a catastrophe. GTP-bound tubulin can bind to the tip of a shrinking microtubule to provide a new cap and to protect the microtubule from shrinking, in an process called rescue [25]. In cells, because of these dynamics, individual microtubules switch between growing and shrinking states in the course of their lifetime (see Figure 1-3).

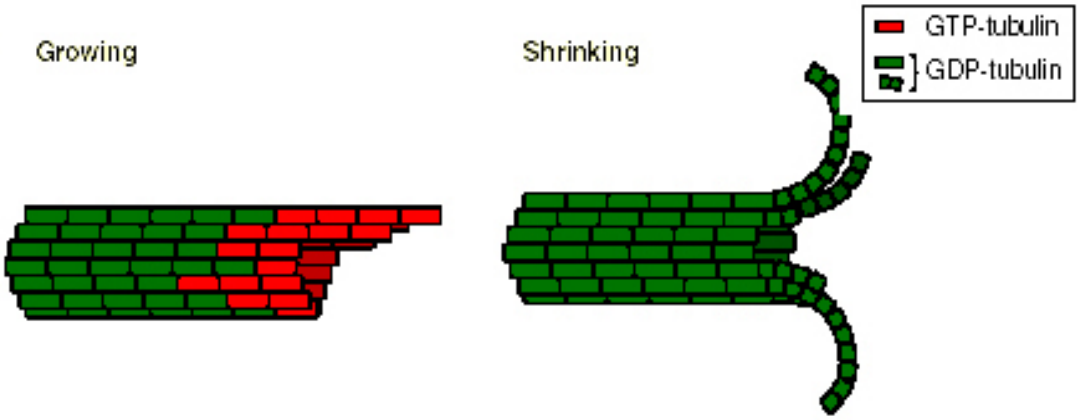

Figure 1-3 The combination of growth, shrinkage and rapid transitions between the two is known as ‘dynamic instability’. The picture was modified from Tim Mitchison’s review [1].

This combination of growth, shrinkage and rapid transitions between the

two is known as ‘dynamic instability’ [1]. Although dynamic instability may be more crucial for microtubule plus end function *in vivo*, both microtubule ends exhibit this behavior *in vitro* [26]. An interesting question might be raised if dynamic instability occurs at the minus end. Current opinion is that anchorage of the microtubule minus-ends at centrosomal and non-centrosomal sites stabilizes the minus end. It is not clear how this will be prevented in Drosophila cells without a functional MTOC. Ninein has been reported as a non-nucleating microtubule minus-end associated protein which may have a dual role as a minus-end capping and anchoring protein [27].

1.4 Cellular Regulation of Microtubule Instability

Dynamic instability is very important for cells. It allows microtubules to rapidly explore cell space, continuously re-using tubulin monomers as the network organisation changes. Although this process consumes energy (GTP), filament turnover can be fast, in the order of seconds. This means that microtubules can adapt quickly to changes in the environment. So, to understand how cells precisely regulate this process will be an essential step to understand many cellular activities.

1.4.1 Microtubule-associated proteins (MAPs) – the Yang of microtubules

In traditional Chinese philosophy, the concept of ‘Yin and Yang’ is used to describe how opposing forces or two aspects of one thing are interconnected and interdependent in the natural world, giving rise to each other in turn. The concept lies at the heart of many branches of classical Chinese science and philosophy as well as being a primary guideline of traditional Chinese medicine. Here, I would like to introduce this concept to the regulation of microtubule instability.

Microtubule-associated proteins (MAPs) are a family of proteins that bind microtubules. A large variety of MAPs have been identified in many different cell types. The proteins in this family usually share a region which can bind to microtubules localized at either their N-terminals or C-terminals. The MAPs can be divided into 4 groups which are MAP1, MAP2, MAP4 and Tau groups.

MAP1a and MAP1b constitute the MAP1 family. They utilize charged interactions to bind to and stabilize microtubules [28]. The C-termini of MAP1 family proteins bind microtubules, and the N-terminals bind other parts of the cytoskeleton or the plasma membrane to control the organisation of microtubules within the cell. MAP1 family proteins are mainly expressed in neurons, where they are thought to be important in

the formation and development of axons and dendrites [29].

MAP2 is found primarily in the dendritic extensions of neurons. MAP2 has been considered as a hallmark of neuronal differentiation [30] and plays a role in stabilizing microtubules.

MAP4 is expressed in nearly all types of cells. It is responsible for stabilization of microtubules. This protein promotes microtubule assembly *in vivo*, and has been shown to counteract interphase microtubule catastrophe [31]. Cyclin B was found to interact with this protein, which targets cell division cycle 2 (CDC2) kinase to microtubules in mitosis [32].

Finally, Tau is the most famous MAP family member because it has been implicated in Alzheimer's disease [33]. It is found primarily in neurons, where its phosphorylated isofoms bind to tubulin to promote polymerization and stabilization of microtubules. Hyperphosphorylation of Tau can make them drop off microtubules, leading to disassembly of the microtubule. The protein has also been widely used as a marker of individual microtubule filaments.

1.4.2 Microtubule destablizers – the Yin of microtubules

The Yin-Yang theory always helps us to understand and describe opposing aspects in one system or phenomenon. If the above MAPs stabilize microtubules can be compared to the Yang aspect in microtubule

instability regulation, there should be a Yin aspect to make the system balanced, which requires a group of proteins to function as microtubule destabilzers. While MAPs bind to lateral side of the polymers to stabilize microtubules, these proteins work in multiple ways to destabilize microtubules. The most important counter-balance to microtubule polymerisation is the intrinsic ability of tubulin in the filament to hydrolyse GTP to GDP. This leads to the loss of the GTP cap and to catastrophe. In addition, several proteins have been identified that can bind to tubulins dimers to inhibit monomer addition at the growing end, and the following proteins have been shown to work as destabilizers of microtubules.

Stathmin/Op18: Stathmin/Op18 was originally identified as an oncoprotein. It is a member of a microtubule-destabilizing protein family which has been shown to play a critical role in the regulation of mitosis [34]. Stathmin has been shown to bind tubulin to inhibit microtubule polymerization [35, 36] and to promote catastrophe by inducing GTP hydrolysis [37]. Stathmin/Op18 is regulated by phosphorylation at four serine residues by a number of protein kinases and dual phosphorylation, particularly of serines 16 and 63, inhibits the microtubule destabilizing activity of Op18 [38].

Spastin/Katanin: Spastin functions as a microtubule severing enzyme. In 1991, the Vale lab first showed the evidence with Xenopus egg mitotic

extracts that microtubule breakage reflects the action of an enzyme rather than just mechanical strain [39]. Two years later McNally identified an ATPase that has the function of severing and disassembling stable microtubules to form tubulin dimers [40]. Microtubule severing is a hard task as the enzyme needs to break both longitudinal and lateral contacts in the microtubule lattice. The most significant thing is that the finding of this protein demonstrates a novel mechanism for cells to disassemble microtubules which utilizes energy from nucleotide hydrolysis to break tubulin-tubulin bonds within a microtubule polymer [40]. Using small-angle X-ray scattering combined with atomic docking, Katanin was seen in hexamers, forming a ring with a prominent central pore and six radiating arms that dock onto the microtubule [41]. The Vale lab has come up with a working model for Katanin published in 2008, in which Spastin pulls the C terminus of tubulin through its central pore, generating a mechanical force that destabilizes tubulin-tubulin interactions within the microtubule lattice [41].

Minispindle/XMAP215: Unlike the other MAPs, XMAP215 has both microtubule plus end stabilizing and destabilizing activities. Gard and Kirschner identified this protein in Xenopus egg extracts in 1987 [42]. *In vitro* data in the following years revealed that it inhibits the activity of XKCM1 a kinesin-13 family member to suppress catastrophe from

microtubule plus ends [43]. However, XMAP215 and its yeast homologue Stu2 can also destabilize microtubules through interfering with tubulin addition to microtubule plus ends [44, 45]. Recent data from Ohkura's lab demonstrate Minispindles acts as an anti-pausing factor to exhibit both microtubule stabilising and destabilising activities. This is a new mechanism for the regulation of microtubule instability [46].

Microtubule filaments can work as a track for motor proteins in addition to generating movements and forces through the regulation of dynamic instability. The major microtubule motor proteins are those of the kinesin superfamily, which generally move towards microtubule plus ends and dynein which moves towards the minus end. Here, I am going to focus on a subset of motor proteins that have effects on the microtubule instability. So, Dynein will not be discussed in the following text.

Kinesin super family proteins (KIFs) are motor proteins that transport membranous organelles and macromolecules for cellular functions along microtubules. They share a 360 amino acid globular ATPase domain to hydrolyze ATP to supply energy for this movement. However, more recent data suggest that some members of this family such as Klp10A and Klp67A also function to regulate microtubule instability. For the historical reasons the nomenclature can cause confusion as different kinesins have different names in various species. In Table 1-1, I try to summarize their

reported functions and localization according the most popular and systematic nomenclature.

Standardized name	*Drosophila* homology	Human homology	Reported function
Kinesin-1	Khc	KIF5B	Vesicle transport, conventional
Kinesin-2	Kif3C	KIF3A/3B	Vesicle-intraflagellar transport
Kinesin-3	Unc-104	KIF1A	Organelle transport
Kinesin-4	Klp3A	KIF21A/B,	Organelle transport, chromosome movement
Kinesin-5	Khc-73	KIF11	Spindle formation, microtubule induced cell polarity
Kinesin-6	Pav	KIF20	Cytokinesis, spindle polarity
Kinesin-7	Cmet	KIF10	Kinetochore microtubule capture
Kinesin-8	Klp67A	KIF18B, KIF19A	Nuclear migration, mitochondrial transport and destabilising MT
Kinesin-9	none	KIF6	Unclear
Kinesin-10	Nod	KIF26A, KIF26B	Chromosome segregation
Kinesin-11	none	KIF22	Signal transduction
Kinesin-12	Klp54D	KIF12	Organelle transport
Kinesin-13	Klp10A, Klp59c	MCAK,KinI	Microtubule depolymerising at plus end/central motor
Kinesin-14A	Ncd	KIFC1	Chromosome segregation
Kinesin-14B	none	KIFC2	Organelle transport

Table 1-1 Kinesin family members and their homologues

As I shown in above table, so far two kinesin subfamilies can function as microtubule destablisers. These are the kinesin-8 and kinesin-13 families. The Kinesin-13 family protein, also known as KinI or Kif2, has been reported to promote the catastrophe of the microtubule polymers at its plus end. In *Drosophila*, there are two members in this subfamily- Klp10A and Klp59C which functionally cooperate to regulate microtubule plus end dynamics in interphase. A model for the mechanism by which these two proteins induce microtubule plus end catastrophe has been proposed by David Sharp's lab [47, 48]. In interphase, they suggest that Klp10A can

target to the plus end of polymerizing microtubules by directly interacting with EB1 [49], whereas Klp59C binds along the lateral side of microtubules. When a microtubule pauses for a long time at the cell cortex, Klp10A will be inactivated and will drop off from the plus end, which allows Klp59C to accumulate at the plus end where it acts to depolymerise microtubules [50]. Thus, the hallmark of this process is its reliance on the paused state during the microtubule dynamic cycle. It is easy to understand how cells could use this mechanism to make microtubule dynamics sensitive to spatial information within the cell.

Kinesin 8 family member Klp67A is present in an active form in the nucleus during interphase. It therefore engages with its microtubule targets during nuclear envelope breakdown (NEB) at the onset of mitosis. The Vale lab also demonstrated that relocalisation of Klp67A to the cytoplasm using a nuclear export signal resulted in the disassembly of the interphase microtubules [51]. This experiment provides support for the hypothesis that this class of kinesins possesses microtubule-destabilizing activity, which is regulated by changes in the subcellular localization of the protein. Kip3p the yeast homologue of Klp67A has several properties that distinguish it from other depolymerising kinesins, such as the kinesin-13 MCAK. The most important one is that Kip3p depolymerises longer microtubules faster than shorter ones, which provides a new mechanism

for controlling the lengths of subcellular structures known as length-dependent depolymerization [52].

1.6 Microtubule plus-end interaction proteins (+TIPs)

The network of Microtubule polymers in a cell quickly adapts to a new internal and external environment. This is because there are many microtubule accessory factors in the cytoplasm which form a system to precisely control the polymerization and depolymerization of microtubule filaments. Apart from the microtubule associated proteins (MAPs) and microtubule based motor proteins I mentioned above, there is another group of proteins that play an important role in the dynamics of microtubules. They regulate the microtubule dynamics through the microtubule plus end to guide the growth of the filament network, by favouring the growth or catastrophe of individual filaments, depending on their local environment in the cytoplasm. They also act as a scaffold for other signalling proteins to regulate the polymerization of microtubule filaments. These are termed plus-end-interaction proteins (+TIPs). To date, two distinct classes of such proteins have been characterized. One is end-binding proteins and end-binding associating proteins; the other is end-binding microtubule destabilizers that induce their depolymerization, which I discussed in 1.4.1. In the following, I will only focus on the first class.

Human	*Drosophila*	*S.pombe*	*S.cerevisiae*
EB1, EB3	EB1	Mal3p	Bim1p
CLIP-170,CLIP115	CLIP-190	Tip1p	Bik1
CLASP1, CLASP2	MAST/Orbit	?	Stu1p

Table 1-2 Homology in different Organisms for +TIPs

1.6.1 Microtubule plus-end binding proteins (EB1)

EB1 (also known as Mal3p in *S. pombe* and Bim1p in *S. cerevisiae*) was first identified as an adenomatous polyosis coli (APC) interacting protein which can bind to the plus-end of growing microtubule polymers in 1995 [53]. In 1998, Morrison and colleagues defined its subcellular localization. In interphase, EB1 was found associated with microtubules along their full length but was particularly concentrated at their tips. During early mitosis, EB1 was localized to centrosomes and their associated microtubules. During cytokinesis EB1 was strongly associated with the midbody microtubules [54]. Importantly, immunofluorescence microscope images suggest the native EB1 is in punctate structures hinting that EB1 may work as part of a large protein complex [55]. Since then, GFP-EB1 fusions have been widely used as a microtubule plus end marker to visualize microtubule dynamics in living cells. In 2000, EB1 was supposed to function in the recruitment of tubulin subunits at microtubule plus ends [56]. In addition, further work done in 2002 revealed that EB1 can stimulate the growth of microtubules at their plus ends and is necessary for the long-

range and dynamic microtubule filament ‘search-capture’ process [57]. This ‘search-and-capture’ mechanism was first proposed in 1986 by Mitchison to explain the way in which the inter-conversion between the growth and shrinking of microtubule plus ends, could enable microtubules to search for cellular space to interact with and capture target structures (e.g. plasma membranes, chromosomes, organelles etc.); a process that is followed by stabilization and reorientation of the microtubule-based cytoskeleton [58]. Current opinion favours this model. In addition, EB1 can control the distribution of other proteins, as Goshima et al. reported in S2 cells, where EB1 mediates the relocation of the minus end microtubule motor protein Ncd (kinesin-14 member function during chromosome segregation process) to microtubule plus ends [59].

1.6.2 Cytoplasmic linker proteins (CLIPs) and CLIP-associating protein (CLASPs)

The first identified member of the CLIP family of proteins was CLIP-170 which functions to protect the microtubule against catastrophe [60]. CLIP family members include the neural-specific protein CLIP-115, CLIP-170 and its homologues CLIP-190 in *Drosophila* and Tip1p in yeast. CLIPs localize at the microtubule plus-end and associate with EB1. CLIP’s localisation to the plus ends of growing microtubules is maintained by its binding to the newly polymerised GTP-cap. CLIPs are then released from

the microtubule lattice once the microtubule has aged. Once bound at the plus end, CLIP works together with EB1 to regulate microtubule dynamics by stabilizing the plus end [61].

CLIP-associating proteins (CLASPs) were firstly identified as interacting partners of CLIPs in a yeast two-hybrid analysis in 2001 [62]. In interphase, CLASPs localize to the Golgi apparatus and at the distal ends of microtubules [62]. Overexpression of CLASPs in COS-1 cells can stabilize microtubules. In contrast, injecting anti-CLASP antibodies suppresses the formation of stabilized microtubules in Hela cells [62, 63]. The middle part of CLASP binds directly to EB1 and to microtubules [63]. Currently, CLIPs and CLASPs are thought to mediate interactions between microtubule plus ends and the cell cortex and to act as local rescue factors through forming a complex with EB1 at microtubule tips [61].

In the following paragraph, STE20 family kinases will be briefly discussed because Tao-1 kinase the most important hit in my screen to regulate the cell shape belongs to this family, and it is necessary to know the history of this kinase family to help us to understand Tao-1's biological function.

1.7 STE20 kinase family

STE20 protein kinases share a typical Serine/Threonine kinase domain. They take their name from budding yeast Ste20p (sterile 20 protein)

kinase, the first member of this family to be identified. There are about 11 Ste20 family members in *Drosophila* and 30 Ste20 kinases in mammals (see Figure 1-4) [5]. Two subgroups have been identified based on the location of the Serine/threonine kinase domain: the Germinal Center Kinases (GCKs) with a N-terminal kinase domain and p21-activated kinases (Paks) with a C-terminal kinase domain. STE20 kinases have been reported to be involved in many important intracellular activities such as cell division through the MAPK pathway, apoptosis and the regulation of cytoskeletal remodelling.

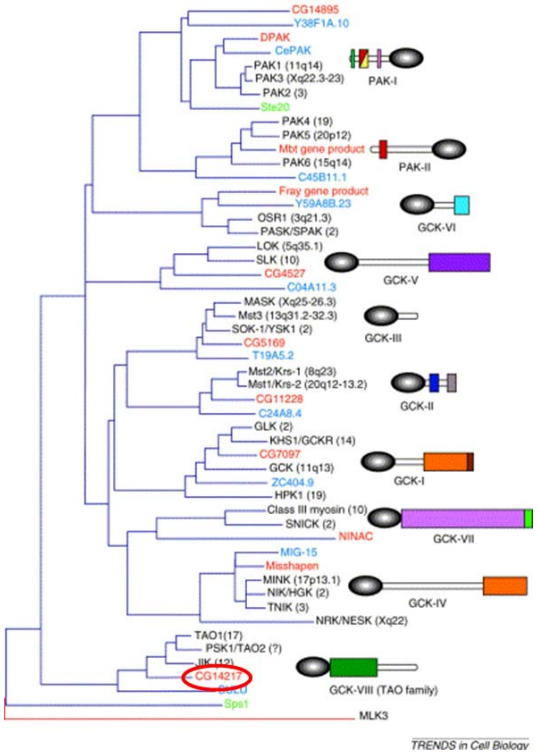

Figure 1-4 Phylogenetic relations among STE20 family kinases.
Letters in red shows the *Drosophila* homology; letters in black shows the mammalian members. *Drosophila* Tao-1 has been circled in red. (The picture was modified from Dan's review in *Trends in cell biology* [5])

Many findings have confirmed that many Ste20 group kinases are able to activate the mitogen-activated protein kinase (MAPK) signal cascade [5, 64, 65]. The MAPK pathway responds to the binding of growth factors to

receptors in the cell membrane, e.g. EGF to EGFR. The basic pathway has been shown in the Figure 1-5, and STE20 kinase works as the upstream regulator of mitogen-activated protein kinase by phosphorylation. In many cases, the activation of this pathway leads to cell growth and cell division.

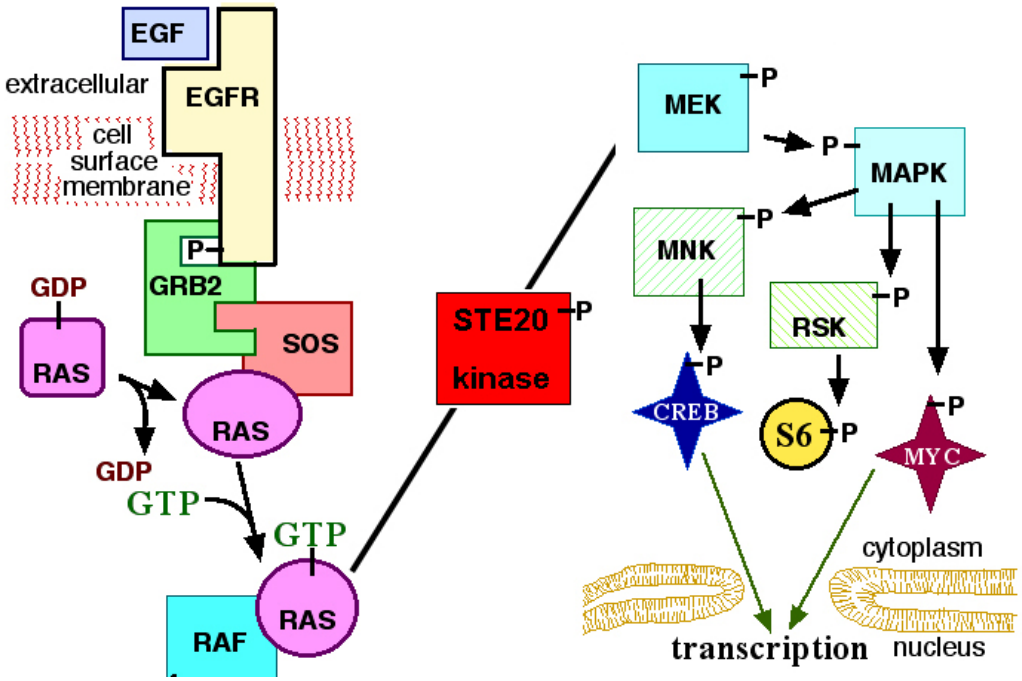

Figure 1-5 STE20 kinase family can active MAPK pathway. (The picture was modified from the website picture at http://en.wikipedia.org/wiki/File:MAPKpathway.png)

Several STE20 group kinases have also been reported to be directly involved in either inducing or preventing apoptosis. For example, in a well-studied apoptosis pathway, activation of Fas by ligand binding induces a sequential cleavage of caspases. Downstream effectors like caspase-3

then activate an Ste20 kinase, such as Mst1, Mst2, Hpk1 and Slk, which are known to be inducers of apoptosis [66, 67] to promote apoptosis.

STE20 group kinases have also been involved in morphogenesis and cytoskeletal rearrangement. The most well-known subgroup with this function is the Pak family. These proteins are characterised by having a Cdc42/Rac binding domain. The Pak I subfamily regulates the actin cytoskeleton by signaling downstream of the small GTPases, Cdc42 and Rac. Frost and colleagues found that Pak1 induces two types of morphological changes [68]. They showed that Pak1 kinase activity is important for the disassembly of focal adhesions, and that kinase-defective Pak1 promotes lamellipodia formation and membrane ruffling [69]. The other subgroup of the STE20 kinase family which has been reported to affect the cytoskeleton is GCK-IV, whose best know representative is Misshapen (Msn). *Drosophila* Msn has been reported to regulate dorsal closure through a JNK MAPK pathway [70] and axon targeting *in vivo* [71]. The human orthologue of Msn, NIK, was recently reported to phosphorylate ERM proteins at the distal margins of lamellipodia [72], as a novel mechanism that allows cells to control membrane protrusion and cell morphology in response to growth factors.

1.8 Background to methodology

1.8.1 RNA interference (RNAi)

Cells in culture have long been used as models for studying the function of proteins. However, until recently it was not possible to use them as a system in which to study loss of function genetics. This changed with the discovery of gene silencing and RNAi. The earliest gene silencing phenomenon, termed co-suppression, was first reported in 1990 [73]. Work over subsequent years identified similar silencing in a wide-variety of yeast, plants and animals. The impact of this work has been so important that 2006 year's Nobel Prize in Physiology or Medicine was shared by Andrew Z. Fire and Craig C. Mello for their discovery that silencing operates on a post-transcriptional level and is mediated by double-stranded RNA, published in their joint paper of 1998 [74]. Their discovery revealed a new mechanism for gene regulation, and the biochemical machinery involved plays a key role in many essential cellular processes. Transcripts with double-stranded character (microRNAs) synthesized within the cell are now know to regulate gene activity by an RNAi-like mechanism, through the inhibition of translation. RNAi has also been shown to protect plants and invertebrates cells against viral infections [75] and may have a similar function in metazoa, and ensures genome stability by keeping mobile elements silent [76].

Today, double-stranded RNA mediated RNA interference of gene expression (RNAi) serves as a powerful tool for determining protein function in a variety of organisms including *C. elegans*, *Drosophila*, mouse embryos, and mammalian cells. The present understanding of the mechanisms underlying dsRNA-induced gene silencing are largely derived from genetic studies in *C. elegans* and plants and from biochemical studies in *Drosophila* extracts [77]. Studies in *Drosophila* extracts showed how long dsRNA substrates could be cleaved into short interfering dsRNA species [78]. The process is initiated by a cytoplasmic RNAse III family double-stranded RNA-specific endoribonuclease, Dicer. It cleaves long dsRNA into short 21-23nt dsRNA fragments to initiate RNAi (see Figure 1-6). Each dsRNA fragment has a characteristic 2bp 3OH' overhang and a recessed 5' end phosphate at each end. In order to induce silencing, these small double-stranded RNA duplexes bind to form what is known as the RNA-Induced Silencing Complex, or RISC. ATP-depending unwinding of the small RNA duplex is required to discard one of the strands of the small double-strand RNA duplex. The activated RISC complex containing an Argonaute family endonuclease bound to a small single stranded guide RNA then targets the homologous transcripts by base pairing interactions, cleaving the mRNA ~10 nucleotides from the 5' terminus of the small RNA. This mRNA is degraded resulting in the eventual loss of the corresponding protein. The entire process is restricted to the cytoplasm [79-81].

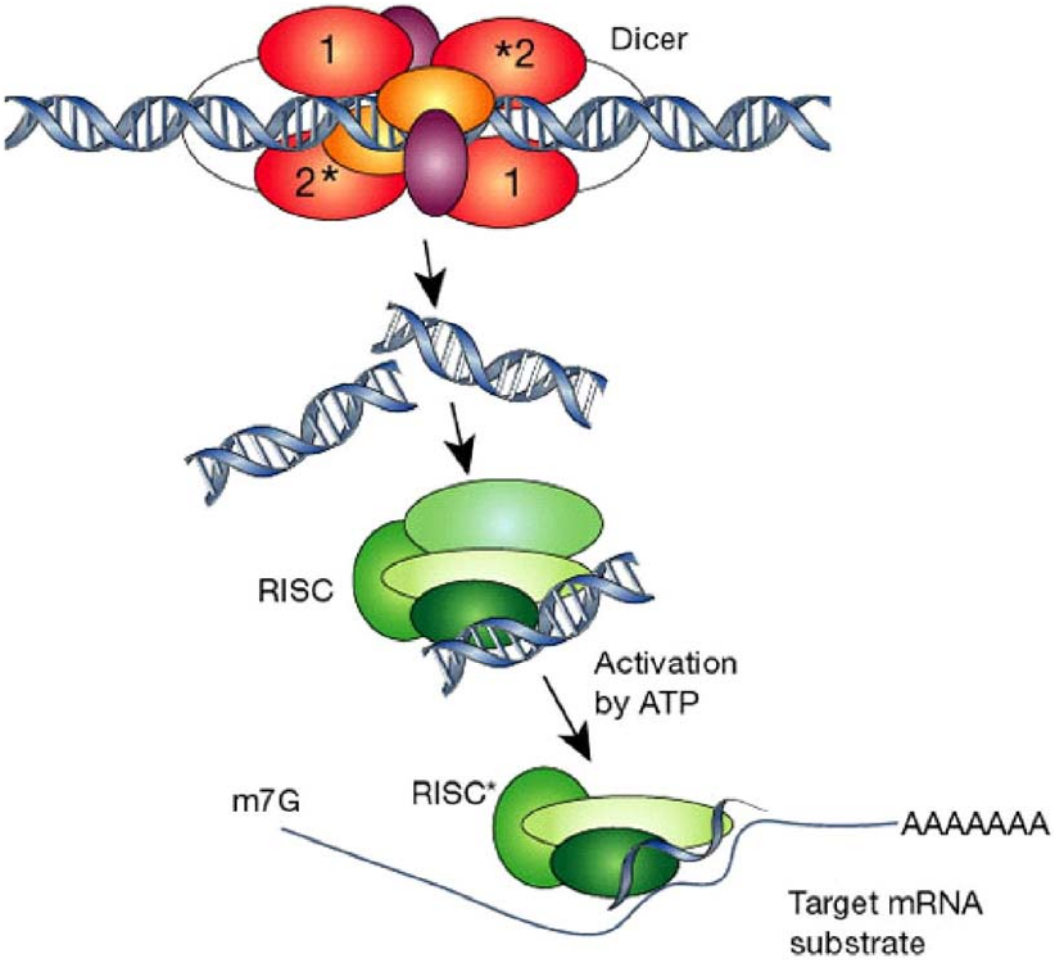

Figure 1-6 The two-step mechanism of RNA-mediated interference in the *Drosophila* cell cytoplasm.
The initiation step: Long dsRNAs are cleaved to for 21-23nt siRNAs by Dicer. The effector step. siRNAs are bound by the RISC complex, which cleaves the sense strand and binds the anti-sense strand, using it as a guide to target homologous mRNAs for degradation. The picture was modified from Hannon's review [4].

Although originally described as a post-transcriptional mechanism, RNAi silencing has now been proven to work on many levels. In plants, exposure to dsRNA induces the methylation of genomic DNA homologous to the trigger. If the trigger shares sequence with a promoter, the targeted gene can become transcriptionally silenced [10]. Studies in *Drosophila*

have suggested that the RNAi machinery may also affect gene expression at the level of chromatin structure. Some reports suggested that RNAi-dependent methylation of genomic DNA causes heritable alterations in gene transcription [82]. Finally, miRNAs, the endogenously encoded inducers of the RNAi machinery inhibit protein synthesis by binding to the 3' UTR of mRNAs without inducing mRNA degradation [83].

1.8.2 High-throughput RNAi Screening using *Drosophila* cell lines

Why fly cells? With the discovery of RNAi, the use of cultured *Drosophila* cells has several advantages as a model system in which to do cell biology. First, there is less genetic redundancy in *Drosophila* than in mammalian systems even though many signaling transduction pathways and other cellular processes are highly conserved from *Drosophila* to mammals. Second, many *Drosophila* cell lines have been established which are easy to grow, at room temperature in normal CO_2, which are ideal for use in studying various cellular processes [84]. Third, results obtained from cell culture studies can be confirmed in the whole organism, because *Drosophila* is also amenable to RNAi analyses and genetics at the organismal level. Fourth, the use of dsRNA to silence expression of specific genes in *Drosophila* cell culture is cheap, technically simple, efficacious, and highly reproducible [85] compared to that in mammalian

cells. This is because *Drosophila* do not respond to dsRNA with an interferon response. Instead, dsRNAs are efficiently internalized by the cells, thereby circumventing the problems generated by variable transfection efficiencies. Finally, the gene-silencing effect can be sustained for many cell divisions, as long as the protein of interest is not necessary for cell survival [86]. Therefore, RNAi in *Drosophila* cell culture provides a highly effective method for determining the function of proteins identified in the *Drosophila* genome sequencing project, as well as for deciphering the functions of mammalian proteins that have *Drosophila* homologues.

RNAi is often used for small-scale gene function studies. Tissue culture cells have also provided a powerful system for studying many fundamental problems in signaling transduction, cell differentiation and cell morphology. With the availability of complete genomic sequence, RNAi provides a cheap, effective and rapid approach to study gene functions on a large scale. A turning point came with the emergence of high-throughput RNAi screening in *Drosophila* cells, with the help of simple robotics, liquid handling devices, sensitive automated microscopes, and control software and data processing tools. In addition, progress in screening technologies and data analysis now allows the adaptation of screening methods to analyse more complex cellular processes [87, 88]. A typical HT RNAi screening consists of several key steps. First of all, a suitable dsRNA

library needs to be generated, which targets all the genes of interest. Second, a choice of cell type and assay conditions needs to be carefully considered, and positive and negative controls designed and tested. Finally, data acquisition and analysis are very important steps that should be considered before embarking on the screen. A typical data analysis process includes phenotype annotation, data normalization and a statistical analysis.

RNAi screens can also be refined through many of the same screening strategies that have been developed and perfected for decades in classic genetic screens. Particularly powerful are modifier screens [89], whereby RNAi is used to identify genes and pathways that, when silenced, can either enhance or suppress a given phenotype of interest. The phenotype to be modified can be the result of an initial drug treatment [90].

1.9 Aims of the Thesis

Different cell lines exhibit different cell shapes, which are generated by the organisation of the actin and microtubule networks. Kinases play very important roles in this process because many signal-transducing cascades result in the phosphorylation of proteins which regulate tubulin and actin dynamics to alter cell shape. Thus, in this study of morphogenesis I focused on all *Drosophila* kinases and used high-throughout RNAi screens to reveal novel genes involved in the regulation of cell shape in 6 different

Drosophila cell lines from 2 different kinds of tissues. This enabled me to identify generic and cell type specific regulators of the cytoskeleton. I then chose to characterize the function of two of these novel cytoskeletal regulators in detail.

Chapter 2

Methods and Materials

2.1 Selection of Drosophila kinases

In biochemical terms, a kinase is a type of enzyme that transfers phosphate groups from high-energy donor molecules to specific target molecules; this process is termed phosphorylation. *Drosophila* kinases consist of several subgroups as shown in the Figure 2-1. Protein Kinases are the largest subgroups, based on the total set of predicted proteins that were identified in the *Drosophila* genome using automated gene predictor methods [91] and published references [92]. In this study, 265 kinases in total were selected to make the kinase library. The percentage of each different subgroup is also shown in the Figure 2-1.

Using genomic information, I constructed a *Drosophila* kinase RNAi library, which was then used to screen six different cell lines from two different tissues originating from embryonic haemocytes and CNS tissues for novel genes involved in the generation of cell form. In doing so, I identified several regulators of cell behaviour and morphology across all cell lines, together with a set of cell-type specific kinases. Importantly, this analysis also revealed that, when considering the kinome, gene expression signatures are a poor measure of cell type specific differences in gene function.

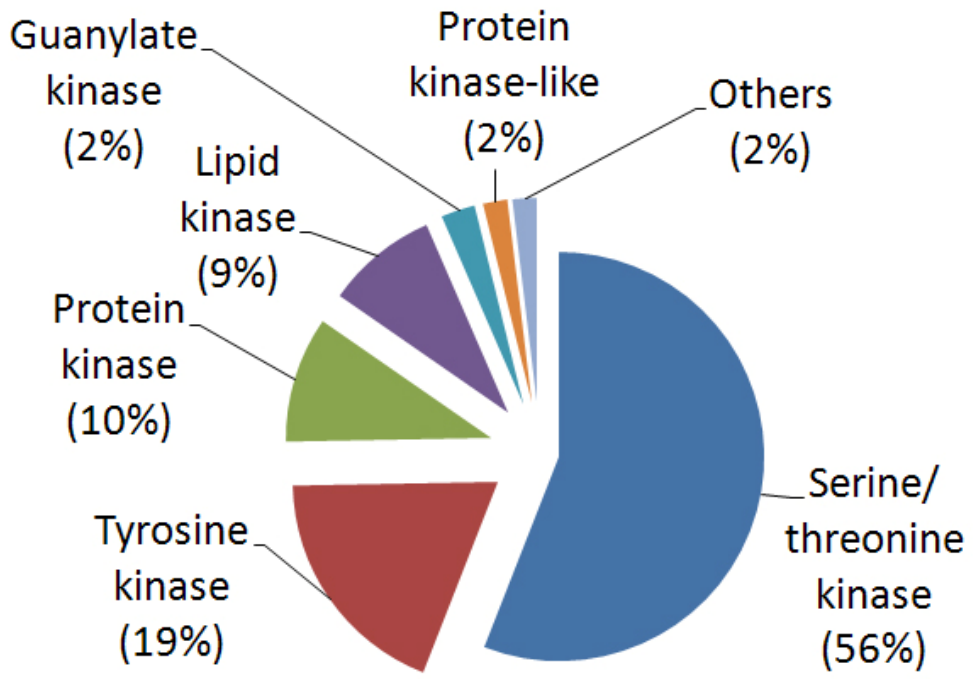

Figure 2-1 Subgroups and percentage of kinases in *Drosophila* dsRNA library

2.2 Genomic DNA Preparation

Approximately 30 pregnant female adult (WT) flies were homogenised in an eppendorf tube and genomic DNA was recovered using the Puregene DNA Isolation kit (Lot No. GS7907), following the protocol as described in the manual.

2.3 dsRNA Synthesis and Kinase library generation

Pairs of gene-specific primers (QIAGEN) were taken from FLIGHT database [93] or designed *de novo* using the E-RNAi primer design tool [94]. Each primer was designed to be ~21bp in length before addition of a

T7 tag ((TAATACGACTCACTATAGGG). Templates for the kinome RNAi library, targeting 265 *Drosophila* kinases and kinase regulatory subunits, were generated by PCR using HotSarTaq DNA polymerase (QIAGEN) in 200 µl PCR tubes (Appleton Woods TA571). PCR was carried out using the following program:

1) 95 ºC 15min
2) 94 ºC 30sec
3) 55 ºC 30sec
4) 72 ºC 30sec
5) go to step 2 for 29 cycles
6) 72 ºC 10min
7) 4 ºC hold

PCR success was confirmed using a 1% agarose DNA gel in 1xTAE. GeneRuler 1kb ladder (Fermentas) was used to confirm the size of bands obtained. DsRNA synthesis was performed using the T7 MegaScript kit (Ambion) according the manual. RNA preparations were purified using Multiscreen PCR purification kit (Millipore) attached to a vacuum pump with 1xTE buffer (pH=8.0). Purified RNAs were annealed by heating at 65°C for 10 minutes and cooling slowly. PCR and dsRNA synthesis was performed in 96-well plates and dsRNA concentrations were adjusted to 1 µg/µl before aliquoting into 384-well assay plates using a Beckman Biomek FX robot. 300 ng dsRNA of each kinase was added in 5 µl PBS to give a final concentration of 0.03 µg/ul in each well in 384-well plate.

2.4 Cell culture and cell lines used in the study

Six *Drosophila* cell lines were used in the parallel RNAi screening study. Kc167 and S2R+ cells were grown in Schneider's medium (Invitrogen) with 10% heat-inactivated fetal bovine serum (JRH Biosciences) and 1% penicillin-streptomycin (Sigma) at 24°C in treated culture flasks (Falcon from BD Biosciences). S2R+ cells were removed from culture flasks using Trypsin-EDTA (Invitrogen). S2 cells were grown in InsectExpress media with L-Glutamin (PAA Laboratories). The BG2-c2, BG3-c2, BG3-c1 cell lines were cultured with Shields and Lang M3 insect medium (Sigma) with FBS and antibiotics (1% GIBCO Penicillin and Streptomycin Lot412045). M3 media was supplemented with insulin for BG3-c2 (10 µg/ml) and BG3-c1 (5 µg/ml) cells. Cell lines used in this study are listed in the Table 2-1.

	cell lines	origination	Media	experimental purpose	original source
1	S2	embryonic haemocytes	InsectExpress (PAA Laboratories)	parellel RNAi screening	Invitrogen
2	Kc	embryonic haemocytes	M3(Sigma)	parellel RNAi screening	Baum's lab
3	S2R+	embryonic haemocytes	M3(Sigma)	parellel RNAi screening	Baum's lab
4	BG2	neuronal tissue	M3(Sigma)	parellel RNAi screening	Baum's lab
5	BG3-C1	neuronal tissue	M3(Sigma)	parellel RNAi screening	Baum's lab
6	BG3-C2	neuronal tissue	M3(Sigma)	parellel RNAi screening	Baum's lab
7	pMT-GFP-EB1 S2	embryonic haemocytes	M3(Sigma)	MT dynamic study	DGRC
8	Act5c-GFP-Tubulin S2	embryonic haemocytes	M3(Sigma)	MT dynamic study	DGRC

Table 2-1 Different cell lines used in either parallel RNAi screening or in

microtubule dynamic studies.

Two modified *Drosophila* S2 cell lines were used in the study of microtubule dynamic regulation: pMT-GFP-EB1 S2 and Act5c-GFP-Tubulin S2 (from DGRC). Both grow in 10% FBS M3 media with 1% P/S antibiotic (Sigma). 0.5 mg/ml G418 was added to inhibit the growth of non-expressing cells.

Cells stocks were stored in liquid nitrogen. For freezing, $1x10^7$ cells were suspended in 1 ml of ice-cold 10% (v/v) DMSO and 90% (v/v) FBS and placed in cryovials (Corning) in an isopropanol cell freezer (Amersham) and frozen gradually (-1°C/hour) to -80°C. After 24 hours, cryovials were transferred to liquid nitrogen for long term storage. Cells were thawed rapidly in a water bath at 37°C. Just before cells were thawed, they were mixed with 5 ml of ice-cold medium and centrifuged at 4°C. DMSO containing supernatant was removed by aspiration and the cell pellet was re-suspended in 5 ml of fresh medium. Cells were allowed to recover for two weeks prior to sampling.

Hela-Kyoto cells used in this study were cultured in pyruvate-free Dulbecco's Modified Eagle Medium (Gibco) containing 4.5 g/L glucose and 1x L-glutamine, supplemented with 10% FBS (PAA), 50 U/ml penicillin (Gibco), and 50 µg/ml streptomycin (Gibco) in a humidified 37 degree incubator at 5% CO_2.

2.5 High-throughput RNAi Screening and Automated Image Acquisition

For RNAi screens, cells in serum-free medium were plated into 384-well assay plates using a multidrop machine (Thermo Scientific Matrix WellMate), centrifuged briefly, and then incubated at 24°C for 15 minutes before addition of complete medium. Cells were grown for 5 days at 24ºC. In each experiment, positive and negative controls (pebble/thread/SCAR/LacZ RNAi) were included. Cells were fixed for 10 minutes in 4% formaldehyde (Polyscience). After fixation, cells were permeabilised by washing with PBS containing 0.1% Triton-X-100 (PBS-T), then blocked with 5% BSA in PBS-T for 15 minutes. Cells were incubated with primary antibody (α-Tubulin) in PBS containing 1% BSA overnight at 4°C. Cells were then washed and incubated with secondary antibody (FITC anti-mouse IgG) combined with TRITC-Phalloidin and DAPI for two hours. After staining, cells were washed and stored in 0.1% Sodium Azide in PBS-T at 4°C sealed with Costar6570 Thermowell sealing tape.

Fluorescent images were acquired using an automated Nikon TE300 microscope with a 20× objective and HTS MetaMorph software (Universal Imaging) running an automated stage, filter wheel and shutter, and a cooled-coupled device camera (Hamamatsu). Automated wide focusing was performed on the DAPI channel first. Images were acquired in three

channels at three sites per well.

2.6 Two step Reverse transcriptase (RT) Quantitative (Q) PCR

Cytoplasmic RNA was harvested from BG3-c2 and S2R+ cells using the RNeasy miniprep kit (Qiagen) according to the manufacturer's guidelines. The SuperScript II Reverse Transcriptase kit (Invitrogen) was used to synthesise the first-strand cDNA according to the manufacturer's guidelines. E. coli RNase H was used to remove RNA complementary to the cDNA. Q-PCR was performed using SYBR green (Molecular Probes) and an MX4000 real-time PCR machine (Stratagene). SYBR green fluorescence was quantified using a serial dilution of template containing PCR products of known concentration. Relative abundance of transcript was normalised against control (rp49) RNA levels. Primer sequences (Eurogentec) for all genes can be found in additional file 1.

2.7 Microarray Gene Expression Analysis

Total mRNA from wild-type cells in exponential growth phase was isolated by TRIzol extraction (Invitrogen). Microarray gene expression analysis was carried out using FlyChip long oligonucleotide spotted microarrays (FL002). Expression data was Loess normalised by intensity and probe location per chip, and rank normalised across chips. Normalised

expression was then averaged across three replicate chips for each cell line. Hierarchical clustering was performed using the Pearson correlation and the average linkage method. All data processing was performed using R/Bioconductor by David Sims [95].

2.8 Image annotation

Morphological phenotypes were annotated by eye from the automatically acquired images. Phenotypes were described using a controlled vocabulary of terms relating to cell shape, size, number and organisation of cytoskeleton protein. Each hit was scored for each relevant annotation term relative to wild type on a scale from -3 to +3. Phenotypic data was recorded using the PHenotype Annotation Tool (PHAT) (http://flight.licr.org) [93]. All annotation was carried out blind and repeated at least twice.

2.9 RNAi and modified RNAi treatment

RNAi experiments were performed in a range of different tissue culture dishes with different starting cell number depending on the assay (Table 2-2).

Plate	Size	cell concentration(cells/ml)	dsRNA(µg)	Assay
4-well	100µl	2×10^6	5.0	IF/WB/Transfection
6-well	400µl	2×10^6	20.0	WB
12-well	200µl	2×10^6	6.0	IF/WB
24-well	100µl	2×10^6	5.0	IF/WB/Transfection
96-well	40µl	2×10^6	1.5	Microscopy
384-well	10µl	2×10^6	0.3	Microscopy

Table 2-2 RNAi treatment in different tissue culture containers for different purposes

Typically, cells suspended in serum-free medium were mixed with dsRNA to give a final concentration of 30 ng/µl, centrifuged briefly, and then incubated at 24°C for 15 minutes before addition of complete medium. Cells were grown for 5 days at 24ºC.

For modifier RNAi experiments, cells were pre-treated in 0.1 µg/ µl dsRNA of gene X in serum free media for 15 minutes before cells were processed using a Multidrop 384 liquid dispenser (Thermo Labsystems).

LacZ (LacZ-f': TAATACGACTCACTATAGGTTGCCGGGAAGCTAGAGTAA; LacZ-r': TAATACGACTCACTATAGGGCCTTCCTGTTTTTGCTCAC) dsRNA was used as a negative control in all experiments if not specially mentioned otherwise.

2.10 Molecular biology and Cloning

2.10.1 Cloning and Sub-cloning Tao-1 (CG14217) from the *Drosophila* cDNA library

Compared to Human Homologues (PSK1α, PSK1β and PSK2), *Drosophila* Tao-1 (CG14217) has only one isoform which has been

confirmed via RNAi and antibodies, although the gene model of Tao-1 from Flybase (http://flybase.bio.indiana.edu/) shows existence of multiple transcripts (PA, PB, PD and PE) based on EST data.

Full length Tao-1 (1039aa) contains a kinase domain, ATPase domain, ERM-like domain and three repeated coiled coil regions from the N to C terminus (see Figure 2-2).

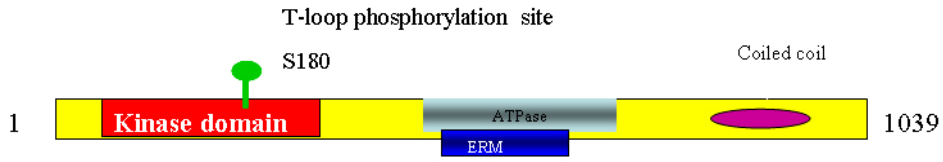

Figure 2-2 Functional domain distribution in Full length *Drosophila* Tao-1

Two pairs of primers were used to amplify the full length Tao-1 from the cDNA library (from NB's lab) as the full length Tao-1 is 3120bp, making it very hard to generate a PCR product free from mutations in one go. Primer pair LT-007 (all cloning primer sequence information can be found in the additional file 2) and LT-004(2) were used to PCR Tao-1 from the start codon to 1722bp giving fragment 1. Primers LT-005: 5' and LT-008 were used to PCR Tao-1 from 1556bp to the stop codon, including the mutant stop code and HindIII restriction enzyme site, to form fragment 2. Fragments 1 and 2 were cloned into the pGEM®-T Vector Systems (promega) as an intermediate step to supply suitable restriction enzyme sites. BglII/ApaI and ApaI/EcoRI were used to cut out Fragment 1 and Fragment 2 from pGEM-T vectors. Subsequently, the two fragments were

ligated with pENTR1A simultaneously to create a Gateway® entry vector (from Invitrogen life technologies, Catalogue Number 11813011) at BamH1 and EcoRI sites. pENTR1A-FL-Tao-1 was sent for sequencing after the purification with PureYiedl plasmid midiprep kit from Promega (Cat.#A2492) to ensure that no mutations occurred during the cloning and subcloning work. There are no mutations in the sequencing results as shown in the sequencing results in additional file 3.

2.10.2 Mutations

In order to study the function of individual domains of Tao-1, mutations based on the entry clone, pENTR1A-FL-Tao, have been made with different strategies, as shown in Figure 2-3 below:

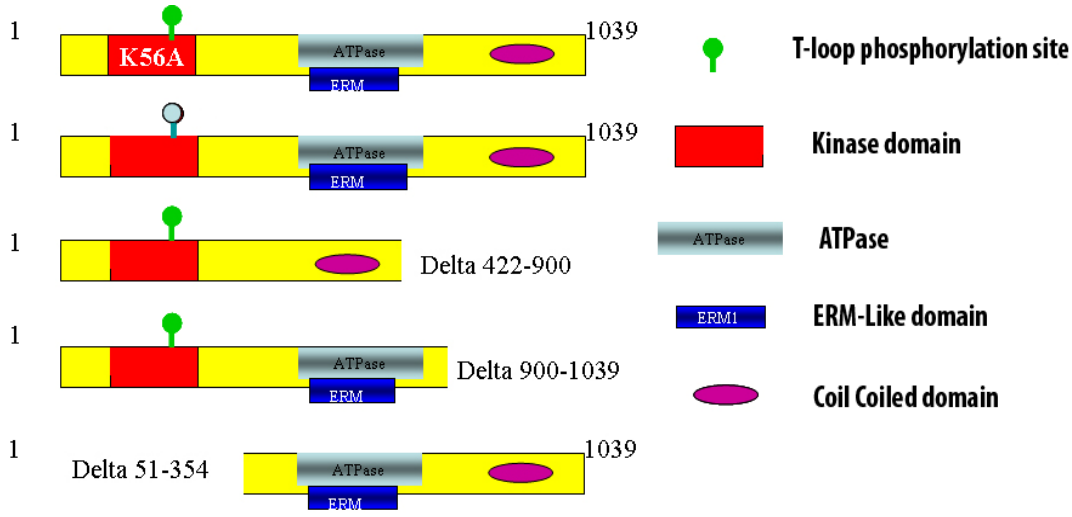

Figure 2-3 Strategy of all mutations made from Full length construct for studying the molecular biological function of Tao-1

K56A is a kinase domain point mutation via that is predicted to destroy

Tao-1's kinase activity, whilst the other protein domains remain unmodified. S180E is a mutant which mimics the T-loop phosphorylated predicted 'active' form of Tao. Δ422-900 is a construct with the ERM-like and ATPase domains missing. Δ900-1039 lacks of two repeated coiled coil domains which were reported to be related to the microtubule binding and/or centrosome localization functions of the protein [96]. Δ51-354 is an N-terminal Kinase domain deletion mutation. All these mutations were made based on the pENTR1A-FL-Tao so that they could be easily recombined into destination vectors with different fusion tags.

The Quikchange site-directed mutagenesis kit from STRATAGENE (Cat.#200519) was used to introduce the point mutations.

S180E-f'(5'- AAGTGTCCGGCCAACGAATTTGTCGGCACGCCC-3') and S180E-r'(5'- GGGCGTGCCGACAAATTCGTTGGCCGGACACTT-3') were designed as forward and reverse primers for making the S180E construct.

K56A-f'(5'- GAGATCGTGGCCATCGCAAAGATGTCGTACACC-3') and K56A-r'(5'- GGTGTACGACATCTTCGTGATGGCCACGATCTC-3') were designed as forward and reverse primers for making the K56A kinase domain mutant.

To make Δ 900-1039 and Δ422-900, pENTR1A-FL-Tao was cut open with KpnI and HindIII respectively at 1266bp and 3120bp. The strategy is

shown in the Figure 2-4.

Forward primer NTaoΔ900-1039-f' (5'-ACAGCCGGTACCGCCTGGAGCCGTGTCCCGC-3') and reverse primer TaoΔ900-1039-r'((5'-CGAAGCTTCTATTTGTAGCTCTGACTTTGGAAC-3') were used to obtain the PCR segment which is approximately 1.4kbp from 1260bp to 2700bp with incorporated KpnI and HindIII. Forward primer-NTaoΔ422-900-f':

(5'-GCGGTACC ACTAGACGAAAGCCAAGTGATTGAGTGC-3') containing a KpnI site and reverse primer-TaoΔ546-900-r':

(5'- CG AAGCTTCTATAGCGAACCAGCCGGAAAACTTG-3') with a HindIII site were used to perform the PCR to obtain the segment which is about 420bp to get the pMT-GFP-TaoΔ422-900 mutation. PCR segments then were subcloned into a pGEM-T vector (from Promega), cut with KpnI and HindIII to generate the sticky ends for re-insertion into the linearized pENTR1A-FL-Tao-1 vector.

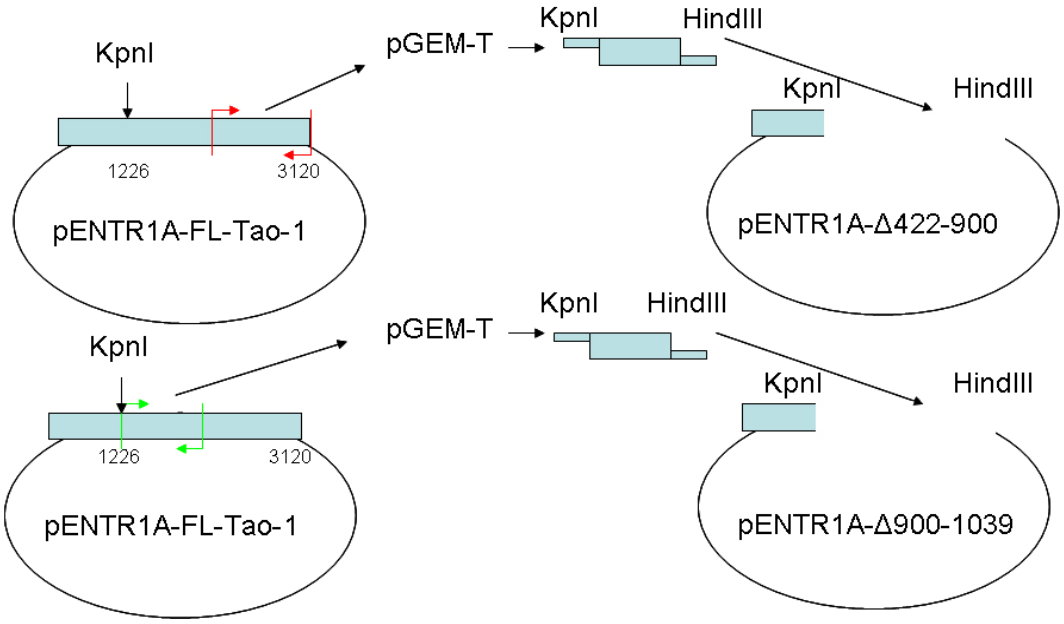

Figure 2-4 The cloning strategy for Δ900-1039 and Δ422-900 mutations

After ligation, final constructs were sequenced and confirmed that no mutations were introduced during the PCR process (sequence results are in additional file 3).

To make Δ51-354, pENTR1-FL-Tao was cut open with XcmI which cuts full-length Tao twice at 153bp and at 1062bp respectively, and the remaining part, which is still inframe, was then ligated to generate the construct pENTR1A- Δ51-354.

PCR was carried out as follows:

1) 1.25 µl primer pair (5 µmol)
2) 1.25 µl dNTP (2.5 mM)
3) 0.2 µl HotstarTaq DNA polymerase (from Qiagen, Cat.#203205)
4) 3 µl 10xBuffer
5) 100 ng pMT-GFP-Tao-1
6) 24 µl dH2O

With a program:

1) 95 ºC 15min
2) 94 ºC 30sec
3) 55 ºC 30sec
4) 72 ºC 1min
5) go to step2 for 24 cycles
6) 72 ºC 10min
7) 4 ºC hold

Samples were sent for sequencing after the purification with PureYield plasmid midiprep kit from Promega (Cat.#A2492). All sequence results showed that the expected residues were mutated, while other parts of the constructs were unaffected (sequence maps as shown in additional file 3).

2.10.3 *Drosophila* Gateway recombination cloning system

A universal cloning method named Gateway Technology based on the site-specific recombination properties of bacteriophage [97] has become more and more popular as a way of simplifying cloning work in life sciences. Gateway Technology provides a rapid and highly efficient way to move DNA sequences into multiple vector systems for functional analysis and protein expression (see Figure 2-5).

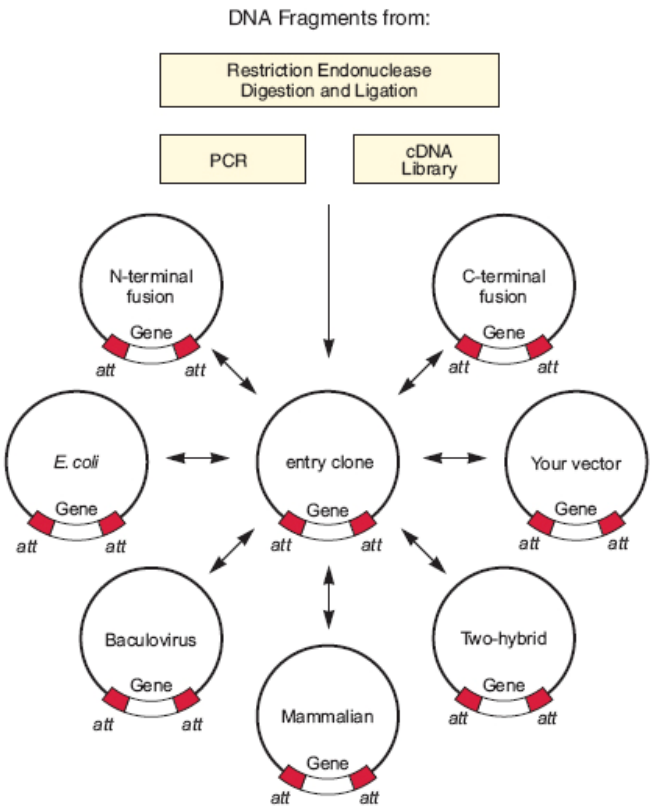

Figure 2-5 Gateway Technology-easy strategy to cloning a gene using different expressed destination vector. (Modified from Invitrogen website)

This technology enabled me to efficiently move various DNA sequences into different constructs for different purposes, such as protein expression and functional analysis, without considering changing the orientation and open reading frame.

Different destination vectors were used to generate constructs with different promoters and fusion tags. The details were as shown in the Table 2-3:

	Construct Name	Promoter	Fusion tag	Antibiotic Resistance	P-element
1	pMT-GFP-FL-Tao	pMT	N-terminal GFP	Amp	no
2	pMT-RFP-FL-Tao	pMT	N-terminal GFP	Amp	no
3	pMT-GFP-S180E	pMT	N-terminal GFP	Amp	no
4	pMT-GFP-K56A	pMT	N-terminal GFP	Amp	no
5	pARW-K56A	Actin5c	N-terminal RFP	Amp	no
6	pARW-delta-900-1039	Actin5c	N-terminal RFP	Amp	no
7	pARW-delta-422-900	Actin5c	N-terminal RFP	Amp	no
8	pARW-delta-51-354	Actin5c	N-terminal RFP	Amp	no
9	pPGW-FL-Tao	UASp	N-terminal GFP	Amp	yes
10	pPGW-K56A	UASp	N-terminal GFP	Amp	yes
11	pPGW-delta-422-900	UASp	N-terminal GFP	Amp	yes

Table 2-3 All the constructs, fusion tags and promoters used in this study

pARW, pPGW (Invitrogen) and N-terminal pMT-GFP/RFP-*ccdB* (a gift from Dr. Jeroen Dobbeleare in Jordan Raff's lab) is a modified gateway destination vector that was used for the LR reaction with pENTR1A-Tao-1 to create a Gateway® expression clone. The protocol of the LR reaction is as follows:

1) Entry vector pENTR1A-Tao-1 (150 ng/µl) 1.5 µl
2) Destination vector pMT-GFP/RFP-ccd (150 ng/µl) 1.5 µl
3) LR Clonase™ II enzyme mix 4.0 µl
4) 10x buffer 2.0 µl
5) Add dH_2O to 20 µl reaction

This was mixed well by vortexing briefly and incubated at 25°C for 4 hours. Next, 100µl Dh5α was transformed with 5µl of the mixture according the protocol from the kit (Invitrogen gateway vector system). Purification of the pMT-GFP-Tao-1 was carried out using the PureYield plasmid midiprep kit from Promega (Cat.#A2492).

2.11 Transfection

Drosophila S2R+ and S2 cells were transiently transfected using FugeneHD (Roche, Lot#93539521) transfection reagent. 1.0 µg plasmid was mixed with 3 µl of FugeneHD reagent in 50 µl of serum-free M3 medium and incubated at room temperature for 60 minutes. Meanwhile, $5x10^5$ S2R+ cells previously plated into a 4-well dish were washed twice in 300µl of serum-free medium. Next, the plasmid and FugeneHD mixture was added to the cells, with an additional 300µl complete media, resulting in a total volume of 700 µl in each well. Cells were incubated for 12 hours at 24°C before changing the media. After 24-48 hours, cells were moved to FCS coated glass bottom coverslips. Where necessary, gene expression was induced the following day by addition of $CuSO_4$ solution (the final concentration of Cu^{++} is 70 nm).

2.12 Cell number measurement

Cell number counts were used to gain a quantitative assessment of the Mnb phenotype in S2, BG2, BG3-C1 and BG3-C2 cells. In each case, $1.5x10^6$ cells were treated with Mnb or LacZ dsRNA in 4 well-dish. On the 5th day, cells were counted in triplicate using a Beckman Z2 Coulter Counter. The average cell number and standard deviation are presented for each.

2.13 Antibody and Western Blotting

We made rat multipeptide-antibody against Tao-1 both on the C-terminal part: 967-981: C+FNQERAERLRMKHEK-CONH2 and the N-terminal part: 2-16: CONH2-PSARPGSLKDPEIAD+C. The rabbit multipeptide-antibody against P-Tao-1 was made based on sequence CONH2-RAQRATS[P]NVFAMC+3, which has been confirmed as the T-loop phosphorylation site [98]. All of these antibodies were ordered from Eurogentec.

Samples were lysed in 2 x laemmli buffer and boiled at 95°C for one minute before loading. Samples were run on a 4-12% graduated SDS-PAGE gel (Invitrogen), and then transferred to nitrocellulose blotting paper (Invitrogen). Membranes were blocked with 5% skimmed milk in TBS-T for 30 minutes, incubated overnight at 4°C with appropriate primary antibodies (1:1000 for P-Tao antibody and 1:500 for non-ph-Tao antibody), and then washed three times with TBS-T for 15 minutes each time. Membranes were then incubated with appropriate horseradish peroxidase (HRP) conjugated secondary antibodies (1:2000) in TBS-T for one hour, and washed as before. The Super Signal West Pico Chemiluminescent Substrate (PIERCE) was used for detection. After incubation with the reagent, the membrane was wrapped in SaranWrap and exposed to Hyperfilm EC (Amersham Biosciences) under dark-room conditions. The

resulting films were scanned and quantified with metamorph6.2 and photoshop7.0 software.

2.14 Tissue staining

I used w118;UASp-GFP-Tao in crosses with different Gal4 drivers to generate homozygous flies in which to observe GFP-Tao's localization in fly egg chambers. Flies were fed yeast for 2 days before the isolation of ovaries. For egg chamber analysis, 5 well-fed females of each genotype were dissected to obtain about 10 ovaries in total. For antibody, TRITC–phalloidin and DAPI staining, tissue was fixed in 4% formaldehyde in PBS for 20 min. Tissue was then pre-washed in 1% Triton X-100 for 4 h at room temperature, blocked in 5% BSA, 0.1% Triton X-100 (PBT) and incubated overnight at 4°C in TRITC–phalloidin (Molecular Probes) and DAPI (1 μg/ml), before mounting in antifade and glycerol.

2.15 Microscopy

2.15.1 Automated stage microscope

A Nikon TE2000E Inverted Microscope with an automated stage was used for capturing data from screen experiments. The TE2000-E has a high precision Z-axis automated focus (with a linearly encoded Z-axis minimum step size of of 0.05 microns), allowing us to take pictures for each well in a wide region in the 384-well plate without losing focus.

2.15.2 Confocal microscopy and Fluorescence time-lapse live imaging acquisition

For immunostaining, S2 and or S2R+ cells were fixed with either –20°C methanol or 4% formaldehyde. Antibodies used in this study were diluted to concentrations ranging from 1 to 20 µg/ml (anti-Tao-1 and anti-P-Tao-1 [our lab], anti-Cnn [J. Raff, University of Cambridge], DM1a α-tubulin [Sigma], phosphohistone H3 [Upstate Biotechnology], anti-GFP [LabVision, Fremont, CA; #MS-1315-PO]. Secondary antibodies (FITC, TRITC,Cy5 and TRITC; Jackson ImmunoResearch, WestGrove, PA) were used at final dilutions of 1:1000 [99]. Cells were mounted in a 0.1 M propyl galate-glycerol solution. DAPI (Sigma) was used at a concentration of 5 µg/ml.

For cold-shock experiments, S2R+ cells pre-spread on Concanavalin A (ConA) coated 35 mm optical quality glass-bottomed culture dishes (MatTek Corporation, USA) were placed on a partially submerged aluminum block in a water-ice bath at 0°C for 2.5 hours in the 4°C cold room environment and allowed to recover at room temperature.

Compared with other microscopy systems, the confocal laser scanning microscope has several advantages, the most important being its high spatial resolution in z compared with non-confocal light microscopy. In this study, a Leica TCS SP5 with a HCxPL 40x/1.25 oil-immersion lens (Leica)

and a Leica DFC400 camera was used for high resolution cell imaging *in vivo* and *in vitro*. The software platform used was LAS AF. An inverted confocal system, Leica TCS SP5 was used to perform all the time-lapse imaging work.

For time-lapse microscopy imaging, cells were plated onto ConA (50 μg/ml) coated 35 mm optical quality glass-bottomed culture dishes (MatTek Corporation, USA). Phase-contrast and fluorescence time-lapse movies were taken on the Leica TCS SP5 with a Leica DFC295 digital camera, using a HCxPL 40x/1.25 oil-immersion lens at 2 seconds intervals. Microtubule dynamics were analysed in live RNAi-treated or transfected cells by time-lapse fluorescence microscopy using GFP or RFP fusion protein. 0.5 μM Latrunculin B (LatB) which sequesters G-actin and promotes actin depolymerization was used for drug treatment experiments.

2.15.3 TIRF microcopy

The Leica multicolor TIRF (Total Internal Reflection Fluorescence) all-in-one system was used in this study to demonstate Tao-1's membrane localization. It has four integrated solid state lasers for excitation of fluorophores in wavelengths 405 nm, 488 nm, 561 nm and 635 nm. The extremely short switching times and constant TIRF penetration depth of 90nm enabled us to study the processes of microtubule plus end dynamics at cell cortex and the interaction between our protein of interest,

Tao-1 and +TIPs in living cells.

$1x10^6$ RNAi treated or transfed cells were plated onto ConA (50 μg/ml) coated 35mm optical quality glass-bottomed culture dishes (MatTek Corporation, USA), and left to attach to the bottom and spread completely for 30 minutes prior to loading onto the TIRF microscope with HCX PL APO 63x/1.40 oil-immersion lens (Leica). Florescent images of both GFP and RFP were acquired every 2 seconds.

Chapter 3

Results: Parallel RNAi screens across different cell lines to identify kinases that regulate cell morphology

3.1 Introduction

In recent years RNAi screening has proven itself to be a powerful tool for dissecting gene function. To date, most RNAi screens have been performed in a single cell line. Results have then been extrapolated to all cell types and other systems. This is the case even though multi-cellular organisms are composed of a large variety of specialised cell types with distinct morphologies and functions.

A diversity of cell shapes is a fundamental feature of multicellular life. Cell type specific forms arise during development as the products of a cell differentiation program that refines patterns of gene expression to yield cells with a form and behaviour appropriate to their function. To establish how the forms that characterise cells from different lineages are generated, we have used *Drosophila* cell lines derived from distinct tissues as a model system.

Drosophila cells lines provide a good model for such an analysis, since multiple cell lines have been derived from diverse tissues, including haemocytes [100-102], neuronal tissue [103] and imaginal discs [104, 105], and because all these cell lines have morphologies that appear consistent with their lineage. Thus, S2 and S2R+ cells have broad lamelliopodia and are similar in both form and behaviour to larval blood cells [105] (Sims et al., unpublished data), while BG1, BG2 and BG3 nervous system-derived

cell lines have a common morphology and cyto-architecture [105], which includes filopodia embedded in lamellipodia [84], reminiscent of those seen in neuronal growth cones [106]. It has long been hypothesised that the morphological diversity of different cells types is decided largely by differential gene expression and consequently differential regulation of signalling pathways and cytoskeletal genes [107]. However, the genes required to establish these different forms remain largely unknown. I used gene expression microarray gene expression analysis together with RNAi screening in a panel of *Drosophila* cell lines to identify cell type-specific cytoskeletal regulators, and to explore the relationship between gene expression and function across a panel of cell lines. Since the structural components of the cytoskeleton and their core regulators (e.g. cofilin and profilin) are likely to function in a broadly similar way across cell types, I focused our analysis on the kinome to identify cell type specific differences in the regulation of this basic cytoskeletal machinery. Kinases are a well-defined family of proteins characterised by a common catalytic domain that regulate myriad cellular processes, including the organization of the cytoskeleton, and hence cell shape [108-110]. They can be divided into a number of sub-families based on the structure of the kinase domain in each case [92]

In doing so, I identified a set of common regulators of cell behaviour and

morphology, together with a group of cell-type specific kinases. Importantly, this analysis also revealed that, when considering the kinome, gene expression signatures are a poor measure of cell type specific differences in gene function.

3.2 Cell Lines from the Same Origin Display Similar Morphologies and Gene Expression Patterns

We chose to use six different cell lines from two different tissues of origins in RNAi screens for novel genes involved in the generation of cell form. In *Drosophila*, S2, Kc167 and S2R+ cells, which originate from embryonic haemocytes [100-102], are relatively symmetrical in shape and are non-motile as shown in (see Figure 3-1).

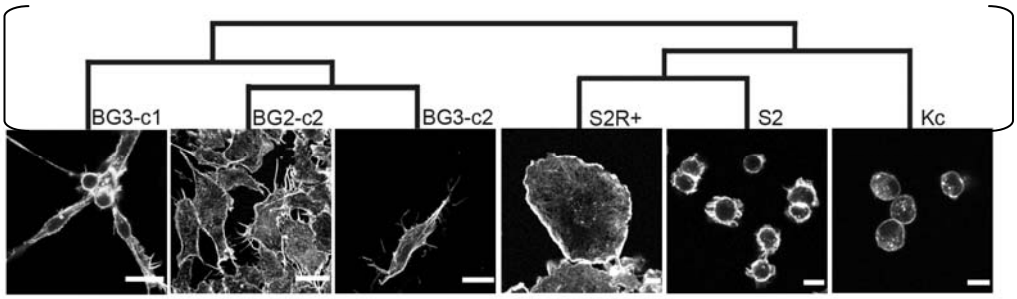

Figure3-1 The three CNS-derived cell lines BG2-c2, BG3-c1 and BG3-c2 have a bipolar, spiky cell shape, whereas the three embryonic haemocyte derived cell lines S2, S2R+ and Kc167 have a symmetrical morphology. Gene expression profiles for each cell line were normalised and hierarchical clustering was used to generate the dendrogram shown. This analysis reveals that cell lines from the same origin have closely related gene expression profiles. (scale bars represent 10 μM in each picture.)

Note that the S2R+ line is an original isolate of the S2 line [102]. In addition, these haemocyte lines have a propensity to develop lamellipodia rather than filopodia [89]. By contrast, BG2-c2, BG3-c1 and BG3-c2 cells originate from neuronal tissue [103], are migratory (Wei-Bai, Baum and Ridley, unpublished), and have a polarised shape characterised by long actin-rich protrusions embedded in lamellipodia [84]. Note that BG3-c1 and BG3-c2 represent different clonal isolates from a single primary culture [103].

To determine whether the common origins of these six cell lines are reflected in their respective gene expression profiles, I compared the microarray gene expression analysis data available in our lab which were done by David Sims on each of the six lines (see materials and methods). By clustering these results, it was clear that cell lines from the same tissue of origin have related patterns of gene expression (see Figure 3-1), leading us to conclude that these cell lines are suitable *in vitro* models in which to study the regulatory networks underlying these two distinct cell-type specific morphologies.

3.3 Parallel High-throughput RNAi screen identified a key set of kinases in charge of regulating cell morphology

I designed and constructed a dsRNA library targeting 265 *Drosophila* kinases and kinase regulatory subunits (list in additional file 4), which

could be screened in 384-well plates using the bathing method [111]. For the screen, cells were added to library plates and incubated for five days to allow for the turnover of existing proteins. Cells were then fixed and stained to visualise actin filaments, microtubules and DNA, and images were acquired using automated microscopy (see methods and materials). Each cell line was screened independently at least twice. All cell images and hit annotations are available online through the online FLIGHT database (http://flight.licr.org/) [93].

Of the kinases screened, 17.7% (47/265) yielded a visible phenotype in at least one of six cell lines as shown in additional file 5. The hit rate however varied considerably across lines (see Figure 3-2).

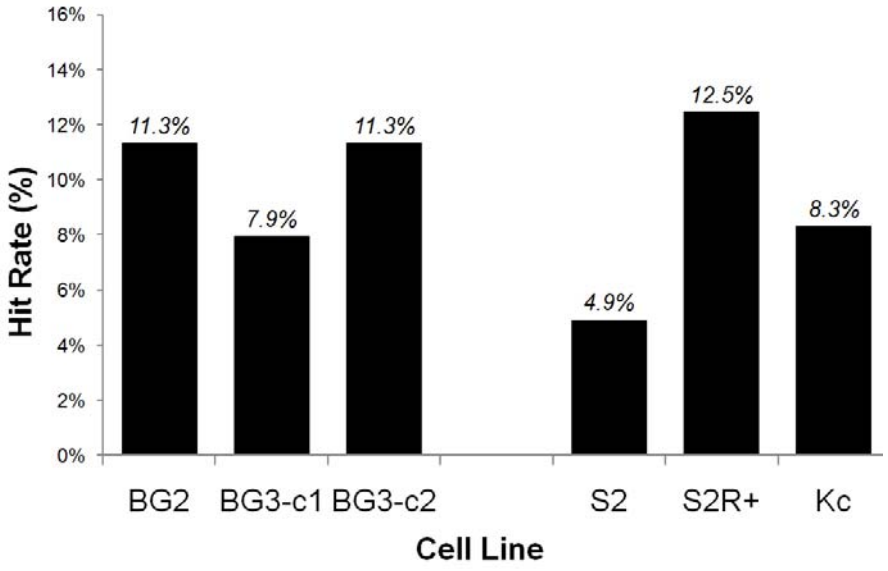

Figure 3-2 Different cell lines exhibit different hit rates in RNAi screens

Based on the results of the positive control Thread RNAi, which led to cell death in all experiments with each cell line, it appears that this variability was not due to differences in the efficacy of RNAi. Instead, the differences appear to be due to variation in the ease of identifying defects in cell morphology in each case. Thus, all the hits identified in the BG3-c1 cell line, which is prone to grow in clumps, were identified in at least one of the more easily visualised CNS lines (see Figure 3-3).

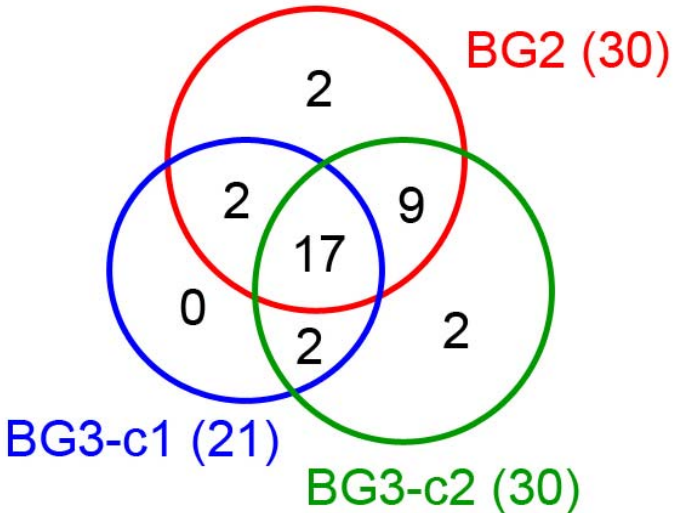

Figure 3-3 Venn diagrams depict the segregation of screen hits between CNS original cell lines

Similarly, only one gene was identified that yielded a phenotype in S2 or Kc167 cells but did not also show up as a hit in the larger, more well-spread S2R+ cell line (Figure 3-4).

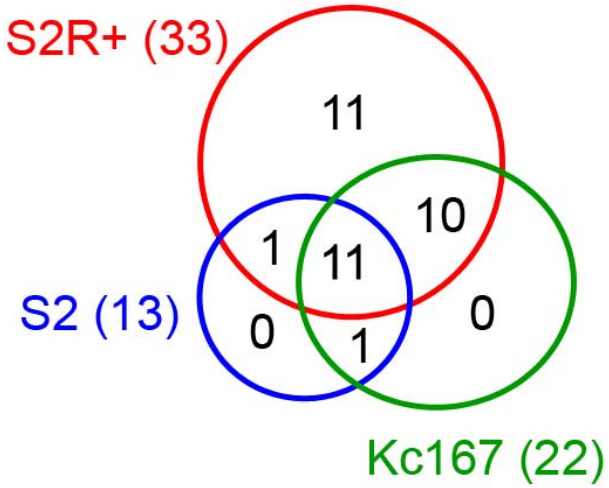

Figure 3-4 Venn diagrams depicting the segregation of screen hits between CNS original cell lines

In contrast, there were significant differences in the kinase requirements of haemocyte and CNS-derived lines (Figure 3-5) that correlate well with the differences in the form and gene expression profiles that separate these two sets of lines (see Figure 3-1).

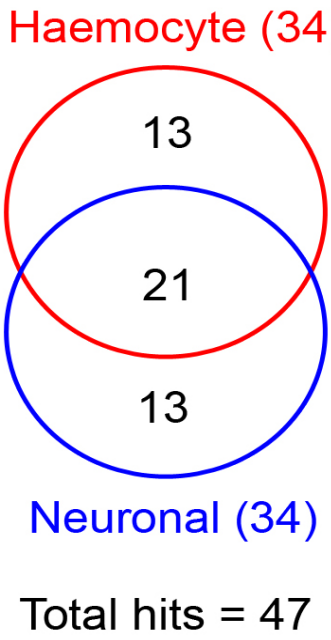

Figure 3-5 A Venn diagram depicting the classification of hits into three distinct classes: those which are hits in both CNS and haemocyte cell lines, those which are hits in neuronal cell lines only and those which are hits in haemocyte cell lines only.

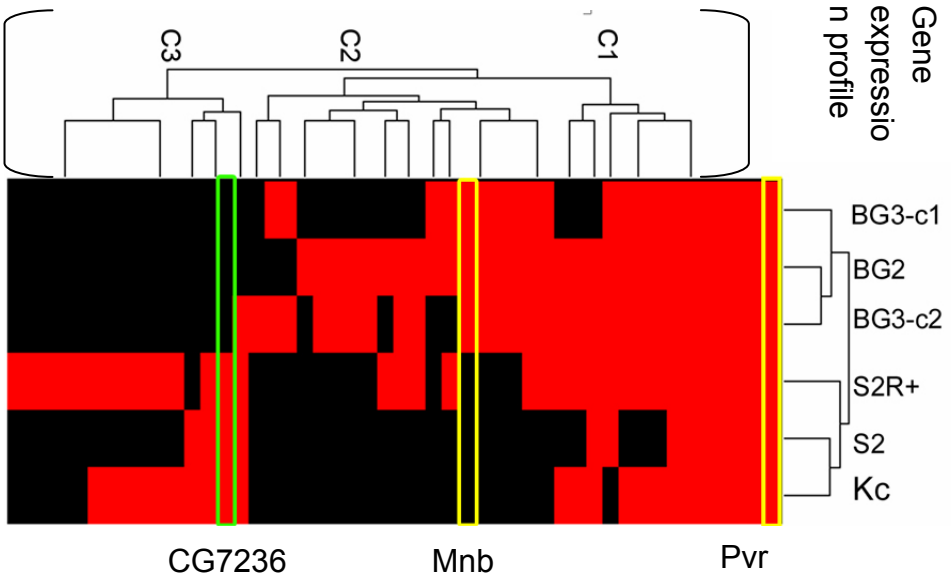

Figure 3-6 Hierarchical clustering of hits across cell lines (depicted in the form of a tree) was used to give a more detailed picture of the three hit classes. Two hits of particular interest; CG7236, Mnb and Pvr are highlighted. Note that the relationships defined by the functional analysis mirror the relationships defined by the microarray analysis

This indicates that both gene expression and function can be used as indicators of a common origin. It was then possible to identify a set of 'cell

type specific' hits and a group of uniform hit across all cell types (Figure 3-6). However, there was no detectable bias in the number of hits in each kinase class between the two different tissues of origin (Table 3-1).

	Total	Neuronal	%	Haemocyte	%
Serine/threonine kinase	146	21	14.4%	22	15.1%
Tyrosine kinase	49	5	10.2%	6	12.2%
Protein kinase	26	3	11.5%	2	7.7%
Lipid kinase	23	3	13.0%	2	8.7%
Guanylate kinase	7	0	0.0%	1	14.3%
Protein kinase-like	5	0	0.0%	0	0.0%
Others	5	2	40.0%	1	20.0%

Table 3-1 Breakdown of RNAi screen hits according to kinase families

As shown in Figure 3-7, a pie chart summarizes the gene expression profiles (present or absent) of genes showing phenotypes in any cell line. The vast majority of genes with expression data available is either present in all cell lines tested, or absent from all. This suggests that cell type specific phenotypes do not arise simply from expression of different subsets of signaling components.

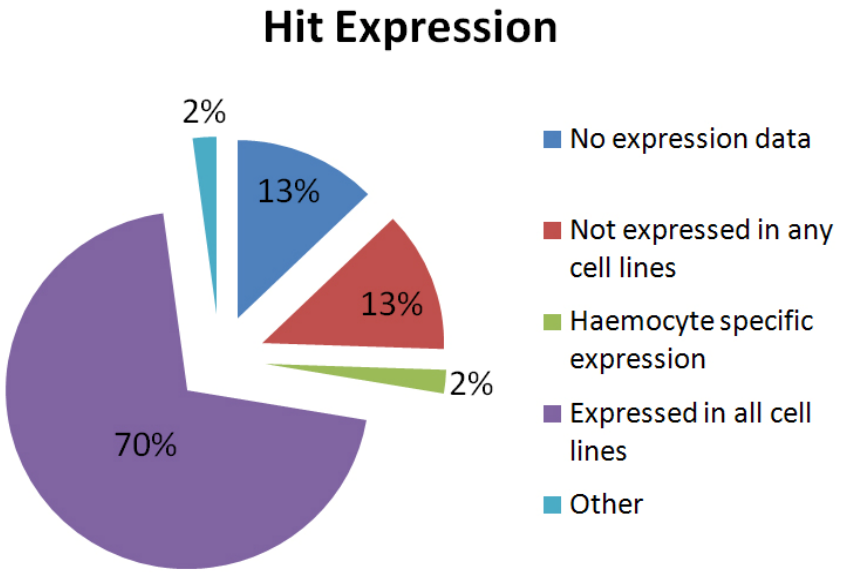

Figure 3-7 Summary of the gene expression of all genes with phenotypes across all cell lines

Using phenotypic clustering to identify genes affecting cell morphology across all six cell lines allows us to identify three strong kinase clusters (Figure 3-6). The first cluster (C1) contains genes which have a strong phenotype in almost all cell lines tested. This cluster appears to be enriched in genes which participate in basic cell biological processes such as cell cycle control (e.g. cdc2, polo and ial). The second cluster (C2) contains genes that are hits in cell lines of haemocyte origin. The final cluster (C3) contains genes which are hits only in CNS-derived cell lines. In the subsequent analysis, I focused on genes with functions specific to one tissue type of origin

3.4 False positive analysis using multiple oligos

Although Dicer-mediated processing of long dsRNAs to generate a

diverse population of siRNAs inside *Drosophila* cells is thought to reduce the probability of off-target effects [87], false positives are always an important issue in high-throughput RNAi screening [112]. In this study, I systematically analysed the false positive rate using multiple oligos. As shown in Figure 3-8, I used a set of genes covered by both library A and B which has different oligos targeted to different part of the genes to do the analysis in 2 cell lines S2R+ and BG2.

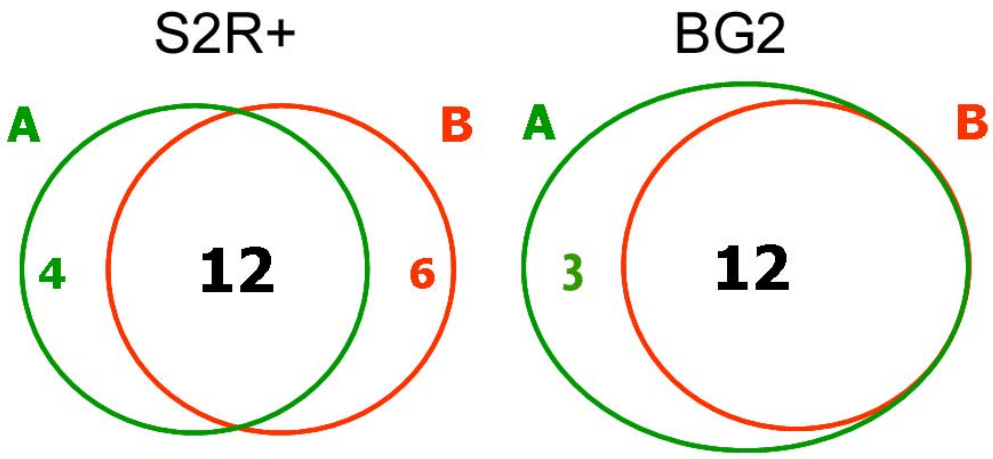

	A	B	C	
Gene 1	✓	✓	✓	True positive
Gene 2	✓	×	×	False positive
			✓	True positive
Gene 3	×	×	×	True negative

Figure 3-8 Using multiple oligos to avoid false positives and estimate the false positives rate
Third oligos have been used for genes which show different results in both libraries A and B in S2R+ and BG2 cell lines

A gene should only be considered a positive if it has been identified as a

hit in two independent experiments using dsRNAs targetting different regions of the same mRNA. Therefore, for those genes that were a hit with only one of the two RNAi libraries (A or B), I designed a 3rd pair of oligos. The idea was to use this 3rd pair of oligos to confirm which of these were true hits. In this way, I hoped to find out whether these represent false positives or false negatives and to estimate the false positive rate. The results from three RNAi experiments are shown in additional file 6. For S2R+ cells, 2 false positives were identified from a total of 16 hits from library A, and two out of 18 hits as false positives in library B. For the BG2 cell line, 1 false positive was identified from a total of 15 hits from both libraries. Based on these data I estimate the false positive rate in our experiment as between 6.7-12.5%.

3.5 Parallel RNAi Screens Reveal Cell-type Specific Phenotypes-CG7236 Displays a Haemocyte-specific Phenotype

The C2 cluster contains genes that were only identified as hits in haemocyte cell lines. One such gene is a Cyclin-dependent kinase (CDK) called CG7236 [113]. CDKs are known to regulate cell cycle dependent changes in cell organisation together with a host of other processes, such as RNA Polymerase II activity [114]. In haemocyte cell lines RNAi-mediated silencing of CG7236 led to the accumulation of large cells with

multiple or enlarged nuclei (Figure 3-9). I quantified the number of multinuclear cells in CG7236 RNAi treated S2R+ cell to confirm that this result is statistically significant.

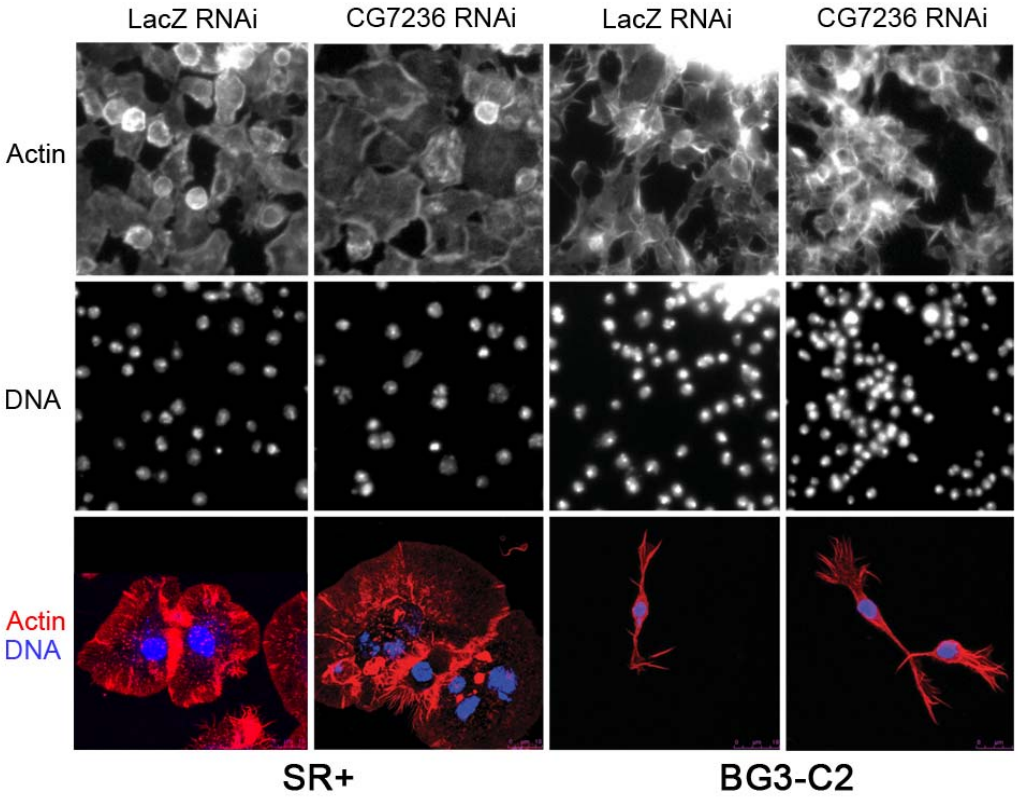

Figure 3-9 CG7236 loss of function shows cell line specific phenotypes Silencing of the Cdc2-related kinase *CG7236* in S2R+ cells gives rise to large cells that frequently contain multiple nuclei or a single large nucleus, whereas silencing in BG3-c2 cells has no discernable phenotype. Note: bottom panel shows confocal images of RNAi treated S2R+ cells and BG3-C2 cells.

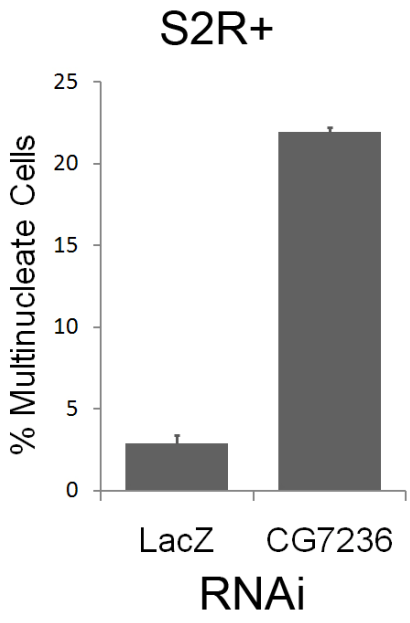

Figure 3-10 Quantification of the CG7236 loss of function phenotype in SR+ cells indicates that the percentage of multinucleate cells in CG7236 RNAi treated cells is much higher than it is in the control.

The phenotype was verified using independent dsRNAs and confocal imaging (Figure 3-9, bottom panels), and suggests a role for CG7236 in the regulation of the cell division cycle. However, silencing of CG7236 caused no detectable change in the appearance of neuronal cell lines such as BG3-c2 (Figure 3-9), even though a Q-PCR analysis revealed that CG7236 is both expressed and effectively silenced by RNAi in both S2R+ and BG3-c2 cells (Figure 3-11).

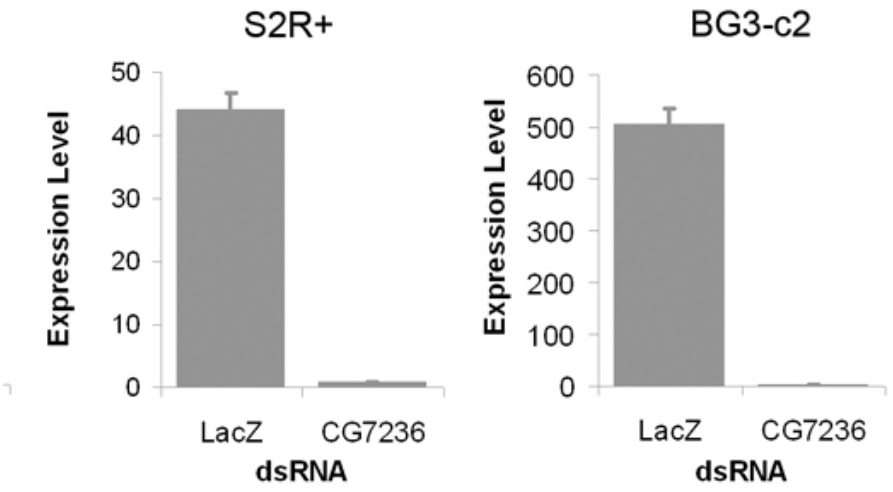

Figure 3-11 Q-PCR analysis revealed that CG7236 is both expressed and effectively silenced by RNAI treatment in both S2R+ and BG3-C2 cells

CG7236 has not been studied in detail before, but was previously identified as a cell cycle kinase in an RNAi screen in S2 cell [115], and as having a cytokinesis defect in RNAi screens in *Drosophila* haemocyte cell line [116, 117]. By analysing its function across cell-types, our analysis suggests that CG7236 differs from many other kinases involved in cell

cycle control in performing a cell type-specific function. Using a Q-PCR analysis revealed that CG7236 was expressed and effectively silenced by RNAi in both S2R+ and BG3-c2 cells.

3.6 Genes with Cell-type Specific Phenotypes are not Differentially Expressed

In order to test whether these phenotypic differences reflect differences in gene expression between different cell lineages I used the gene expression data available in our lab (it is open access in FLIGHT website. http://flight.licr.org/search/expression) to determine whether the differences in gene expression correlate with differences in function, as ascertained using RNAi across the kinome (see Figure 3-12).

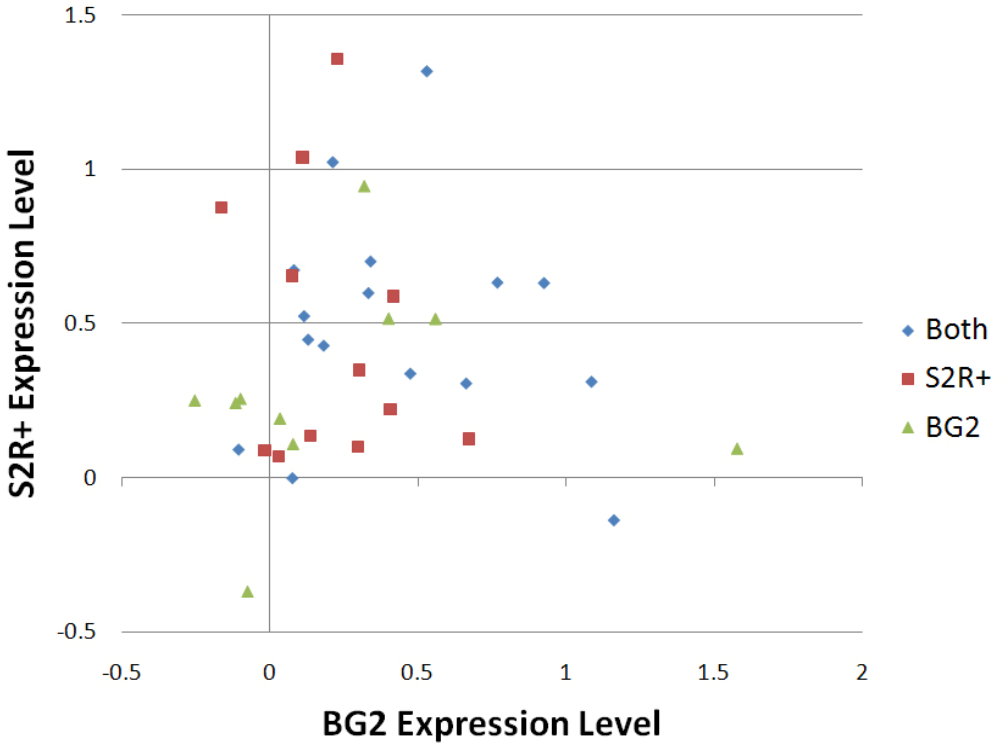

Figure 3-12 Comparison of microarray gene expression levels of genes displaying phenotypes in S2R+ and BG3-c2 cells
Chart of the gene expression levels determined in the microarray analysis for genes showing phenotypes in both S2R+ and BG3-c2 cells compared to those with phenotypes in BG3-c2 or S2R+ cells. There is no strong pattern of gene expression associated with genes with cell-type specific phenotypes.

I was unable to identify a correlation between gene function and expression. However, given the potential problems with a global microarray analysis, I followed this up using Q-PCR to establish whether the relative levels CG7236 expression in S2R+ and BG3-c2 cells correlate with their cell type specific functions. Pvr, a gene that displayed similar strong phenotypes in all cell types screened (see Figure 3-6) was used as a control for this analysis.

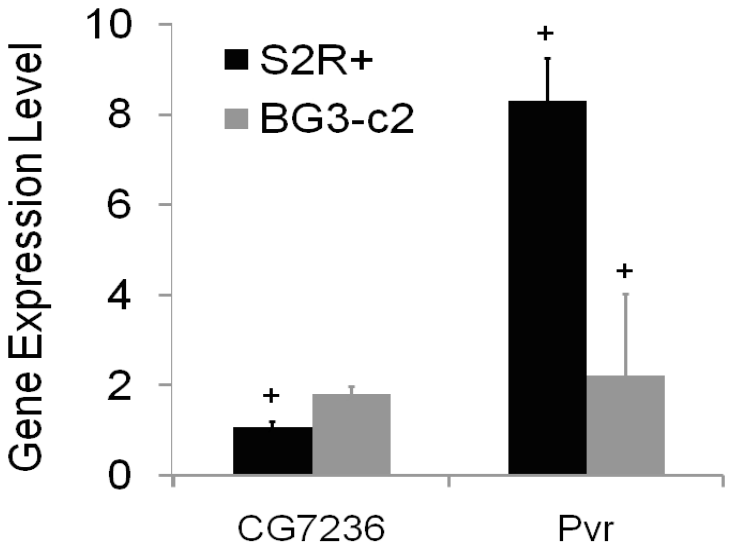

Figure 3-13 Genes with cell line specific phenotypes are not differentially expressed

The result shows no clear correlations between expression at the mRNA level and function (Figure 3-13). Thus, CG7236 mRNA levels are similar in BG3-C2 cells and in S2R+ cells, despite its only having a phenotype in the S2R+ cells (Figure 3-13). Furthermore, Pvr, which displayed strong phenotypes in both S2R+ and BG3-c2 cells, was expressed at very different levels in the different cell lines. These data suggest that there is little relationship between gene expression level and function – at least for kinases.

3.7 Conclusions

In this chapter presents the results from parallel RNAi screens across multiple *Drosophila* cell lines. It is not surprising to see that cells derived from the same tissue appear similar in their morphology and gene

expression patterns by comparison of my screening data and gene expression data available in our lab. However, more interestingly my results prove that different type cells have their own cell type specific gene functions. This means the screening result from one cell line can not be extrapolated to all the other cell types and other systems. Importantly, I estimated the false positive rate in my high-throughput RNAi as between 6.7-12.5%. This result suggests that false positives are likely to be a problem in high-throughput RNAi screens in fly cells. It may therefore be better to minimize the false positive rate by using multiple non-overlapping dsRNA libraries for screens.

Chapter 4

Identification of Minibrain/DYRK1A as a cell-type specific regulator of actin organization

4.1 Introduction- Drosophila Mnb and its human orthologue DRYK1A

In this parallel RNAi screening analysis, I identified a set of kinases which have functional phenotypes in neuronal cells but not in haemocytes as C3 cluster (see Figure3-6). One of these cell type specific kinases is *minibrain* (*mnb*). It belongs to the Serine/Threonine kinase subgroup [118]. Mnb was firstly identified by Tejedor et al in 1995 as a regulator of postembryonic neurogenesis in *Drosophila,* since *mnb* mutant adult flies exhibit a specific and marked size reduction of the optic lobes and central brain hemispheres[119]. More recently, DYRK1A, a human orthologue of *mnb*, was mapped within the Down's Syndrome (DS) critical region of chromosome 21 and found to be over-expressed in DS embryonic brains [120]. An analysis of the distribution of DYRK1A in primary cell culture showed the presence of this protein in the nucleus and the cytoplasm of both neurons and astrocytes [121]. Moreover, studies on the biochemical function of DYRK1A show that Mnb/DYRK1A can phospohorylate Dynamin1 to alter its interactions with several SH3 domain-containing endocytic accessory proteins [118], which hints at a function for *mnb* in the regulation of the actin cortex. Recent published data identified Bmh1/2p, the yeast homologue of protein 14-3-3, as a regulator of Yak1p the *S. cereviaise* orthologue of DYRK1A [122]. The data in human cells show

that a small peptide inhibiting 14-3-3 binding, sc138, decreased DYRK1A kinase activity, implicating 14-3-3 in the regulation of DYRK1A activity [123, 124]. However, so far, there is no report about Mnb's function in the regulation of cell morphology.

4.2 Mnb has a specific role in the regulation of neuronal cell morphology and modulates Actin-based Protrusions in CNS-derived Cell Lines

I identified Minibrain (Mnb) as a kinase that has strong morphological RNAi phenotypes in all neuronal cell lines tested, without eliciting a visible RNAi phenotype in haemocyte cell lines. As before, the specificity of the RNAi phenotype was confirmed using two sequence independent dsRNAs in BG3-c2 cells to minimise the chances of sequence-specific off-target effects [88]. In all neuronal cell lines tested, Mnb RNAi treated cells had a spiky cell shape caused by the formation of extra actin based protrusions (phenotypes shown as Figure 4-2). The Mnb loss function phenotype was similar across all the 3 neuronal cell lines tested, leading to a significant >2-fold increase in the number of long finger-like protrusions around the cell body (Figure 4-3), an increase in cortical F-actin levels (see Figure 4-2), and reduced cell numbers (see Figure 4-1). Cell number of each condition was quantified using a Beckman Z2 Coulter Counter (see materials and methods 2.11). By contrast, S2R+ cells had no detectable

phenotype and kept their flat cell shape and smooth edges. Interestingly, RNAi mediated silencing of *Drosophila* Smi35A (the closest human homologue of this gene is DYRK4) a close homologue of Mnb (there are only 2 isoforms in *Drosophila*) had no visible actin phenotype, while a knock-down of Smi35A enhanced the Mnb finger-like actin protrusion phenotype by 30% compared to a LacZ dsRNA control. This may suggest thatthese two isoforms have functional redundancy in *Drosophila*. DYRK4 has been reported to function as a testis-specific kinase with a very restricted expression to stage VIII postmeiotic spermatids in mice [125].

The reduction in cell number following *mnb* silencing in CNS-cell lines could be due to the activation of apoptosis rather than inhibition of cell proliferation, as a recent study demonstrated that Mnb/DYRK1A phosphorylates caspase-9 on threonine residue 125, a phosphorylation event that is crucial for protecting cells from apoptotic cell death [126].

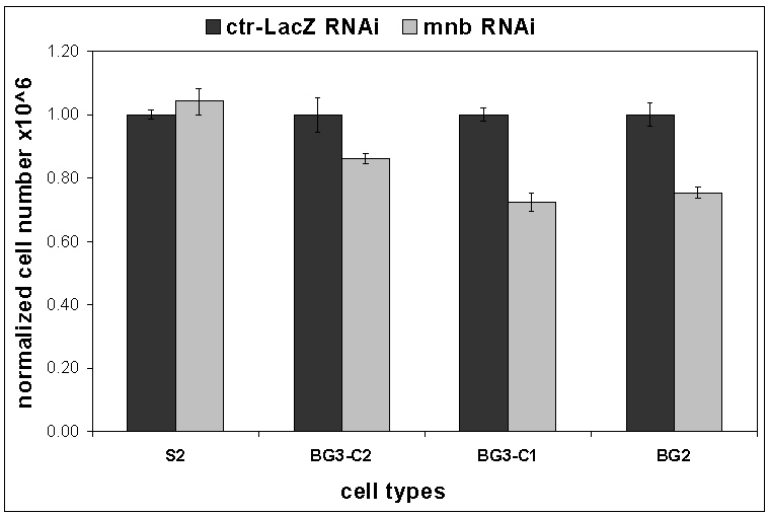

Figure 4-1 Mnb silencing cells reduce their cell number

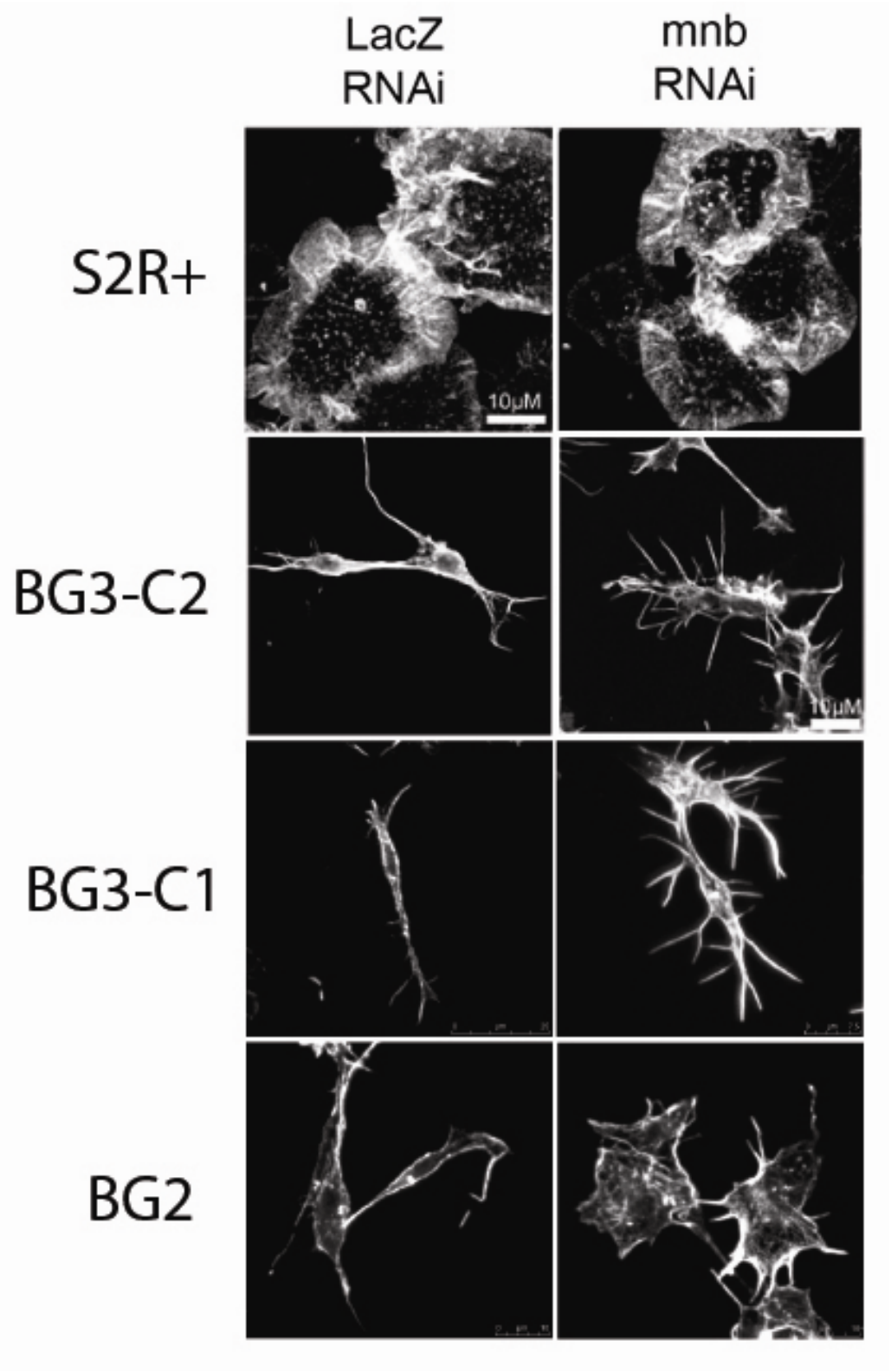

Figure 4-2 Mnb has cell type specific phenotype only in neuronal cell lines (serum coated substrate)

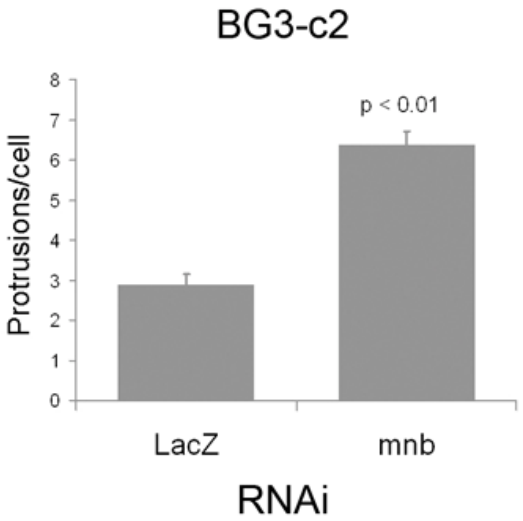

Figure 4-3 Quantification of filopodia around bipolar cell body shows significant incense in Mnb-silenced cells

Significantly, filopodia are absent from the blood cell lines, but are seen in all CNS-derived *Drosophila* cell lines tested [127]. Moreover, these actin structures are superficially similar to actin-based protrusive structures seen embedded in the growth cones of migrating neurons [128, 129], where such finger-like processes are thought to sense local cues to guide the migrating neuron to its target [130], whilst the large mesh-like lamellipodium in which they are embedded generates the forces required to drive the growth cone or cell forwards [131-133]. Given this role for *mnb* in shaping actin-based protrusions, I considered two explanations for its neuronal-specific RNAi phenotype. First, it is possible that the dsRNA failed to silence the *mnb* expression in haemocyte cell lines or that *mnb* is not expressed in haemocyte-derived cells. However, a Q-PCR analysis

revealed that Mnb effectively silenced by RNAi in both S2R+ and BG3-c2 cells (see Figure 4-4 a) and that *mnb* was expressed in both cell lines (see Figure 4-4 b), ruling out this explanation.

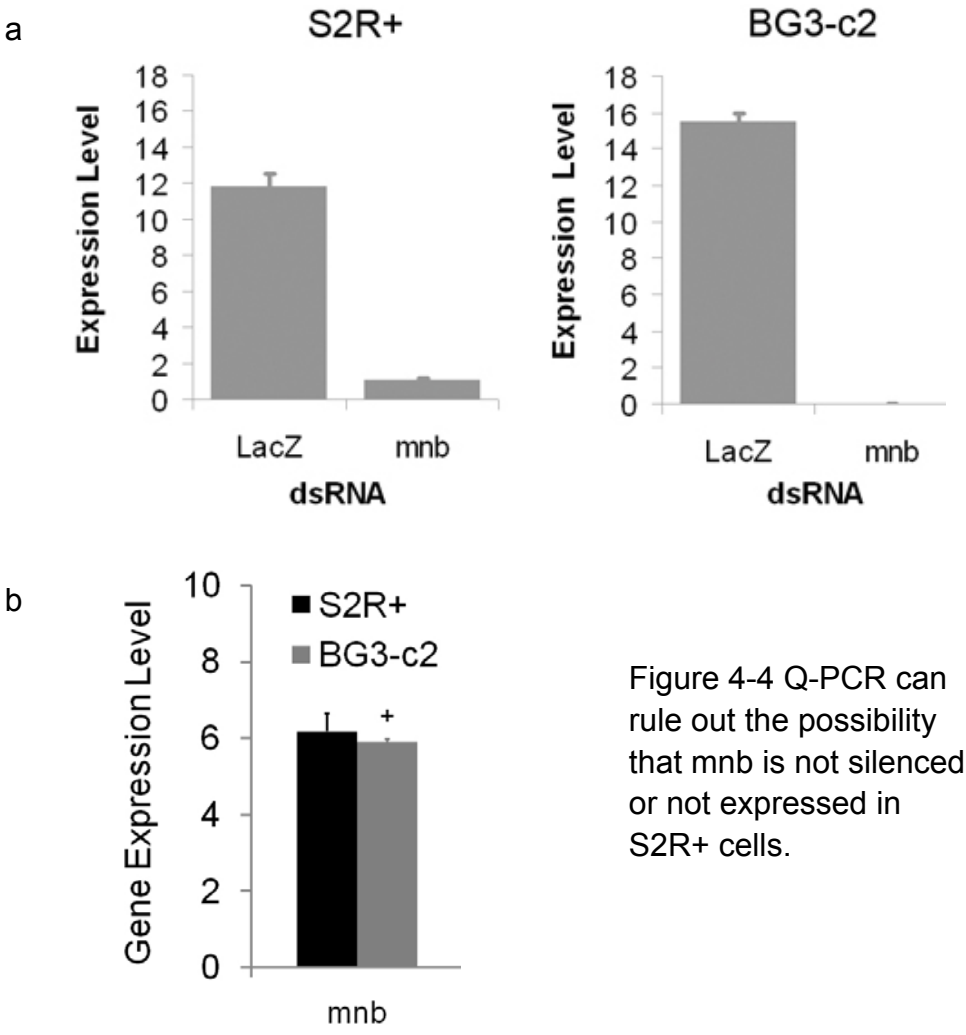

Figure 4-4 Q-PCR can rule out the possibility that mnb is not silenced or not expressed in S2R+ cells.

Second, I considered the possibility that the ability to visualise a morphological phenotype associated with the loss of *mnb* was dependent on the shape of the cells used in the analysis. To test whether this, I forced BG3-c2 cells to spread on a Conconavalin A coated substrate (see Figure 4-5).

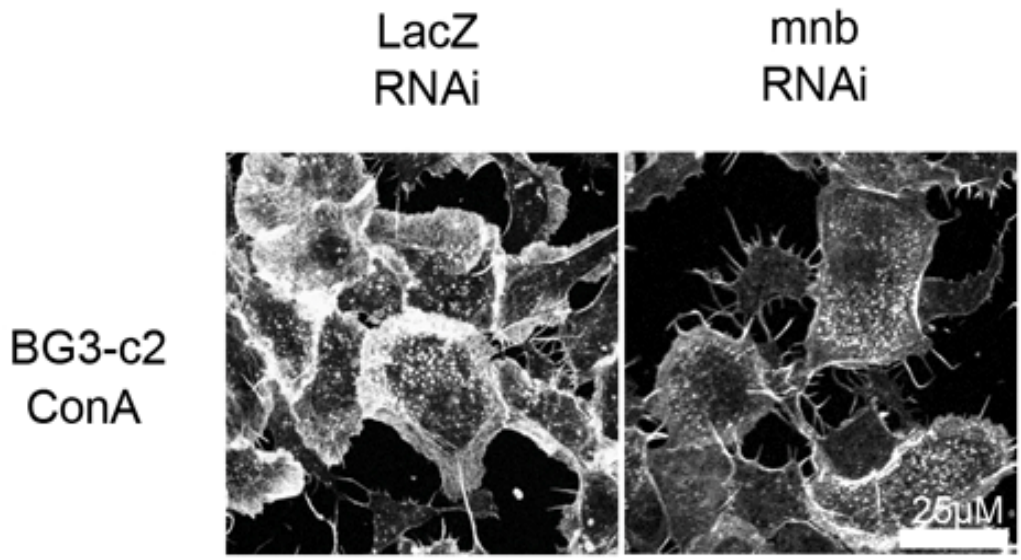

Figure 4-5 Forcing BG3-C2 cell spread on ConA substrate to form broad lamellipodia can not inhibit *mnb* depletion phenotype.

Although this led to the formation of broad lamellipodia in control (lacZ RNAi treated) BG3-c2 cells, it was unable to suppress the induction of ectopic filopodia induced by Mnb depletion. Thus, I cannot attribute the failure of *mnb* dsRNA to elicit an RNAi phenotype in Kc, S2 and S2R+ cells to differences in their form. Instead, these results suggest that *mnb* specifically acts to inhibit the transition between filopodia and lamellipodia in CNS-derived cells. Since *mnb* plays a conserved role in neurogenesis, and has a strong cell morphological RNAi phenotype in CNS-derived cell lines, it seems likely that its represents a cell type specific regulator of cell morphology and behaviour.

BG3-c2 cells originate from neuronal tissue [103], are migratory (Wei-Bai, Baum and Ridley, unpublished), and have a polarised shape characterised by long actin-rich protrusions embedded in lamellipodia and filopodia [84].

The first step for a cell to migrate is to re-organise its actin filaments and generate a leading edge in response to extracellular or cellular signals [16]. Actin assembly drives the extension of flat membrane protrusions-lamellipodia and finger-like protrusions-filopodia. Thus, using BG3-C2 cells in culture enables us to study the role that *mnb* plays in the dynamic regulation of actin based finger-like protrusions. I found that by silencing *mnb* in BG3-C2 cells not only can many finger-like protrusions be generated in a short time scale but also that they are very dynamic structures as shown in the Figure 4-6. The kymograph shows that the cell edge in Mnb RNAi cells is much more dynamic than that of control cells. In addition, BG3-C2 cells lose their big lamellipodia at a time when they generate more finger-like protrusions, implying that Mnb may induce a switch in actin structure. It has been reported that the function of N-WASP in cell migration is restricted to filopodia formation in response to Cdc42 [134], whereas WAVE/Scar is responsible for lamellipodium protrusion in response to Rac1 [10]. It remains to be tested whether Mnb acts by promoting the formation of lamellipodial actin or by inhibiting filopodial actin formation, e.g. via Cdc42-WASP-Arp2/3 or Formins.

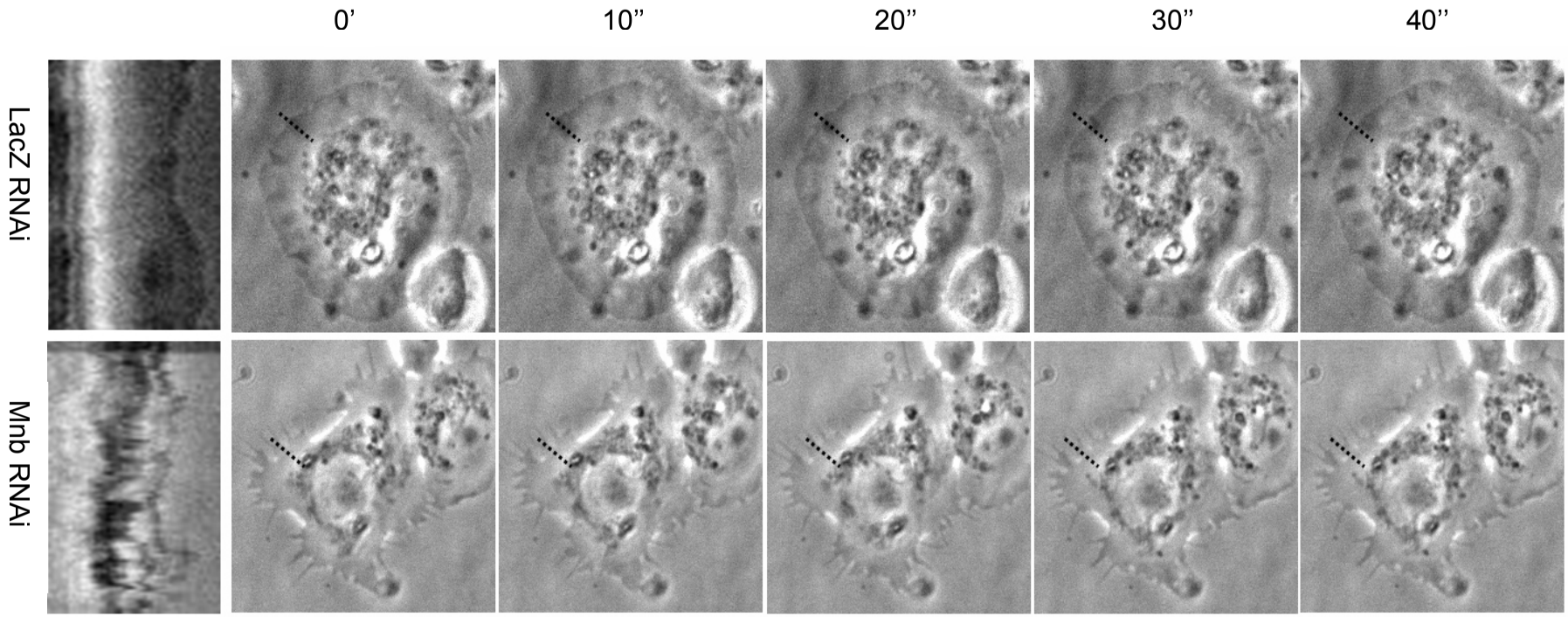

Figure 4-6 Mnb silenced BG3-C2 cell showing high dynamic finger-like protrusions in live cell imaging. (Note: the kymograph was generated based on the movie which is 2 second per frame, and cells were plated on 50 μg/ml ConA for 20 min before the start of the movie.)

4.3 Conclusions

In this chapter, I characterized the function of a second cell type specific kinase (in addition to CG7236). Mnb RNAi only induces strong actin-based cell morphological phenotypes in CNS-derived cells. Importantly, I showed that the differences between the effects of Mnb RNAi on S2R+ and BG3-c2 cells are not due to different gene expression levels in these 2 cell types by measuring mRNA levels. This result strengthens the idea that it is important to use different cell types to gain a thorough understanding of gene function across the genome, and the difficulties of using gene expression to predict gene function. Although I didn't have the chance to follow up the work on Mnb to explore whether Mnb is directly involved in the regulation of actin dynamics , my analysis gives a clue that helps to explain the findings in Mnb null mutant flies which lead to viable, externally normal animals that display strong behavioural defects and a reduction in brain mass [119].

Chapter 5 Results:

The Identification of the Tao-1 Kinase as a Key Regulator of Microtubule Dynamics

5.1 Introduction

The Tao-1 kinase was first identified as a MAPKK isolated from a rat cDNA library in 1998 [135]. Since then, several different functions have been attributed to this STE20 kinase family member in different species: in the regulation of the cytoskeleton, apoptosis, in c-Jun N-terminal kinase, p38 mitogen-activated pathway and spindle-checkpoint signaling [96, 136-141]. The kinase derives its name from its Thousand-And-One amino acids in rat and is highly conserved across animals. Its *C. elegans* homologue named KIN-18 has been reported to be able to reduce worm feeding, which results in slow growing and fewer eggs laying in an expressing active form [142]. In *S. cerevisiae*, USO1 could be considered a Tao-1 homologue, but has only 56% similarity with *Drosophila* Tao-1. It is been thought to function as a vesicle docking protein [143]. *Drosophila* Tao-1 has 90% amino acid sequence similarity with its human homologues, PSK1 and PSK2, which were identified as MAPKKs in human prostatic carcinoma cells [96]. The earliest report of the Tao-1 kinase being functionally related to the cytoskeleton comes from Jonathan Morris's lab [96]. They cloned PSK from a T-47D breast carcinoma cell line using reverse transcription [96]. The p21-activated protein kinases (PAKs) subgroup of the STE20 kinases have long been thought to regulate the cytoskeleton, while the germinal center kinases (GCK) subgroup of the

STE20 kinase family activate the mitogen-activated protein kinase (MAPK) pathway. The Morris lab identified PSK as the first member of the STE20 family lacking a Cdc42/Rac binding domain that could regulate both the c-Jun N-terminal kinase mitogen-activated protein kinase pathway and the cytoskeleton. Three years later, they showed that there are two Tao-1 homologues in humans, which are called PSK1 and PSK2. Following on from this report, they showed that PSK1 alters actin cytoskeletal organisation and binds to and stabilizes microtubules; PSK2 which lacks a microtubule-binding site, activates c-Jun N-terminal kinase (JNK), and induces apoptotic morphological changes that include cell contraction, membrane blebbing, and apoptotic body formation in human Swiss 3T3 cells [137]. By contrast, Mandelkow's lab later reported an analysis of the Tao-1 kinase in human CHO cells when they searched for upstream regulators of Par-1/MARK. They showed that MARKK/Tao-1 destabilizes microtubules via the activation of MARK/Par-1, which hyper-phosphorylates the Tau protein, causing it to detach from microtubules to reduce microtubules stability [144, 145]. Furthermore, this group identified 2 novel proteins, Spred1 and Tesk1, as interaction partners for TAO kinase, which they propose modulate the cross-talk between actin and microtubules [146]. In a functional genomic screen study in Hela cells performed by Stephen J. Elledge's lab, Tao-1 was identified as a regulator of spindle-checkpoint signaling via the interaction with the checkpoint

kinase BubR1 which promotes activation of the checkpoint protein Mad2 [139]. Thus far, most of the published work on Tao-1 kinase has been done in human cells in culture and with biochemistry. Moreover, taken together these papers paint a confused picture of Tao-1's function and mechanism of action. Therefore when I identified Tao-1 as an important cytoskeletal regulator in parallel RNAi screens in fly cell lines, I decided to explore its cellular and molecular function in detail.

5.2 RNAi screens across multiple cell lines identify Tao-1 as a regulator of microtubule organisation

One of the main goals of my RNAi screen work was to identify novel cytoskeletal regulators. Studying gene function using *Drosophila* cells can simplify the research work because there is less genetic redundancy in the fly genome compared to the human genome, even though many genes are functionally conserved between humans and flies. In my parallel screening work, I identified a set of kinases which have morphological phenotypes across all cell lines tested (clustered in C1 group in Figure 3-6). Tao-1 kinase is one of the strongest hits in this group. Tao-1 RNAi cells show strong morphological phenotypes which include a spiky cell shape, bundled microtubule filaments and a disorganized microtubule network (see Figure 5-1 and Figure 5-2). Similar Tao-1 RNAi phenotypes were seen in S2R+, BG3-C2 and Dm16 cell lines, which derive respectively

from haemacytes, CNS tissue, and from the *Drosophila* wing disc.

This implicates a role for Tao-1 as a core regulator of cell shape across different cell types, making research on the *tao-1* gene significant. The latest release of Flybase predicts the existence of 4 annotated transcriptions based on mRNA sequencing data, PA, PB, PD and PE (PA and PB encode same polypeptide and are shorter at 2.08kb in length; PB and PD encode the same peptide but are longer at 4kb in length). PA and PB don't encode a kinase domain, whereas PD and PE encode a 1039 amio acid mutipeptide that contains the conserved serine/threonine kinase domain which was identified in the human protein. My analysis is based on the long PD and PE transcripts.

During the course of my RNAi analysis I used two sets of primer pairs to target different regions of the Tao-1 PD and PE transcripts (one pair target the N-terminal kinase domain and the other target the C-terminus) in order to confirm that the phenotype identified in the screens was not the result of an off-target-effect (primer sequence information can be found in the additional file 4). Both dsRNAs showed the same phenotype. Based on this analysis, the phenotypes seen in Tao-1 RNAi cells are likely to be real and caused by the loss-function of the PD and PE Tao-1 mRNA.

To confirm the Tao-1 knockdown in each cell line, I had custom antibodies made for this purpose by Eurogentec. A rat monoclonal peptide antibody

was generated against the C-terminal part of *Drosophila* Tao-1 : 967-981: C+FNQERAERLRMKHEK-CONH2[144] and a rabbit multipeptide antibody was generated to recognize the phosphorylated form of the highly conserved T-loop phosphorylation site CONH2-RAQRATS[P]NVFAMC+3 [96]. For unknown reasons, the C-terminal anti-Tao-1 antibody didn't work in Western blots although it worked in immunoflourescent staining. Nevertheless, the P-Tao-1 antibody worked for both western blotting and immunoflourescent staining. The Morris lab [141] used our P-Tao-1 antibody to show that it also recognises human PSK1/2.

I then used P-Tao-1 to test the extent to which Tao-1 protein was knocked down following RNAi. In extracts from control cells, the P-Tao-1 antibody identifies a protein of 120KD which probably corresponds to PD and PE (see Figure 5-1 b). For this analysis I used a P-Moesin antibody as a loading control, since I suspected that Tao-1 RNAi might affect α-Tubulin or actin levels. I checked the protein bands with Ponceau after the gel transformation and they correspond in levels to the bands revealed by P-Moesin. I decided to use a cocktail of phosphatase inhibitors (I+II) to inhibit the dephosphorylation during the lysis of RNAi treated cells, as phosphorylated Tao-1 is likely to be unstable in the cell extracts. Analysed in this way, quantification of the western blot gel picture shows that the

RNAi treatment reduced the levels of endogenesis Tao-1 by ~75-80% (see Figure 5-1 c).

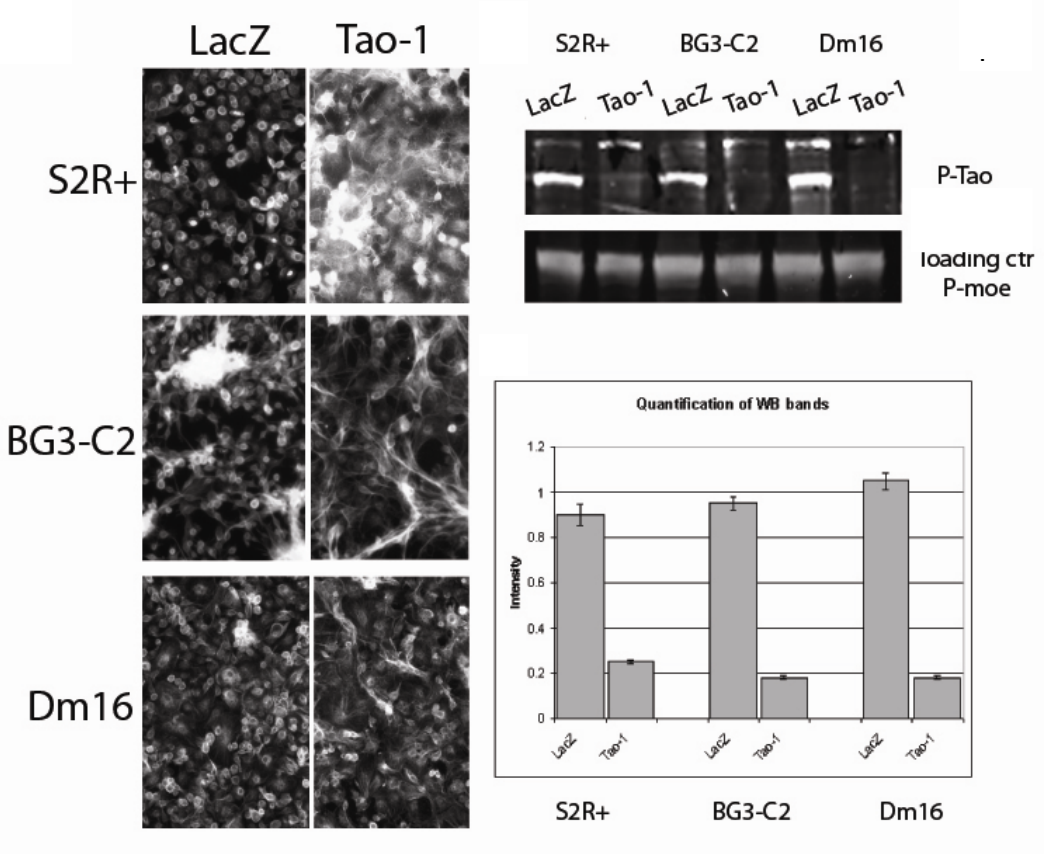

Figure 5-1 Parallel screening in 3 different cell lines demonstrates Tao-1 has strong microtubule phenotypes. a. Images from automated screen for S2R+, BG3-C2 and Dm16 cell lines demonstrate that Tao-1 silenced cells have strong microtubule phenotypes (cell stained with Dm1α (sigma) antibody 1:500). b. Westernblot with P-Tao-1 antibody staining confirms the efficiency of Tao-1 silencing. c. Quantification of Westernblot bands using P-Moe as loading control.

To know more details of the Tao-1 RNAi phenotypes, confocal images were also obtained. This revealed that microtubules accumulate in bundles in spiky Tao-1 RNAi cells and become very straight. Moreover, the microtubule network loses its normal organization in Tao-1 RNAi cells (as

shown in Figure 5-2 a). Quantification of levels of protein knock-down (see Figure 5-2 b), show that the Tao RNAi worked very well. Based on all above, these data suggest that Tao-1 kinase plays an important role in the regulation of microtubule organization. However, it is still not clear how Tao-1 functions as a microtubule regulator.

a

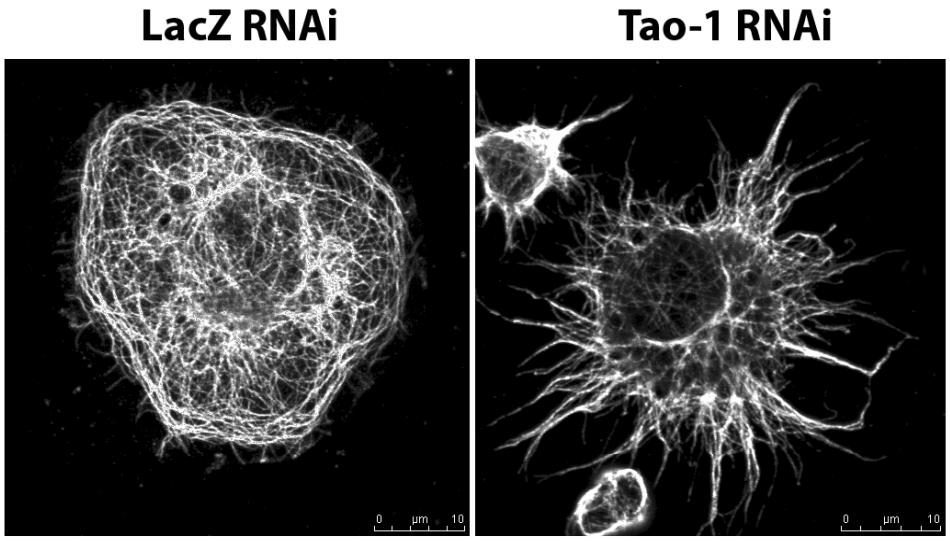

b

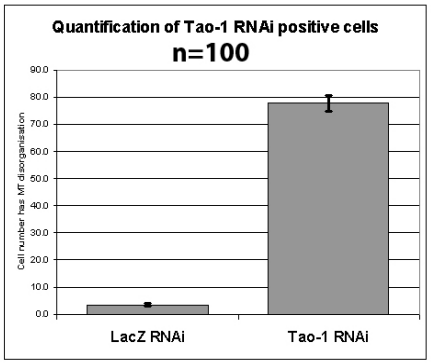

Figure 5-2 Tao-1 RNAi phenotype in S2R+
a. Confocal images of Tao-1 RNAi treated S2R+ cell demonstrate MT phenotypes (1:500 Dm1α antibody stain used to visualise MTs); b. Quantification of Tao-1 RNAi positive cells shows about 78% cells has these phenotypes. Three independent replicates were used to generate the error bar.

5.3 Tao-1 regulates cell morphology by destabilizing microtubules

The fact that Tao-1 RNAi generates microtubule bundles, suggests that

Tao-1 may function as a microtubule destabilizer. As a further study of this hypothesis, I decided to test the effects of Tao-1 overexpression in *Drosophila* cell lines. Using *Drosophila* gateway cloning system, I generated a GFP/RFP tagged full length Tao-1 which has the fusion protein at its N-terminus (see methods and materials). The reason I chose to fuse GFP/RFP at its N-terminus was to avoid perturbing its microtubule binding activity, which has been reported to reside in its coiled coil C-terminal domain [137]. As expected, in contrast to the Tao-1 loss-of-function phenotype, Tao-1 over-expression resulted in the loss of microtubules. Interestingly, in Tao-1 over-expressing cells microtubules filaments fail to reach to the cell edge of interphase S2R+ cells (see Figure 5-3 top panel). Similarly, in GFP-Tubulin-S2 cells, overexpression of RFP-Tao-1 clearly limits microtubules to the perinuclear region and reduces the microtubule network (as shown in Figure 5-3 bottom panel). 27 out of 30 transfected S2R+ cells quantified displayed this phenotype. The remaining 3 cells in my quantification which had a normal microtubule distribution, might have expressed lower levels of GFP-Tao-1. Unfortunately, I could not find many cells in mitosis with GFP-Tao-1 overexpressed to confirm the effect of overexpression of Tao-1 on the mitotic spindle probably due to the low mitotic index combined with moderate transfection efficiency. Nevertheless, so far, I know that in interphase Tao-1 RNAi appears to increases the microtubule filaments

while overexpression of Tao-1 can destroy the microtubule network. These data suggest that Tao-1 could function to destabilize microtubules in interphase *Drosophila* cell lines.

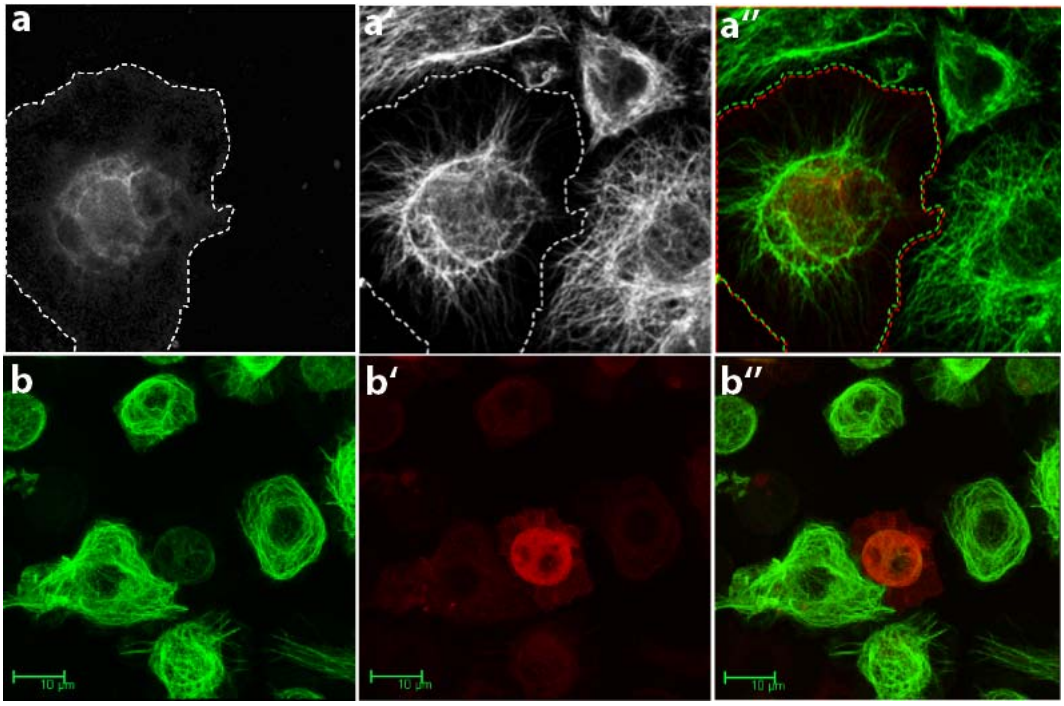

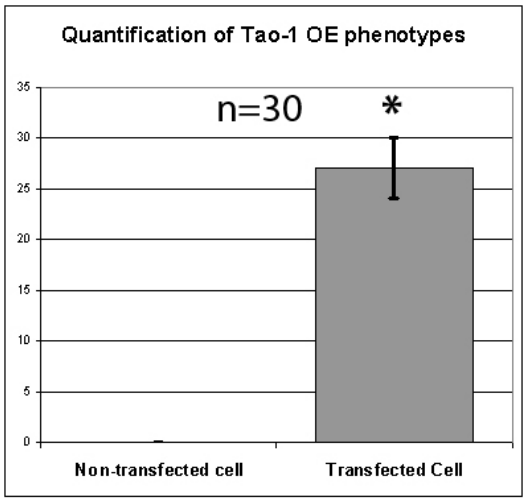

Figure 5-3 Overexpression(OE) of Tao-1 causes MT network disassembly in both S2R+ and S2 cells.
(The Y-axis represents the number of cells and the error bar is calculated from 3 times quantification replicates.)
Top panel demonstrates GFP-Tao-1 OE phenotypes in S2R+; bottom panel demonstrates RFP-Tao-1 OE phenotypes in GFP-tub S2 cell (a. shows GFP-Tao, a' shows MT channel and a'' shows merged image with a and a'; b shows GFP-α-Tub channel, b' shows RFP-Tao, b'' is merged images with both b and b').Note: The red signal in the other cells is background due to increased gain used to see the cell edges.

5.4 Localisation of Drosophila Tao-1

The localization of a protein can often help strengthen the understanding of its function and mechanism of action. Hence, I studied the localisation

of Tao-1 using anti-Tao-1 multipeptide-antibody which recognizes the C-terminal part 967-981: C+FNQERAERLRMKHEK-CONH2 and GFP-Tao-1 in S2R+ cells.

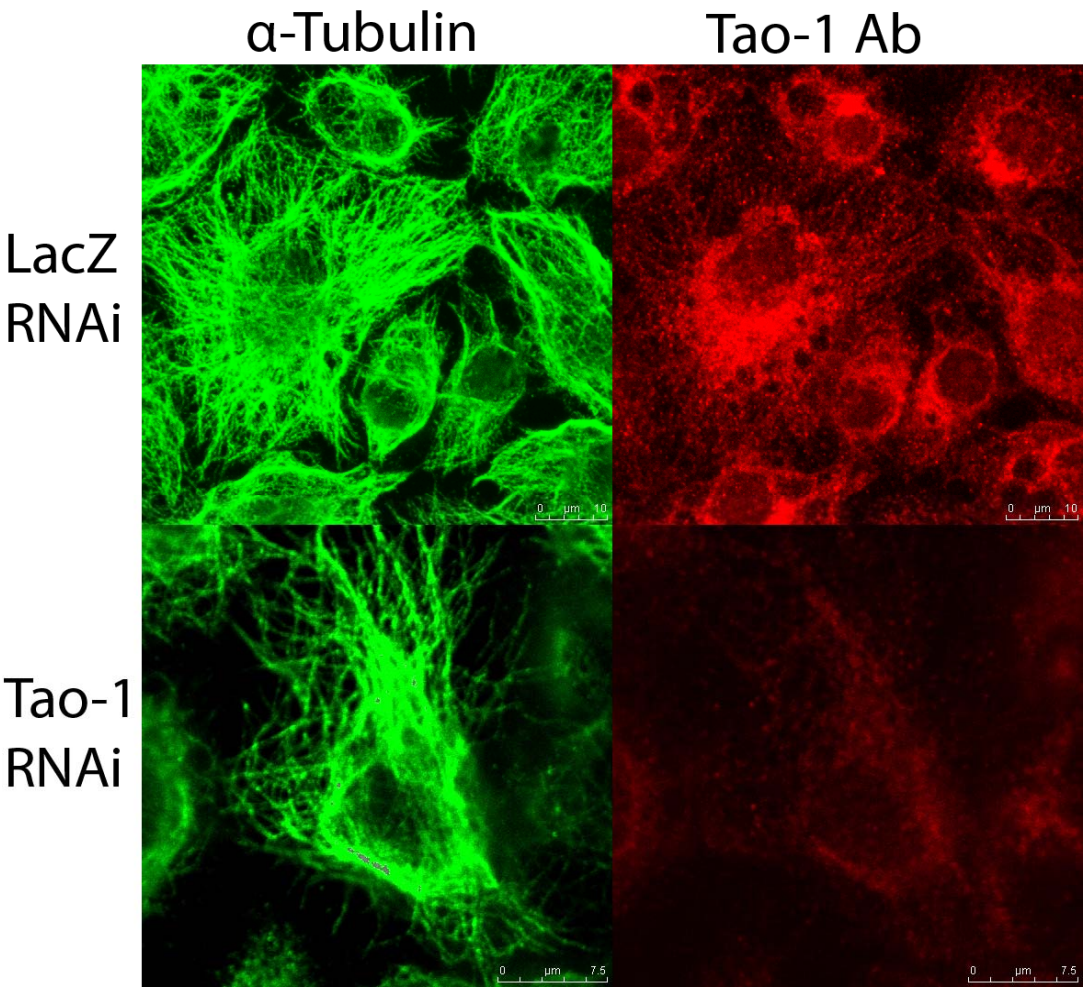

Figure 5-4 Tao-1 antibody reveals Tao-1 colocalises with MTs and reveals that RNAi works because the signal of the immunoflourescent staining in Tao-1 RNAi cells was lower than that of control S2R+ cells when using the same settings.

As I mentioned above, this non-phospho-Tao-1 antibody didn't work for my westernblot, but it works for the immunoflourescent staining. The level of Tao-1 protein was assessed in Tao-1 RNAi cells and control LacZ RNAi treated cells, 5 day after dsRNA addition (see Figure 5-4). The results

show that the antibody works for immunoflourescent staining and confirms the efficacy of the RNAi. The results also show that Tao-1 is weakly co-localized with microtubules and can also be seen at the cell cortex in interphase. This is most clear in Figure 5-5.

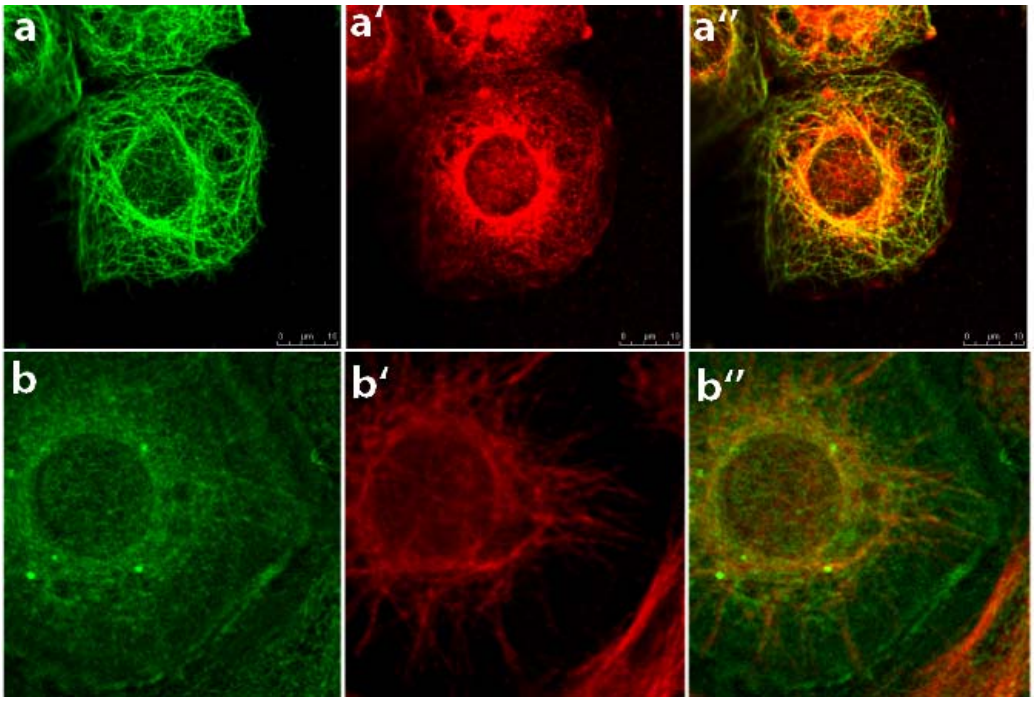

Figure 5-5 Tao-1's localisation in interphase S2R+ cells.
Panels demonstrate that Tao-1 is co-localized with MTs and at cortex. a. shows MTs stained with in 1:500 α-Tubulin; a' shows Tao-1 antibody staining; a'' shows merged image. Bottom panel reveals the localization of GFP-Tao over-expressed in an S2R+ cell. b shows GPF-Tao b' shows MTs; b'' is merged image for both.

Interestingly, using the Tao-1 antibody I also found that endogenous Tao-1 co-localises with the mitotic spindle in mitotic cells (see Figure 5-6). In addition, I was able to compare the localization of both endogenous and GFP-tagged Tao-1 using this antibody. GFP-Tao-1's localization in mitotic S2R+ cells confirmed the Tao-1 antibody staining result (Figure 5-7), and

suggests that GFP-Tao-1 is likely to function normally in these cells. In this experiment, I used phospho-Histone H3 as a marker of mitotic chromosomes (see Figure 5-7). The failure of the chromosomes to align suggests that Tao-1 overexpression may perturb mitosis, as suggested by Elledge ‘s lab [139]. Since I didn’t find any more mitotic cells transfected with GFP-Tao-1, I decided to leave the analysis of Tao-1 in mitosis to the future.

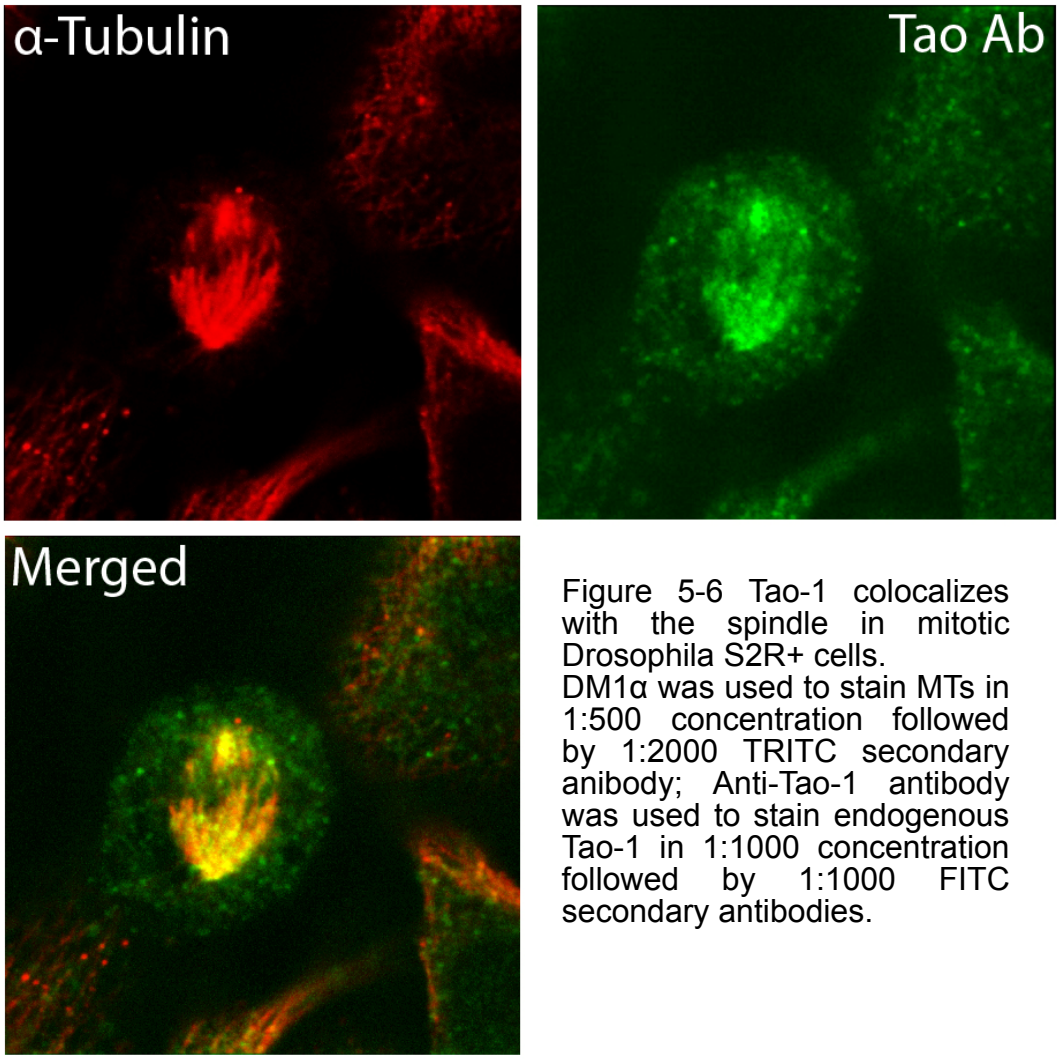

Figure 5-6 Tao-1 colocalizes with the spindle in mitotic Drosophila S2R+ cells.
DM1α was used to stain MTs in 1:500 concentration followed by 1:2000 TRITC secondary anibody; Anti-Tao-1 antibody was used to stain endogenous Tao-1 in 1:1000 concentration followed by 1:1000 FITC secondary antibodies.

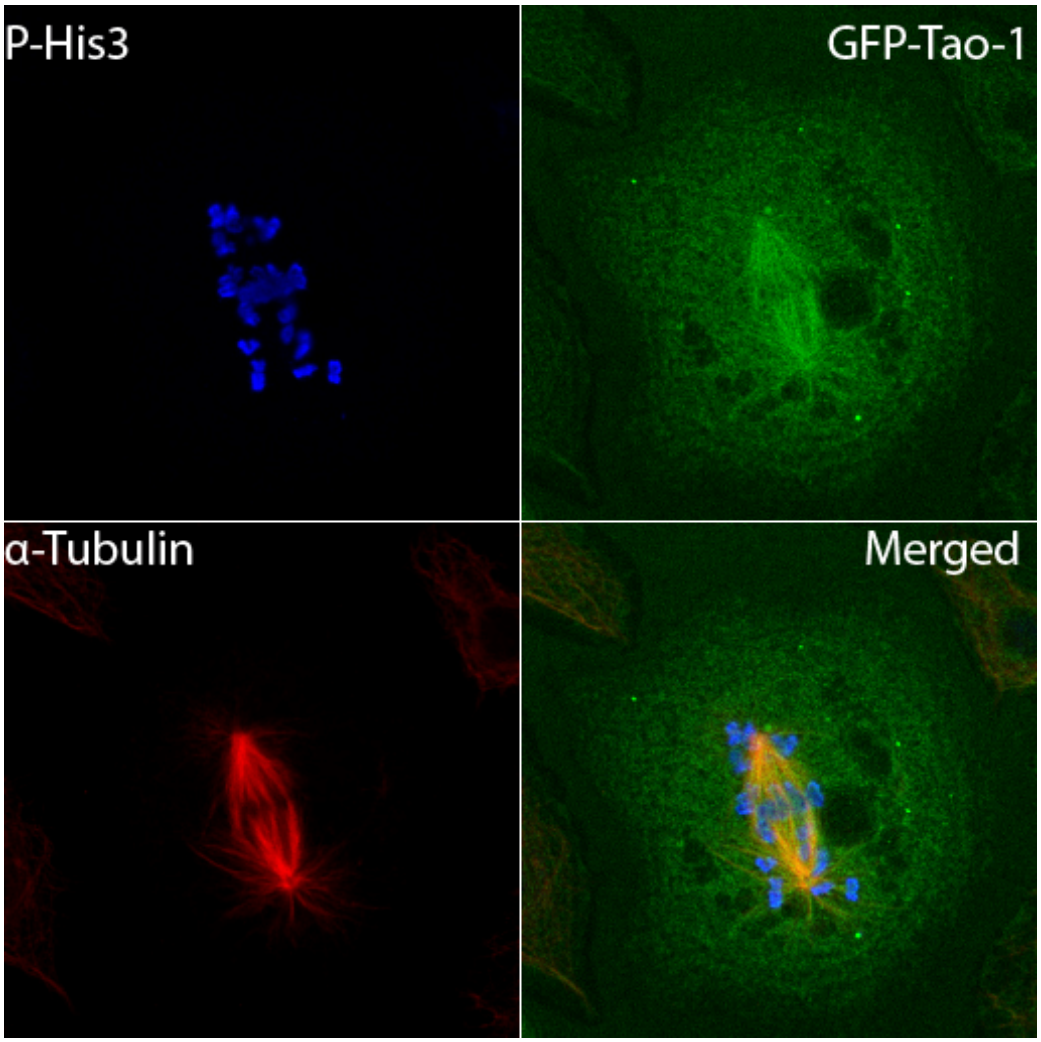

Figure 5-7 GFP-Tao-1 colocalizes with the spindle in mitotic S2R+ cells and may disturb chromosome segregation.

Taken together, these data show that Tao-1 colocalises with microtubules in interphase and in mitotic stage. In interphase, it seems Tao-1 is also localized at the cell cortex. These results support the RNAi and overexpression results which suggest that Tao-1 has an effect on microtubules.

5.5 Molecular and cellular biological function of Tao-1

5.5.1 Tao-1 regulates microtubules organization via it kinase domain

By using the bioinformatics database SMART (http://smart.embl-heidelberg.de/) I analysed Tao-1's functional domains based on its protein sequence. *Drosophila* Tao-1 has a typical serine/threonine kinase domain, an ATPase domain, an ERM-like domain and three repeated coiled coil domains, moving from the N to the C-terminus. Based on this structure, I began by studying the function of its kinase domain, since previous works suggested that human Tao-1 homologue-PSK regulates cell morphology through its kinase domain [138]. By comparing the Tao-1 sequence with the PSK sequence I identified K56 as a conserved residue in the catalytic core of the kinase domain, and introduced a point mutation to change this Lysine (K) to an Alanine (A), which would be expected to generate a kinase dead Tao-1. This could cause a dominant negative effect indirectly by sequestration of its substrates. It was also tagged with either GFP or RFP at its N-terminus (see methods and materials).

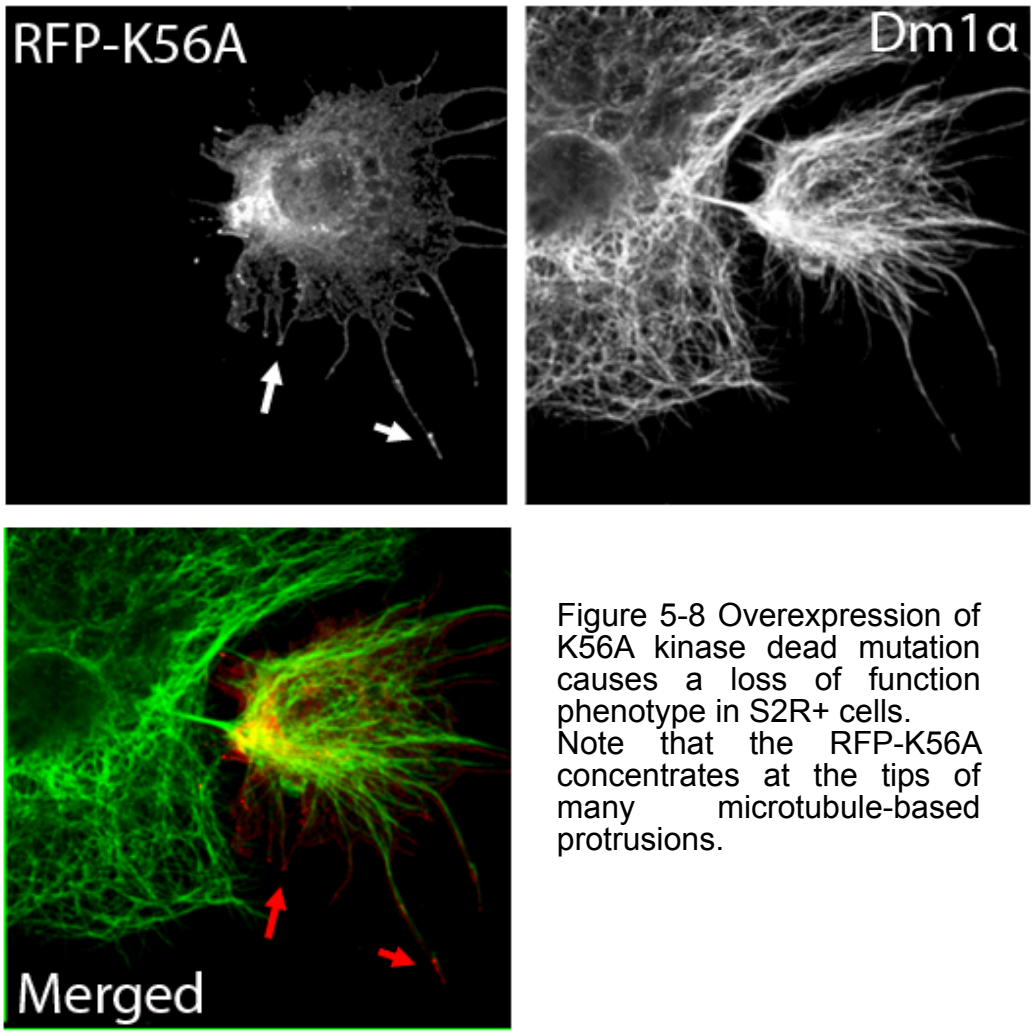

Figure 5-8 Overexpression of K56A kinase dead mutation causes a loss of function phenotype in S2R+ cells.
Note that the RFP-K56A concentrates at the tips of many microtubule-based protrusions.

Overexpression of RFP-K56A Tao-1 in S2R+ cells results in a very similar phenotype to seen in loss-of-function of Tao-1 RNAi cells (Figure 5-8), with an accumulation of microtubules in bundles, microtubule spikes and a disorganized microtubule network (all 11 of the cells quantified in this experiment showed this phenotype.)

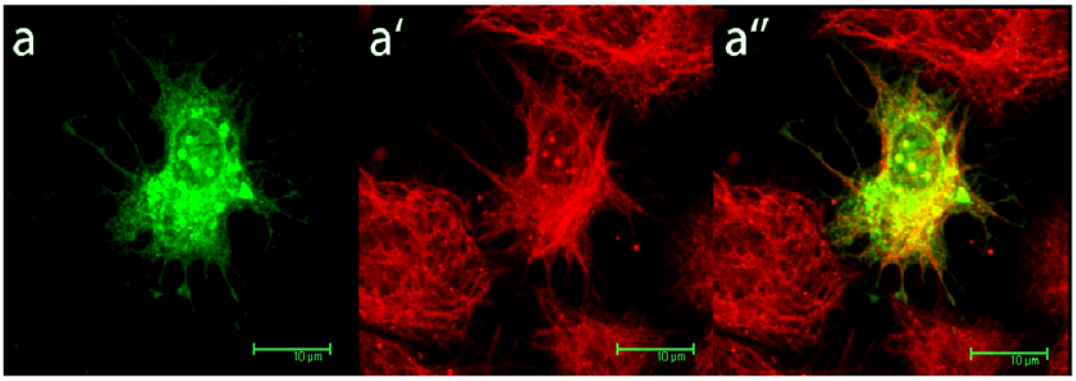

Figure 5-9 Overexpression of GFP-delta-51-345 results in dominant negative Tao-1 phenotypes.
a. shows GFP-delta-51-345 channel; a' shows microtubule staining with DM1α; a'' shows the merged image

To confirm this requirement for the kinase activity for Tao-1 function, I also generated another mutation, GFP-delta-51-345-Tao-1, in which the N-terminal kinase domain was deleted. Once again, this had dominant negative effects on cell morphology in 6/6 randomly identified transfected cells in this experiment. Since Tao-1 can bind to itself in a yeast two hybrid analysis, as shown in the following section, it is possible that the overexpression of GFP-delta-51-345-Tao-1 leads to the similar phenotypes as the kinase domain point mutation (see Figure 5-9) because it sequesters active Tao-1 by forming heterodimers. This is something I plan to test in the future.

Another interested observation from this experiment was the fact that RFP-K56A can be seen concentrating at the cortex and at the tip of each microtubule-based protrusion. This raises two possibilities: First, Tao-1 could stay and wait at the cell cortex for growing microtubule plus ends to

stop them by inducing catastrophe. When K56A is overexpressed in the cell, microtubules are not able to be stopped when they hit the cell cortex as usual, leading to the dominant negative phenotype and to the further recruitment of Tao-1 to the local area as observed. The second is that inactive Tao-1 could function as microtubule plus end tracking protein. These ideas will be explored further in the following sections. However, all the above data confirm that Tao-1 functions as a microtubule destabilizer via its kinase domain.

5.5.2 The ERM-Like domain of Tao-1 is necessary for the formation of lamellipodium and cell spreading

Recently, we found that *Drosophila* FERM protein, moesin, is necessary for the increase in cortical rigidity and cell rounding when cells enter mitosis, and that overexpression of the phospho-mimetic activated form of moesin causes cells to round up and stop the formation of lamellipodia [99]. This raised my interest in ERM proteins. In general the FERM domain proteins bind to the sides of actin filaments and regulate cell morphology by cross-linking actin filaments to the plasma membrane [147]. When looking at the *Drosophila* Tao-1 amino acid sequence using the protein domain prediction database SMART (http://smart.embl-heidelberg.de/) I identified a putative ERM domain within a putative ATPase domain. I therefore wanted to know what this domain might do. A

RFP fused mutation Delta-422-900 Tao-1 was designed and generated. I then expressed the non-ERM mutant Tao-1 in S2R+ cells. The overexpression of the ERM-like domain deletion mutant delta-422-900-Tao-1 (see method and materials and Figure 5-10) prevented cells forming large lamellipodia and spreading as usual.

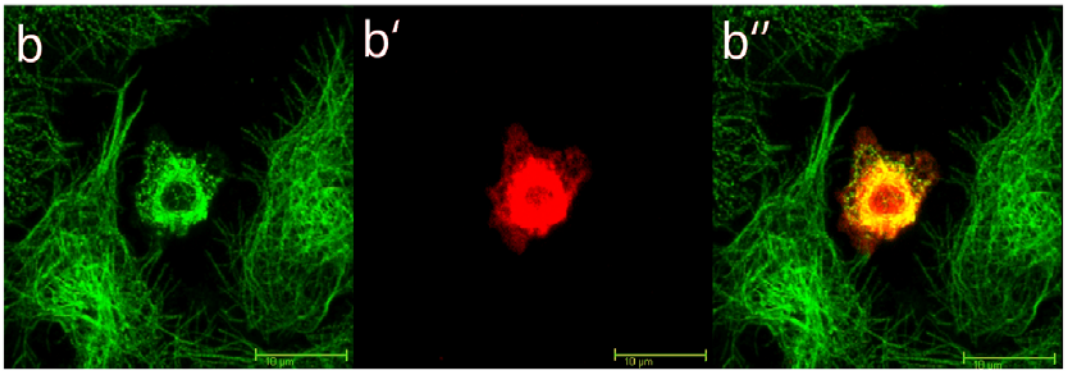

Figure 5-10 Overexpression of RFP-delta-422-900 stops cells spreading while the microtubules are completely destroyed.
b is Mts stained with Dm1α followed FITC; b' is RFP-delta-422-900-Tao-1; b'' is merged image

Moreover, the microtubule network appeared completely destroyed in 7/7 randomly picked cells in which RFP-delta-422-900-Tao-1 had been overexpressed. This phenotype was much stronger than that seen when full length Tao-1 was overexpressed. As a simple test of whether this dramatic effect on microtubules is likely to be direct or via a *Drosophila* specific pathway, I decide to repeat this experiment in human cells. I used Hela cells for this purpose. Hela cells are big and have nice big lamellipodia when completely spread. I subcloned this ERM-like deletion mutation of fly Tao-1 into a human gateway expression vector pDEST-YFP

(a gift from Michael Wer in Nic Tapon's lab). Overexpressing pDEST-YFP-delta-422-900-Tao-1 in Hela cells had a very strong phenotype as shown in Figure 5-11. YFP positive cells overexpressing delta-422-900-Tao-1 were prevented from generating lamellipodia and from spreading like control cells (see Figure 5-10 top panel YFP overexpression only). Again, the microtubule netwoks appeared completely disassembled when compared to a control cell which overpexpressed YFP alone. This result suggests the possibility that Tao-1 may have a more or less direct effect on microtubule stability or dynamics. There are several reasons why this mutated version of the kinase may have an overexpression phenotype which is much stronger than that of the active full length kinase. First, it suggests that in the context of full length Tao-1 a part of this domain limits Tao-1's activity. Since ERM domains enable proteins to bind to F-actin [148], it is possible that the stronger microtubule phenotype seen in this experiment is due to the release of an inactive pool of Tao-1 from the cell cortex. If so, the functional kinase part can still work and the strong phenotype may result from the increase of functional protein levels in the cytoplasm. Alternatively, the deleted ATPase domain may have some function. Finally, since the deleted domain also contains a nuclear localisation sequence, this region of the protein may be required to sequester active Tao-1 in the nucleus. I will discuss this further in the Tao-1 signaling section. This analysis also proves that *Drosophila* Tao-1 has a

conserved function.

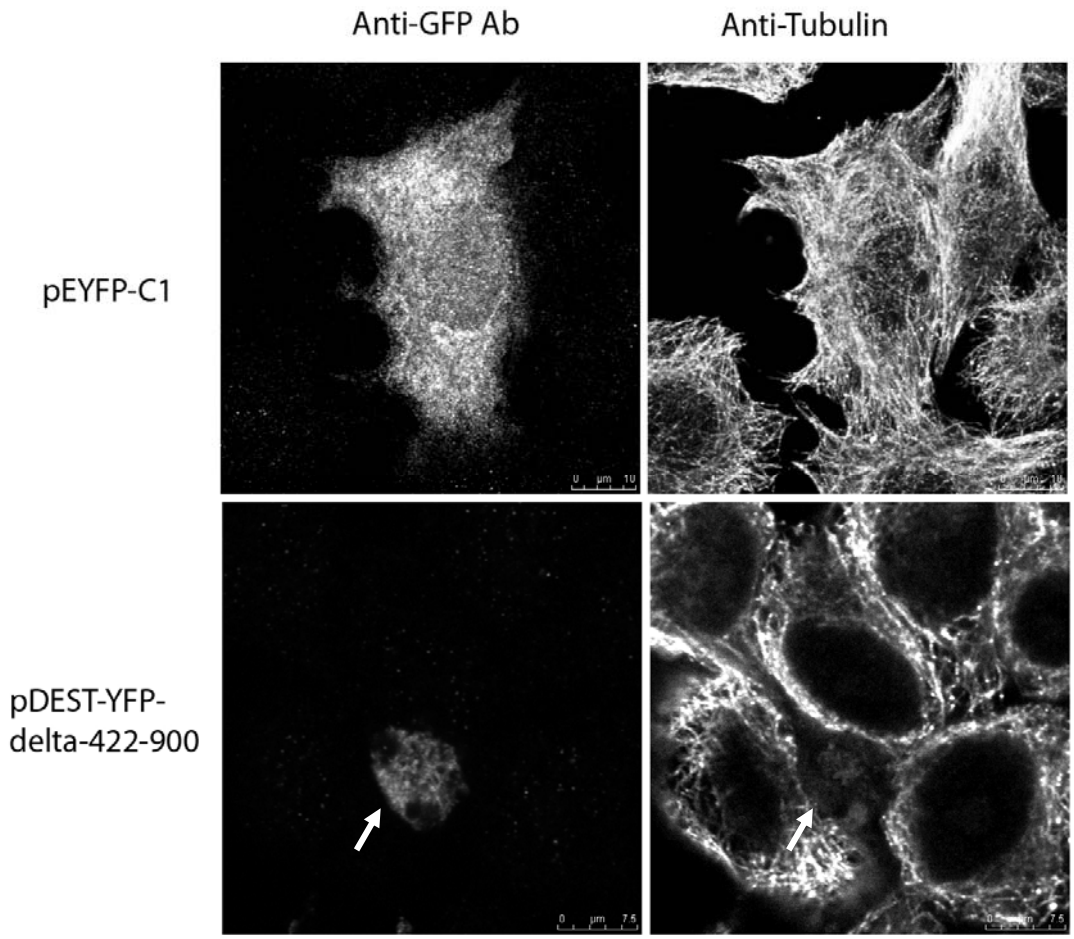

Figure 5-11 *Drosophila* Tao-1 can stop cell spreading and lamellipodial formation in Hela cells, and destroy the microtubule network
Top panel: YFP was used as a control to overexpress in Hela cell
Bottom panel: Delta-433-900 Tao-1 expression.

5.5.3 Coiled-coil domains enable Tao-1 to associate with centrosomes and microtubules

As I mentioned above, *Drosophila* Tao-1 has 3 repeated coiled coil domains at its C-terminus, which are supposed to help Tao-1 bind microtubules and which are required for its function [96, 137]. To test this, I

generated a construct in which are three coiled-coil domains from 900 to 1039 amino acid at the C-terminus of Tao-1 are deleted (the stop codon was replaced during the subcloning work). Overexpression of RFP-delta-900-1039-Tao-1 shows that it doesnt remain in the cytoplasm or associate with microtubules and centrosomes any more (see Figure 5-12).

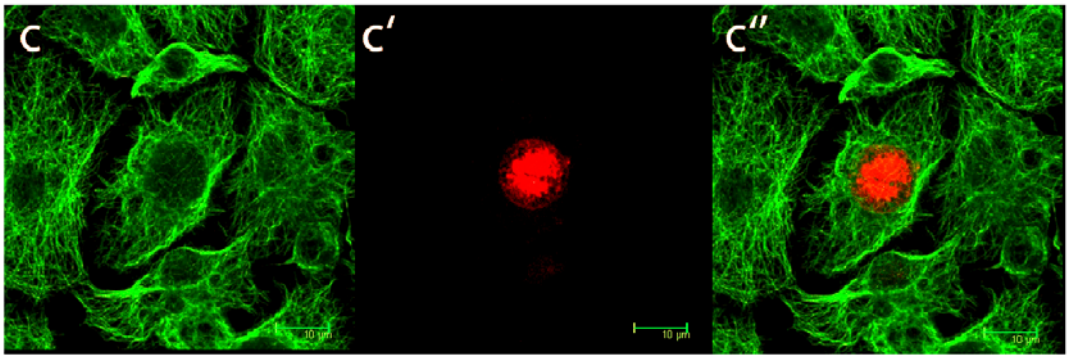

Figure 5-12 The coiled coil domain deletion mutant RFP-delta-900-1039 re-localizes to the nucleus
c is is MTs stained with Dm1α followed by FITC; c' represents RFP-delta-900-1039-Tao-1; c'' is merged image

Instead, almost all RFP-delta-900-1039-Tao-1 localises in the nucleus. Thus, the coiled-coil domains help to give Tao-1 its functional localization, perhaps through binding microtubules. In addition, the microtubule network looks normal when RFP-delta-900-1039-Tao-1 display their localization in the nucleus, suggesting that the Tao-1 kinase domain cannot perform its function when Tao-1 localises in the nucleus. This change of localisation when deleting Tao-1's coiled-coil domains raised my interest as the full length Tao-1 is seen in the nucleus and cytoplasm, whereas the ERM-like domain deletion mutant Tao-1 protein failed to enter the nucleus, as seen by confocal Z mode scanning (I scanned these cells

in a z-stack and the picture showed above is a maximum projection to overview the microtubule phenotypes.) Thus it seems possible that Tao-1 may normally undergo a dynamic change in its localisation which requires both the ERM / nuclear localisation sequence and the coiled coil domains acting in opposition. Does this have a functional meaning? I will return to this topic in the discussion section Chapter 6.

5.5.4 Tao-1 RNAi can stabilise microtubules

The Tao-1 overexpression phenotype suggests that Tao-1 functions as a microtubule destabilizer. However, more direct evidence is required to show the effect of endogenous Tao-1 on microtubules. In order to do this, I decided to perform a cold shock experiment followed by 5 day RNAi treatment in S2R+ cell, following a protocol used in the Rogers's lab [23] (see methods and materials). The idea was to observe the effect of Tao-1 on microtubules during the recovery process after microtubules have been completely destroyed by cold treatment by comparing the recovery in control and Tao-1 RNAI cells. As shown in Figure 5-13, microtubules in control cells have disassembled after 2.5 hours 0 degree cold treatment. However, the same effect was not seen in Tao-1 RNAi cells. This result proves that Tao-1 activity destabilizes microtubules in the face of cold shock. Importantly, however during the period of cold shock, Tao-1 RNAi cells lost their spikes, restoring the circularly symmetrical shape seen in

control cells. After 10 minutes recovery at 25 degrees, however, the shape of Tao-1 RNAi cells dramatically changed from symmetrical to spiky as microtubules became bundled and straight, while the control cells regenerated a normal microtubule organization. This result contains some important information. First, it shows that the spiky cell shape in Tao-1 RNAi cells originates from the effect of Tao-1 on microtubule dynamics. Second, it shows that Tao-1 is required to destabilize the microtubules in cells, and its removal leads to the formation of microtubules that are stable even in the presence of cold shock. Finally, microtubule filaments stop at the cell cortex in control cells during their repolymerization, but fail to do so in Tao-1 RNAi cells.

Taking all the above together, *Drosophila* Tao-1 is likely to function to destabilize microtubules.

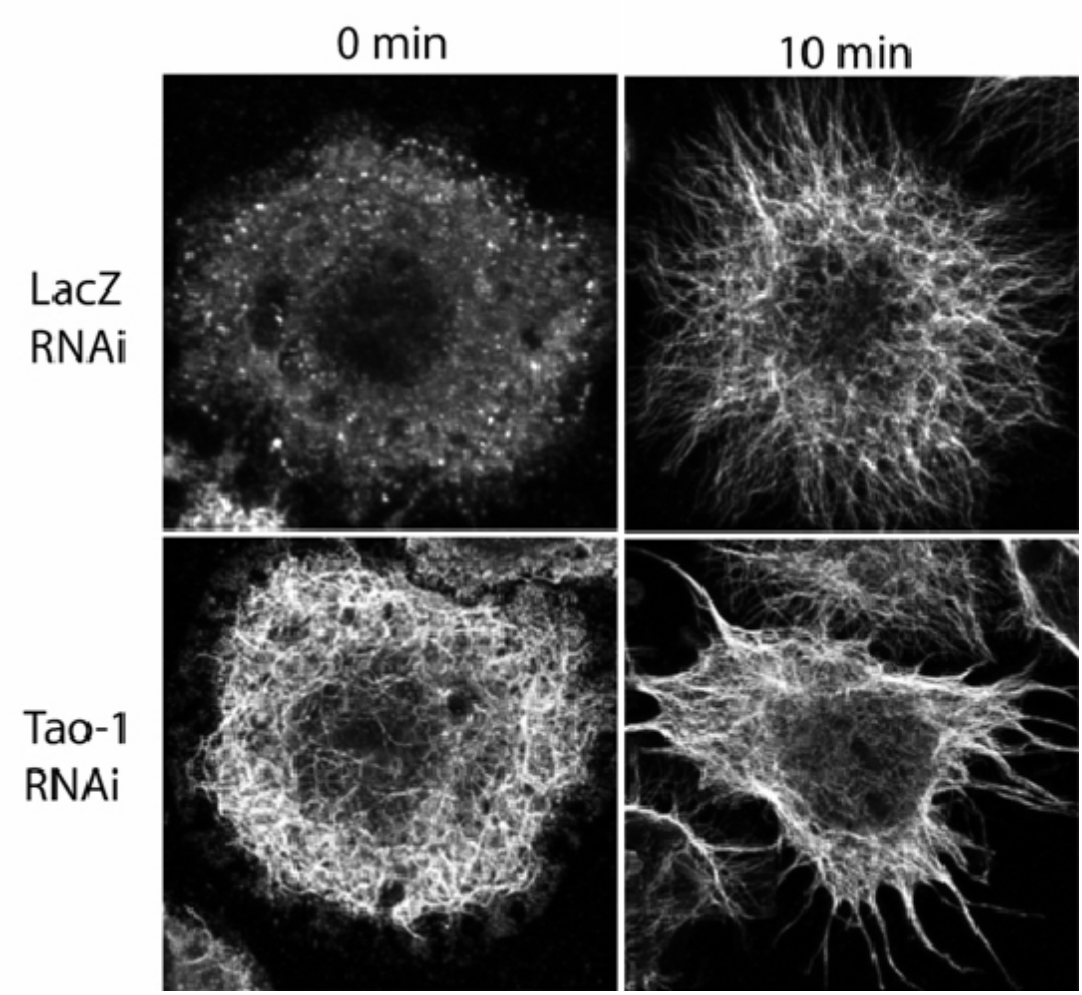

Figure 5-13 Cold shock experiment proves that the Tao-1 RNAi phenotypes are derived from MTs rather than the secondary actin phenotypes. Further more, it shows that Tao-1 activity destablises microtubules. (76% of quantified cells shows the similar phenotype in Tao-1 RNAi treat S2R+. N=30)

5.6 Tao-1 regulates microtubule organization independently of the Par-1/Tau pathway in Drosophila S2R+ cells.

As mentioned at the beginning of this chapter, in human CHO and PC12 cells MARKKs/Tao-1 has been shown to act as a microtubule destabilizer

in a pathway involving Par-1/Tau pathway [144], in which the activity of MARKK/Tao-1 enhances microtubule dynamics through the activation of the conserved serine/threonine kinase MARK/Par-1, which leads to hyperphosphorylation and detachment of Tau or equivalent MAPs from microtubules. Hence, I wondered whether *Drosophila* Tao-1 has its function via the same pathway.

In *Drosophila* there is only one isoform of Tao-1, and this protein has extraordinarily strong effects on microtubule organization. Similarly, there is one Par-1 kinase in the *Drosophila* genome which has been implicated in the regulation of cell polarity [149-151] and in *Drosophila* axis formation, where it helps to organize the polarised oocyte microtubule array [151]. Thus, to test whether Tao-1 regulates microtubule organization through Par-1 pathway I looked for a similar microtubule phenotype in Par-1 loss-of-function cells. Par1 RNAi failed to induce a comparably strong phenotype in the RNAi screens I carried out in multiple cell lines (data can be seen online at http://flight.licr.org/). However, to compare the microtubule organization in both Par-1 and Tao-1 RNAi treated cells in more detail, I looked at confocal images of both Par-1 and Tao-1 5 day RNAi treated cells (Figure 5-14). In Par-1 RNAi cells, there was a marked increase in the density of microtubules and microtubules appeared straighter than they do in control cells. This phenotype was displayed in

73.3% of the randomly picked cells, as quantified by eye (N=30) and resembles the phenotype of Par-1 null mutant follicle cells [152]. However, the global organization of microtubule network appeared unaffected in Par1 RNAi cells.

Interestingly, previous studies in flies show that microtubules are less stable in *par-1* mutant cells as confirmed by both microtubule-depolymerising drug and cold shock experiments [152]. Thus, *par-1* mutant follicle cells lack visible microtubules after short microtubule-depolymerization drug treatments (5 minutes) while the microtubules in control cells are extraordinarily resistant to this drug. Thus, Par-1 is required to stabilize the microtubules in cells in *Drosophila* [152].

However, in my study, Tao-1 shows different a effect on microtubules from Par-1. First, Tao-1 RNAi leads to more microtubules while OE of Tao-1 results in microtubule disassembly as I showed above. Second, the cold shock experiment results show 2.5 hour cold treatment in S2R+ cells is not able to lead to the disappearance of the microtubules in Tao-1 RNAi cells (under the same condition control cell microtubules have disappeared.) while 1 hour cold shock can do so in *par-1* mutant clones as reported in the reference [152].

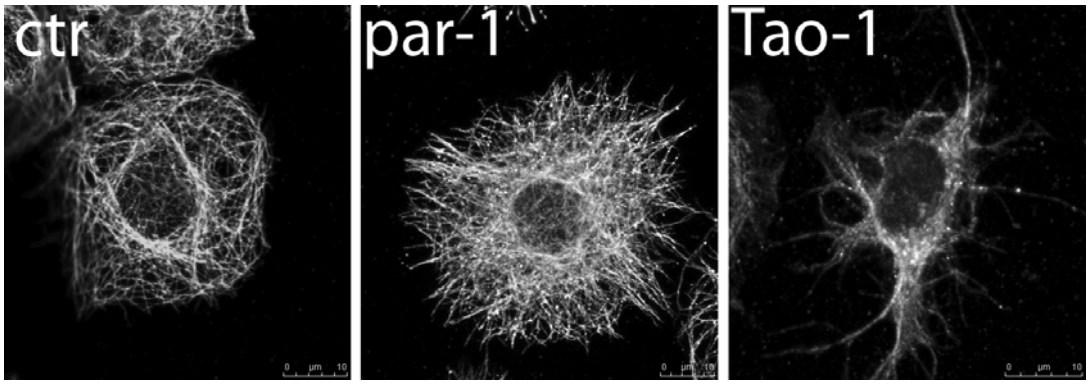

Figure 5-14 Par-1 and Tao-1 have distinct microtubule phenotypes in S2R+ cells. (These Par-1 phenotype was displayed in 73.3% of the cells as quantified by eye. N=30)

I also tested whether Tao-1 overexpression can cause destabilization of microtubules in Par-1 RNAi cells. If Par-1 is an obligatory downstream effector of Tao-1, Tao-1 overexpression should not alter the Par-1 RNAi microtubule phenotypes. In fact, the overexpression of GFP-Tao-1 in Par-1 RNAi treated S2R+ cells induced the disruption of microtubules as shown in Figure 5-15 (This effect was seen in 10/10 GFP-Tao-1 positive Par-1 RNAi cells). To avoid the possibility of an incomplete Par-1 knock-down, I verified that non-transfected cells showed the typical Par-1 RNAi phenotype.

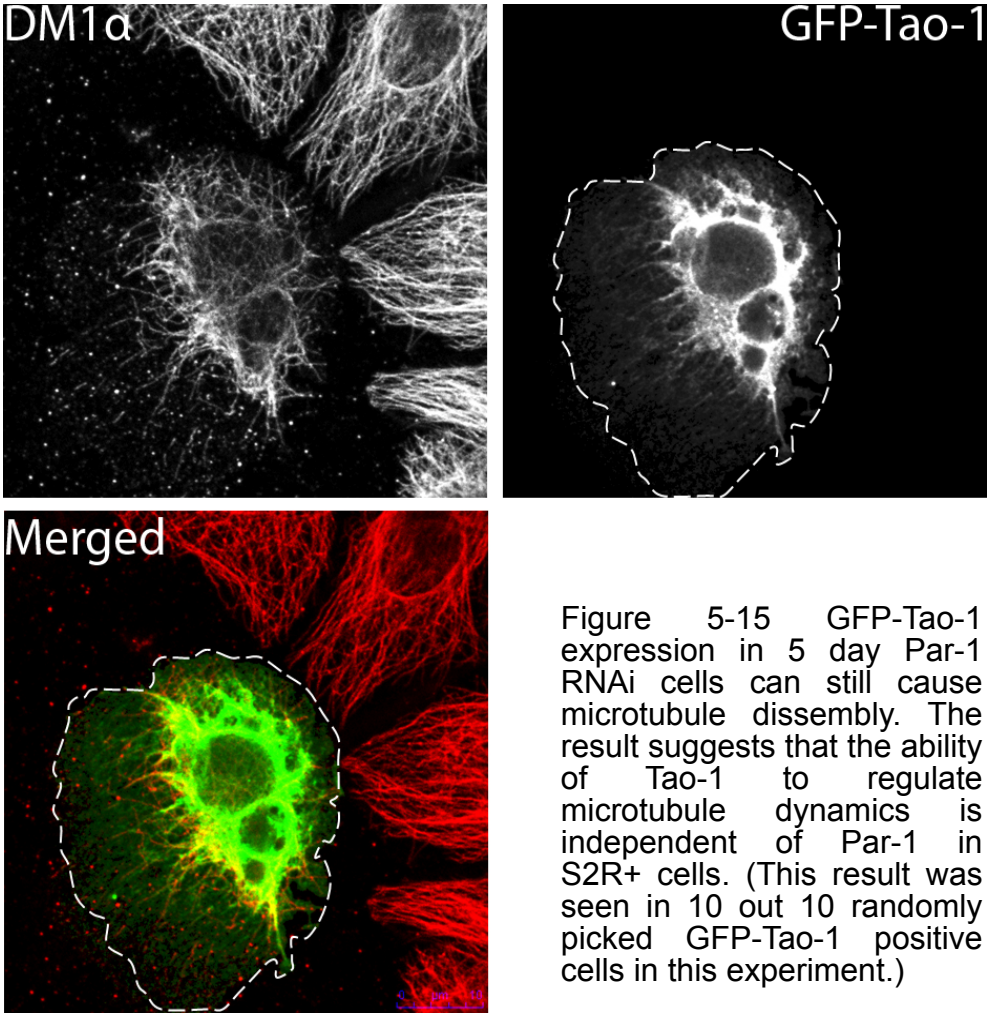

Figure 5-15 GFP-Tao-1 expression in 5 day Par-1 RNAi cells can still cause microtubule dissembly. The result suggests that the ability of Tao-1 to regulate microtubule dynamics is independent of Par-1 in S2R+ cells. (This result was seen in 10 out 10 randomly picked GFP-Tao-1 positive cells in this experiment.)

Moreover, I didn't find any detectable microtubule phenotypes in *tau* knock-down S2R+ cells, which fits with corresponding data from experiments looking at the role of *Drosophila* Tau *in vivo* [152]. Below I compare the different roles of Par-1 and Tao-1 in *Drosophila* in order to make the relationship easier to understand (Table 5-1).

	par-1 null mutant cell or Par-1RNAi in S2R+	Tao-1 RNAi in S2R+
Density of microtubules	Increased [152]	Increased
microtubule filaments	straight (my data)	Bundled rigid microtubules fail to stop at the cell cortex
microtubule network organization	no effect (my data)	Severely disrupted
microtubule stability	Stabiliser [152]	destabilizer
Cell shape	Symmetric (my data)	spiky

Table 5-1 Comparison of the effects on microtubules for Par-1 and Tao-1 in Drosophila cells

Taken all together, these data show that *Drosophila* Tao-1 is unlikely to regulate microtubules via the mechanism proposed for mammalian Tao-1 (via Par-1), even though Tao-1 has the same overexpression effect in fly and human cells. How then does *Drosophila* Tao-1 regulate microtubule organization in interphase?

5.7 Tao-1 changes microtubule dynamic instability

The data presented above show that *Drosophila* Tao-1 functions as a microtubule destabilizer, and argue against Tao-1 functioning via the Par-1/Tau pathway in S2R+ cells. It was therefore necessary to clarify the mechanism for *Drosophila* Tao-1 to regulate the microtubule polymerization.

Microtubules are very highly dynamic structures. They grow and retract, continually probing the cellular environment. One of the interesting results

from the cold shock recovery experiment was that microtubule filaments keep polymerizing when they reach the edge of the cell in Tao-1 RNAi cells, whereas microtubules undergo catastrophe when they reach the cortex in control cells. This led me to wonder whether Tao-1 might act on the microtubule plus end. In order to track and analysis the behavior of microtubule plus end, I chose GFP-EB1 as a marker to take live images. EB1 has been well-known to localize to the microtubule plus-end, and has been successfully used to mark the growth of microtubule filaments in living cells. Steve Rogers developed a *Drosophila* cell line stably expressing pMT-GFP-EB1, which I got from DGRC (*Drosophila* Gene Resource Center) for this purpose [57].

Microtubules undergo dynamic instability in which they undergo rounds of growth and shrinkage. GTP-loaded tubulin subunits from the cytoplasm are added to this plus ends during microtubule filament growth, and microtubules shrink when they loose their GTP-tubulin cap. Recently, several studies have identified a third state, pausing, in which microtubules undergo no significant growth or shrinkage in cells [153-155] (see Figure 5-16), which likely represents a symptom of a change in the microtubule's dynamic state. Thus, Hiroyuki Ohkura's lab found evidence to support the hypothesis that *mini spindles* is an antipausing factor that can work as either a microtubule stabilizer or destabilizer [46].

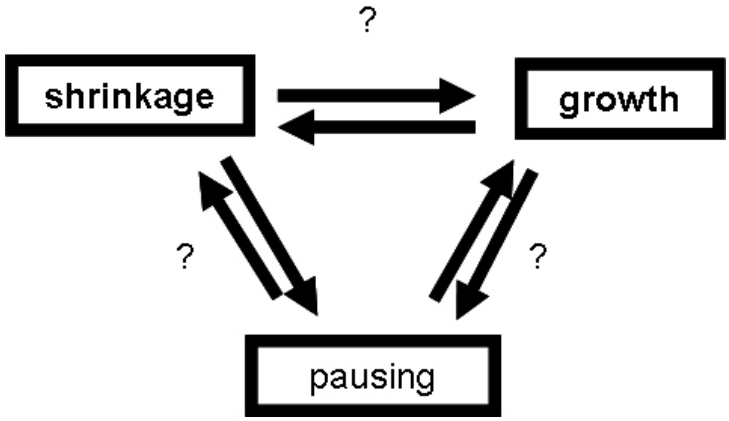

Figure 5-16 Three different states of microtubule instability.

I reasoned that by investigating the effect of Tao-1 on the dynamic state of microtubules would certainly help me to understand its function. Thus, I tracked and measured about 300 microtubule plus ends in different cells made visible using GFP-EB1 under several conditions including control cells, cells expressing Tao-1, a kinase dead K56A-Tao-1, or Tao-1 RNAi cells. Part of work was carried out with the help of Remigio Picone, another PhD student in the Baum lab, who developed a script for Image-j enabling the automatic recognition and thresholding of the cell edge. I then tracked GFP-EB1 comets manually. Remigio Picone also generated the plots in Figure 5-16 and Figure 5-17 using 'R' program and data generated through my analysis. The results of this experiment proved informative. Firstly, in control cells, two groups of microtubules were identified by the growth rate distribution. A slow group and a fast group. Interestingly, the growth speed of a microtubule filament was related to its

location. Microtubule plus ends in central parts of the cell grew faster than those at the edge (see Figure 5-17). This could be due to some factors which regulate microtubule plus ends that are located at the cell edge, which send a signal that restricts peripheral microtubule growth to maintain the normal cell shape.

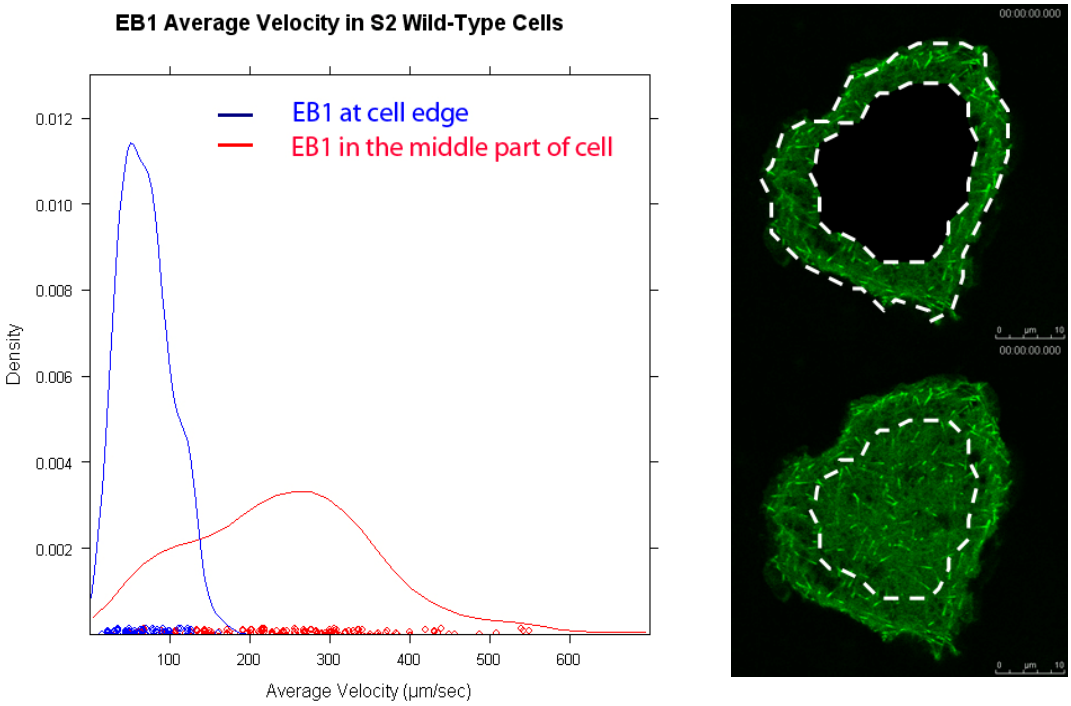

Figure 5-17 Microtubule growth speed can be divided in to two groups depending on the location.
Left graph demonstrates the different distributions of EB1 velocity depending on the location
Region highlighted on up right panel corresponds to MTs in rim of cell while the down right panel shows the central region (The actual data for this analysis has been put in the additional file 10.)

I then studied microtubule dynamics in cells following perturbation of Tao-1 function. In this way, I could determine how Tao-1 affects microtubule dynamics. Following the overexpression of K56A-Tao-1 or in Tao-1 RNAi cells, the distribution of microtubule plus end growth speeds merged to

form one large group instead of the two distinct groups seen in control cells (see Figure 5-18). In other words, a loss of Tao-1 function causes microtubule plus ends to become blind to their location. This is due both to the slowing down of central fast growing microtubules, perhaps due to the increase in microtubules and the concentration reduction in tubulin, and to an increase in the speed of peripheral microtubules. Conversely, the overexpression of Tao-1 led to a marginal reduction in the speed of both peaks (see Figure 5-18). The mild effect may be due to the effects of any increase in microtubule depolymerization being countered by the increase in the level of tubulin monomers. It would be interesting, if challenging, to test the effects of the hyperactive ERM-like domain deletion mutant Tao-1 in a similar way.

Taken all together, these results show that Tao-1 can destabilize microtubules and is required for microtubules to undergo a change in speed/pause rate at the cell periphery. This is the first report of a kinase altering microtubule plus end dynamics at the cell periphery.

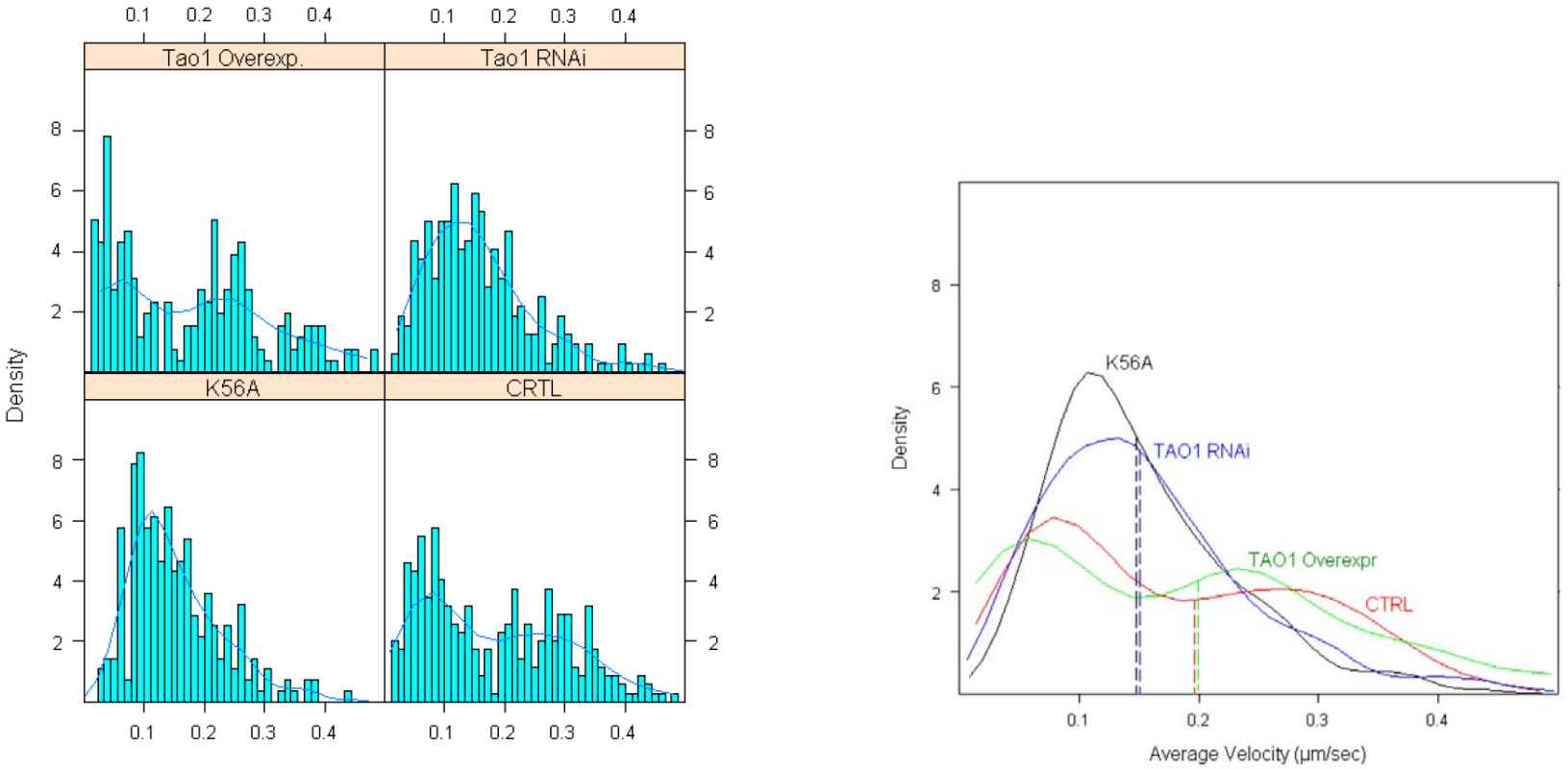

Figure 5-18 Overexpress K56A and Tao-1 RNAi lead to a change in the distribution of microtubule plus ends growth speed.

5.8 Tao-1 can regulate the growing plus end of microtubules at the cell cortex

The dynamic analysis shows that Tao-1 may act at the cell periphery. Moreover, one of the important microtubule phenotypes in Tao-1 loss-of-function cells is that long bundled and straight microtubule filaments push on the cell membrane to generate a spiky cell shape. The simplest hypothesis to explain this phenotype is that Tao-1 works as a signal protein at the cell cortex to let the growing microtubule filament know their spatial information. To test this hypothesis there are 2 questions need to be answered:

1) Does Tao-1 localize at the cell cortex?

2) Does Tao-1 regulate the growing plus end of microtubules at the cell cortex?

Although my studies on Tao-1 localization suggested that a portion of cellular pool of Tao-1 is concentrated on the cell cortex, this effect is a frequent artifact of the folding of the cell edge for cytoplasm proteins. To get around this problem and to clarify the cortical localization of Tao-1, I turned to an analysis in the fly. I crossed homozygous UASp-GFP-Tao-1 flies to heatshock Gal4 flies to induce the expression of GFP-Tao-1 *in vivo*. I checked the localization of GFP-Tao-1 in the egg chambers where Tao-1

localization can be seen in a 3D tissue context. I also tried to use Tao-1 antibody to observe endogenous Tao-1, but was unable to determine the localisation of the endogenous protein.

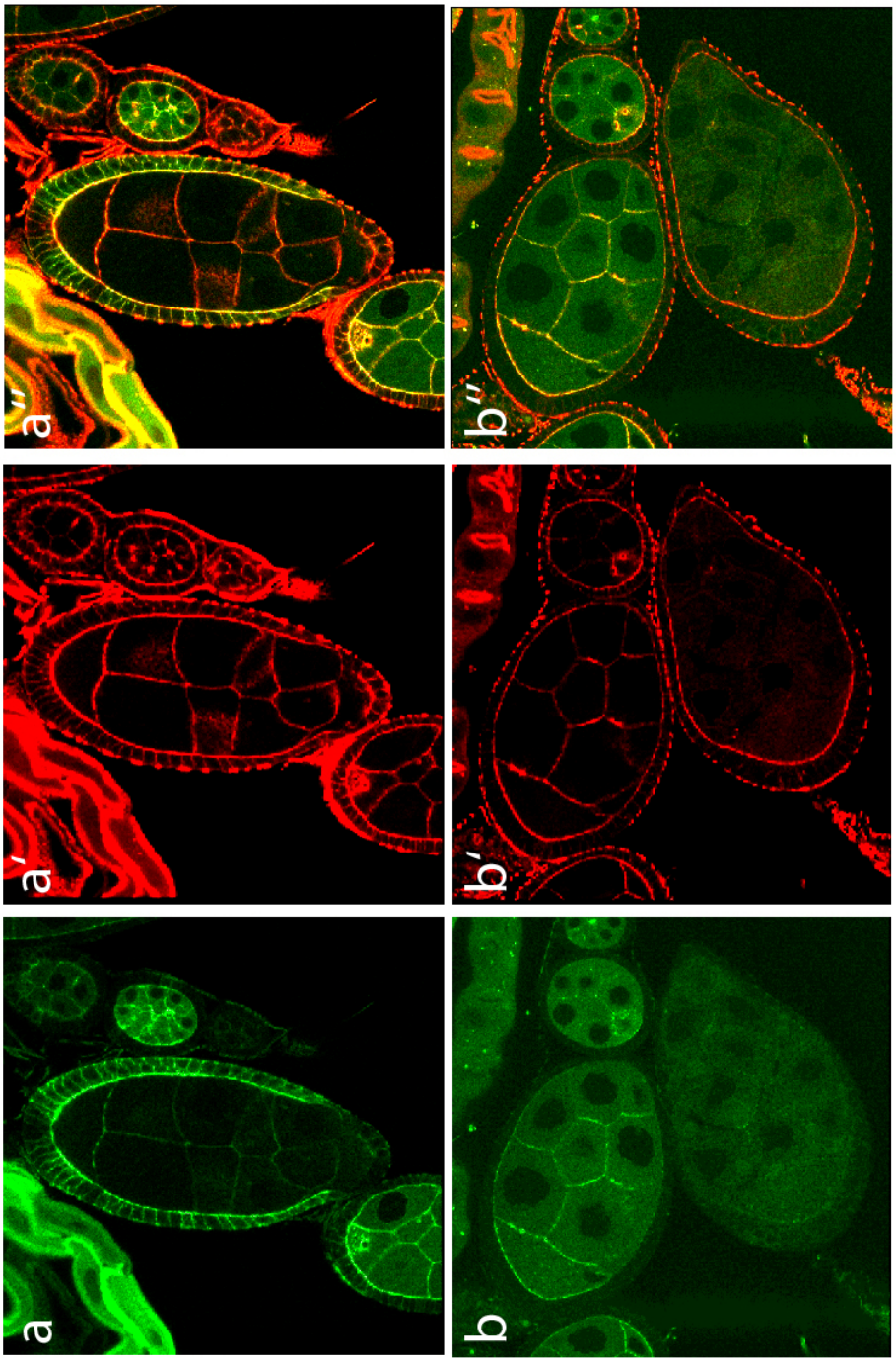

Figure 5-19 GFP-Tao-1 concentrates at the cell cortex and its localization can be destroyed by LatrunculinB.
Top panel shows GFP-Tao-1 localisation in fly egg chambers, while bottom panel shows GFP-Tao-1 was after feeding LatB yeast to flies.(a and b represents GFP-Tao-1; a' and b' represent actin staining; a" and b"shows merged image.)

As shown in Figure 5-19, I found that GFP-Tao-1 was concentrated on the cell cortex *in vivo*. Further more, Tao-1's localization in follicle cells could be disrupted by feeding Latrunculin B containing food to the flies for 24 hours. Latrunculin B inhibits actin polymerization and disrupts microfilament organization. This result implies that *in vivo* Tao-1 binds to actin at the cell cortex rather than microtubules. To confirm this, I carried out a similar experiment using RFP-Tao-1 transfected S2 cells (see Figure 5-20 top panel). Again the Tao-1 signal at the cell cortex was gone within 1 minute following the addition of 0.25 μg/ml Latrunculin B. In another experiment, I added Latrunculin B (0.25 μg/ml) to GFP-EB1 expressing S2 cells to test the behaviour of microtubule plus ends in cells lacking Tao-1 at the cell cortex (see Figure 5-20 top panel). After 10 minutes, single microtubule filaments failed to stop at the cell cortex anymore. Instead they continued to grow without undergoing catastrophe. Eventually, the loss of actin and Tao-1 from the cortex led to a Tao-1 loss-of-function phenotype, suggesting that in cells in culture Tao-1 may function as part of the actin cortex to induce microtubule catastrophe.

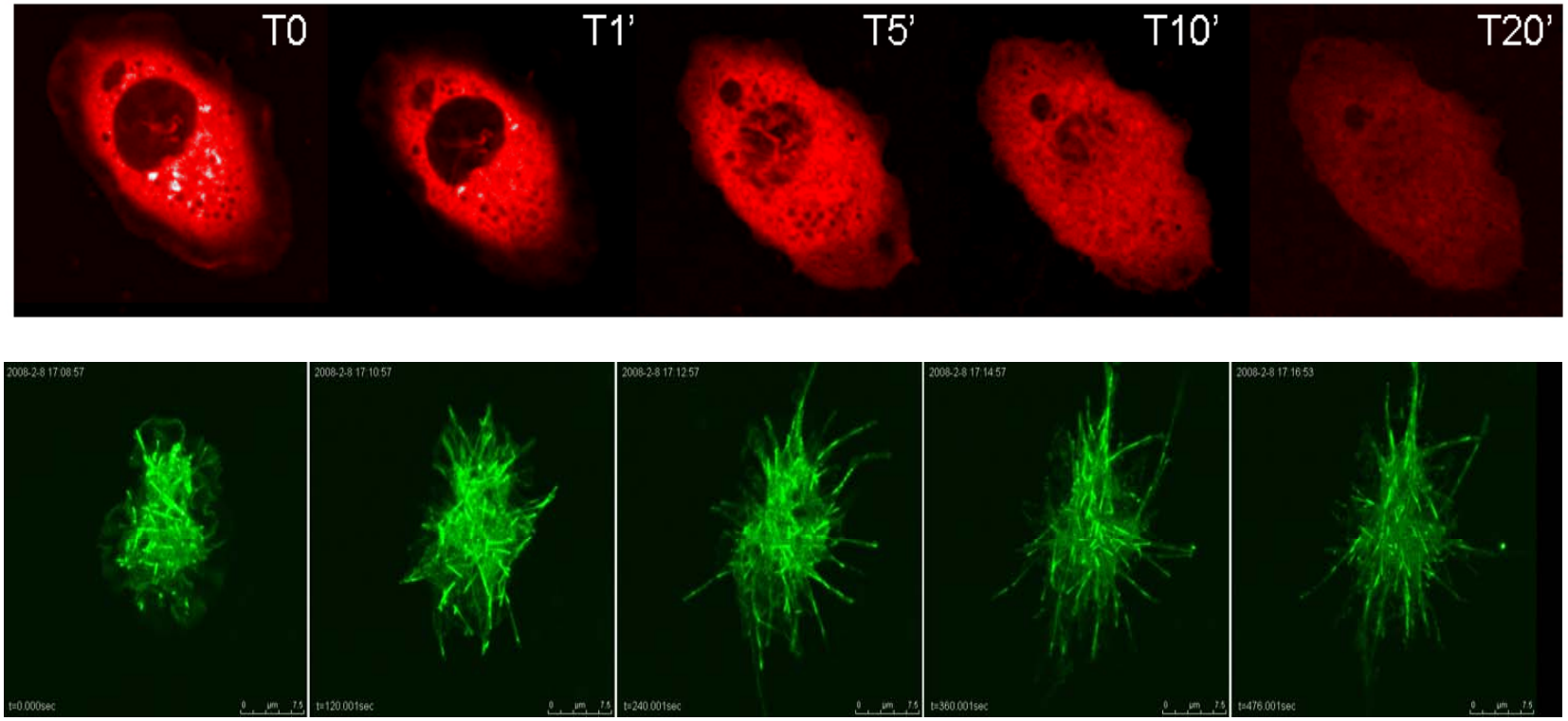

Figure 5-20 Tao-1 can bind to actin and Latrunculin B treatment causes a Tao-1 loss-function phenotype in 10min
Top panel: RFP-Tao-1 loses its localization at cell cortex when the cell was treated by latrunculin B at 0.25μg/ml
Bottom panel: Live imaging shows control cell treated with Latrunculin B at 0.25μg/ml leads to a Tao-1 loss function phenotype in 10 minutes

In summary, Tao-1 localizes at the cell cortex *in vivo* and *in vitro*. Tao-1's cortex localization can be removed by disrupting actin structure *in vivo* and *in vitro.* Microtubule filaments fail to stop at the cortex when Tao-1 comes off from the cell cortex and in Tao-1 RNAi cells.

Here, there is also a possibility that this effect is dependent on cortex tension when actin structure was disrupted. So, the microtubule filaments keep on their growing because there are no forces to make them bend to undergo force-induced catastrophe [156]. To test if this is the case, I repeated the Latrunculin B experiment and took the live image using Total Internal Reflection Fluorescence microscope (TIRF). Using TIRF allowed me to take images at a height that is 90nm above the level of the slide, i.e. at the exact bottom of the cell. So, any GFP-EB1 dots recorded in this image represent the microtubule plus ends which are hitting the cell cortex and/or sliding along the bottom cortex of the cell. At the same time, the glass bottom of the dish acts like a wall that blocks microtubule growth. The aim of this experiment was to test whether the presence of Tao-1 bound to actin at the cell cortex is required to regulate the dynamics of microtubule plus ends in the absence of a change in the physical properties of the cortex as experienced by microtubule tips (since they hit the glass). I compared the GFP-EB1's movement at the cell cortex before and after adding Latrunculin B using TIRF in live movies. To visualize

microtubule dynamics, I combined three sequential pictures from the TIRF movie in the different channels of an RGB image to generate a combined picture which illustrates the movement of the EB1 comets. A white dot therefore is a paused microtubule filament, coloured dots show where the position of EB1 has changed in during the time course (Figure 5-21).

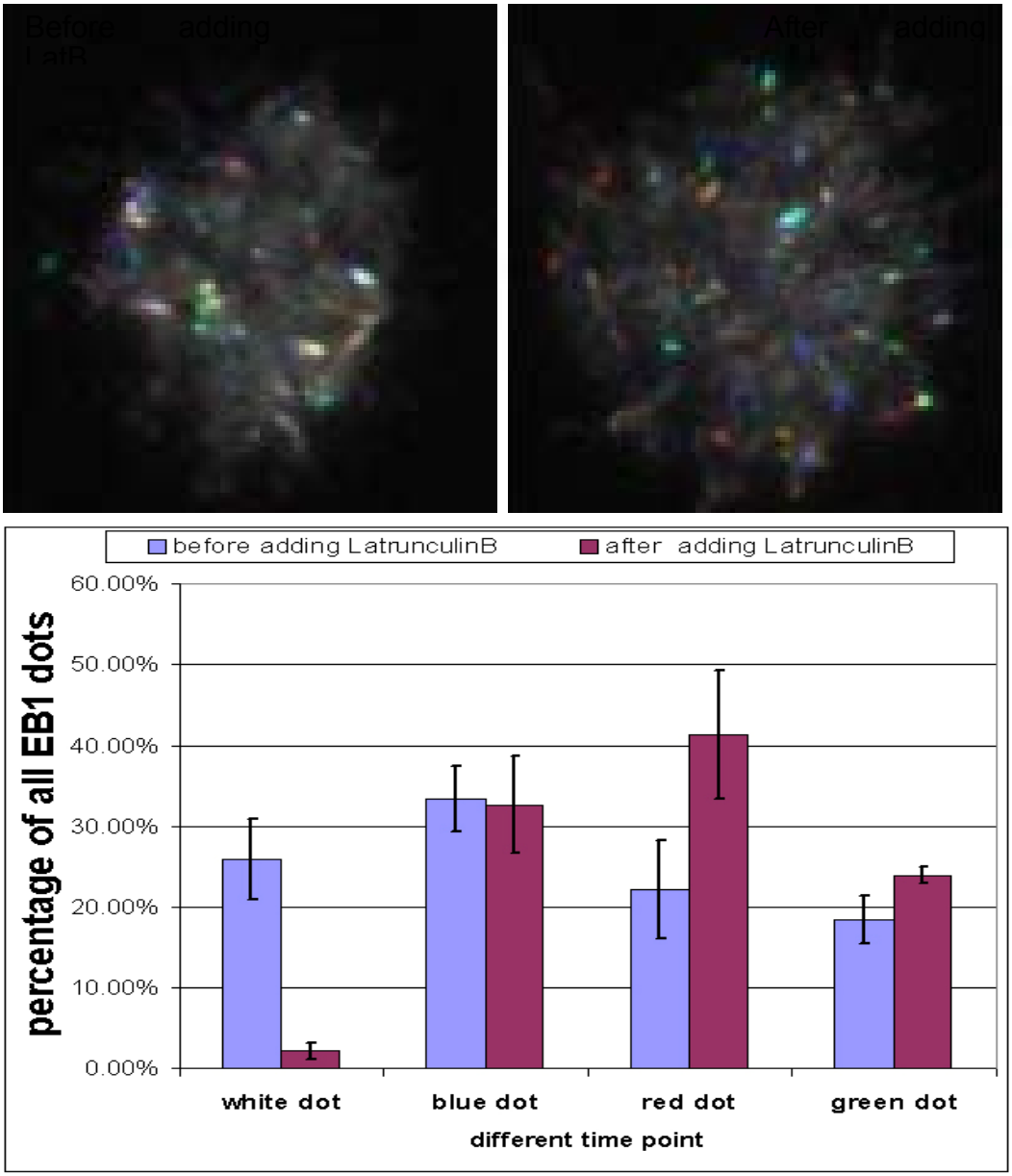

Figure 5-21 When actin structures are disrupted by LatB using TIRF microscope microtubule plus end become more dynamic and less EB1 dots stacked at cell cortex. By superimposing three sequential pictures from a TIRF movie in the different channels of an RGB image I illustrate the movement of EB1 dot before and after LatB treatment. A white dot means no change, blue, red and green dots appear when the position of EB1 dot has changed.

This quantification shows that while many GFP-EB1 dots pause at the cell cortex before drug treatment (white), most GFP-EB1 dots appear to move between timepoints after the addition of Latrunculin B. While this might suggest that Tao-1, actin filaments or other actin associated factors are

required to induce cortical microtubule catastrophe, independently of physical force, it is also possible that the cortex is frictionless in the absence of the actin cortical mesh, allowing microtubule plus ends to slide when they hit the membrane and the glass. If Tao-1 could be bound to the membrane in this experiment, however, I would be able to tell whether Tao-1 on the cortex can induce microtubule catastophe in the absence of actin.

Taken together, I think the answer for the first question is clear, that Tao-1 is on the cell cortex (dominant negative Tao-1 especially so). Furthermore, it seems likely that Tao-1 plays a role in helping microtubule plus end to know their location with respect to the cortex and to regulate their dynamic behavior appropriately.

Next, in order to test whether Tao-1 also changes the rate of catastrophe as microtubules hit the cell cortex, I took the advantage of GFP-EB1 stable S2 cell line to enable measurement of the life time of visible GFP-EB1 comets in interphase cells. Using images taken every 2 seconds I calculated the length of the time between the moment a GFP-EB1 tip hits the cell cortex and when it disappears to estimate the life-time of the growing microtubule filament by counting the number of frames between the first image when microtubule plus end contacts the cell membrane and last image when the GFP-EB1 disappeared. Using these data allows me

to test for statistical differences between the life time of a growing microtubule plus at the cell cortex in control cells, and cells expressing K56A-Tao-1 or and full-length Tao-1. The analysis showed that the survival time of a growing microtubule filament hitting the cell cortex in a K56A expressing cell, that has less active Tao-1, is significantly prolonged compared to a control (>2 fold increased) (see Figure 5-22). This suggests that kinase-dead Tao-1 prevents cortex dependent microtubule catastrophe. Conversely, overexpression of RFP-full-length Tao-1 slightly decreases the life-time of microtubule plus ends at the cortex. Why is the effect of Tao-1 overexpression so weak? I think a possible reason could be the confounding factor, mentioned previously, which is that the disruption of growing microtubules filaments leads to an increase of supply of subunits (α-tubulins and β-tubulins) in the cytoplasm, which drive filament growth. So the life time of surviving microtubules will not decrease too much. In addition, I might have missed catastrophes events which happened in less than 2 seconds. Nevertheless, taken together these data suggest that Tao-1 plays an important role during the interaction between the microtubule plus end and the cell cortex. Thus, Tao-1 may help to induce the catastrophe of a microtubule plus end when it hits the cell cortex. Summarizing all these data, the answer for second question is yes - Tao-1 does appear to be able to regulate the growing plus end of microtubules at the cell cortex.

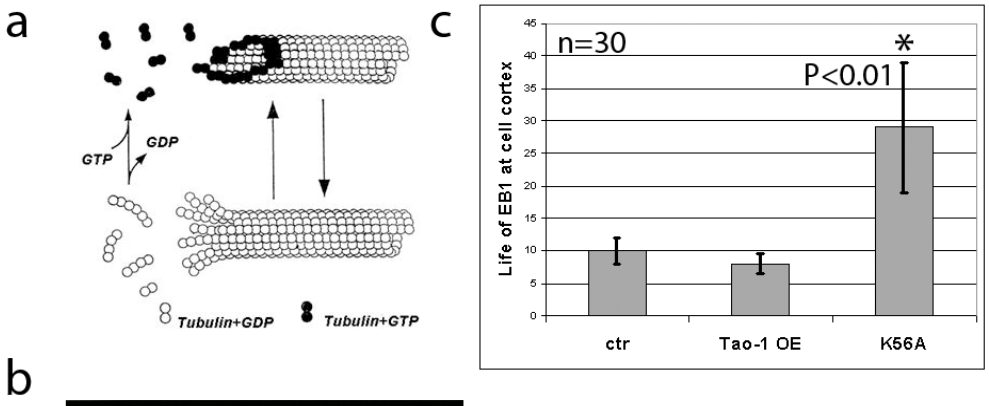

Figure 5-22 Tao-1 activates catastrophe of microtubule plus end at the cell cortex.
a. demonstrates the high dynamics of MT filament; b GFP-EB1 S2 cell has been used as a model to study the life time of EB1 at the cell cortex; c.EB1 Life time analysis shows K56A largely prolong the life time of EB1 in cell when they hit the cell cortex; Full length Tao-1 overexpression causes a slight decrease of the EB1 surviving time.

However, the results so far do not reveal the mechanism by which Tao-1 destabilizes microtubules and stops the growth of microtubule plus end at the cell cortex or the downstream substrate(s) for Tao-1.

5.9 EB1- A potential substrate for the Tao-1 kinase

It was shown above that the kinase domain is necessary for Tao-1's function. Thus, the next step is to find out the substrate of Tao-1 kinase. In order to get at this, I designed a small scale dsRNA library which targets mRNAs for all microtubule plus end binding proteins, all known microtubule destabilizers, kinesin-8 family members and kinesin-13 family members (all genes in this library has been listed in the additional file 6) .

Using this small RNAi library I carried out a modifier screen (see methods and materials). The aim for doing this experiment was to find potential downstream substrates of Tao-1 that may act in opposition to Tao-1 to rescue the Tao-1 RNAi phenotypes.

5.9.1 EB1 RNAi can partially rescue the Tao-1 loss-function phenotype.

In the Tao-1 RNAi modified screen, EB1 silencing was the only hit which could partially rescue the Tao-1 RNAi phenotype (see Figure 5-23). EB1 is a plus end binding protein that prevents microtubule catastrophe to stabilize microtubule growth [157]. It therefore seemed likely that EB1 RNAi would lead to an increase in the rate of catastrophe countering the ability of Tao-1 RNAi to stabilize microtubule plus ends in interphase. If this was the case, why didn't EB1 have a strong RNAi phenotype in S2R+ cells, like that of Tao-1 overexpression? In budding yeast, the double mutant CLIP170 and EB1 is dead but the fact that the single mutant can survive seems imply their function may largely overlap [158]. Moreover, previous work has shown loss-function of MAL3p (EB1 homologue in fission yeast) and TIP1p (CLIP-170 homology in fission yeast) result in a similar defect in polarized morphogenesis [159, 160]. This type of redundancy might explain why neither EB1 nor CLIP170 RNAi had any obvious morphological phenotype. In fact, the Rogers's lab recently

showed a kinesin-13 family member Klp10A can bind EB1 and induce the catastrophe [50].

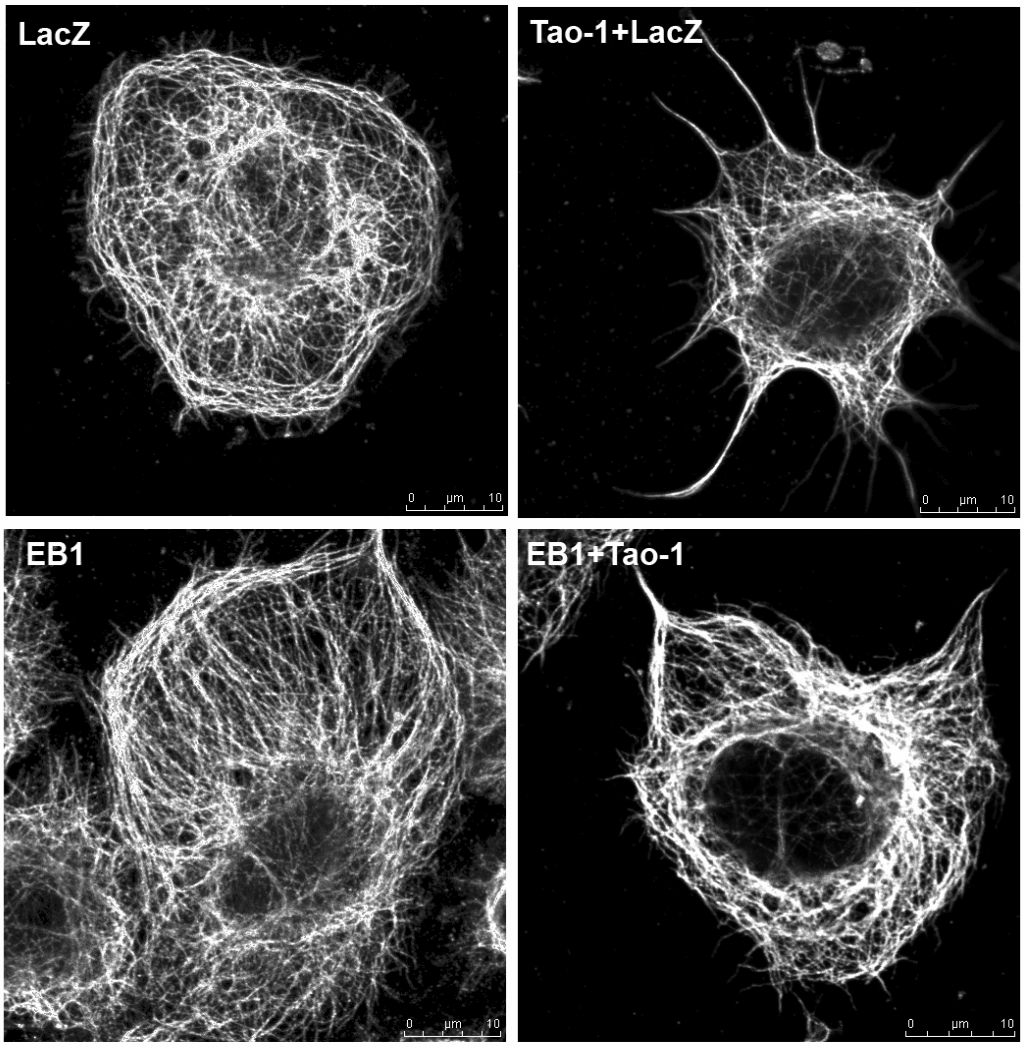

Figure 5-23 Tao-1 RNAi modifier screen identifies EB1 as a hit. EB1 RNAi can partially rescue the Tao-1 RNAi phenotype in S2R+ cells.

Although EB1 and Tao-1 could work in parallel, a potential model to explain this result could be that Tao-1 specifically inhibits the ability of EB1 to bind to or to remain bound to microtubule plus ends. Once EB1 has left, other microtubule plus end destabilizers like Klp10A will then be able to

induce catastrophe from the plus end [51]. If this is true, I should see less EB1 comets at the cell cortex in Tao-1 overexpression cells.

5.9.2 Overexpression of Tao-1 can inhibit EB1 binding to microtubule plus ends.

In order to explore if Tao-1 can have its effect on microtubule plus end binding protein EB1 at the cell cortex, I used the TIRF microscope to study the GFP-EB1 comet density at the cell cortex. The TIRF microscope images at the bottom 90nm of the cell cortex. This analysis showed that there are many fewer GFP-EB1 comets existing in RFP-Tao-1 overexpressed cell surface (see Figure 5-24). Thus, one function of Tao-1 may be to inhibit EB1 binding, increasing the rate of catastrophe.

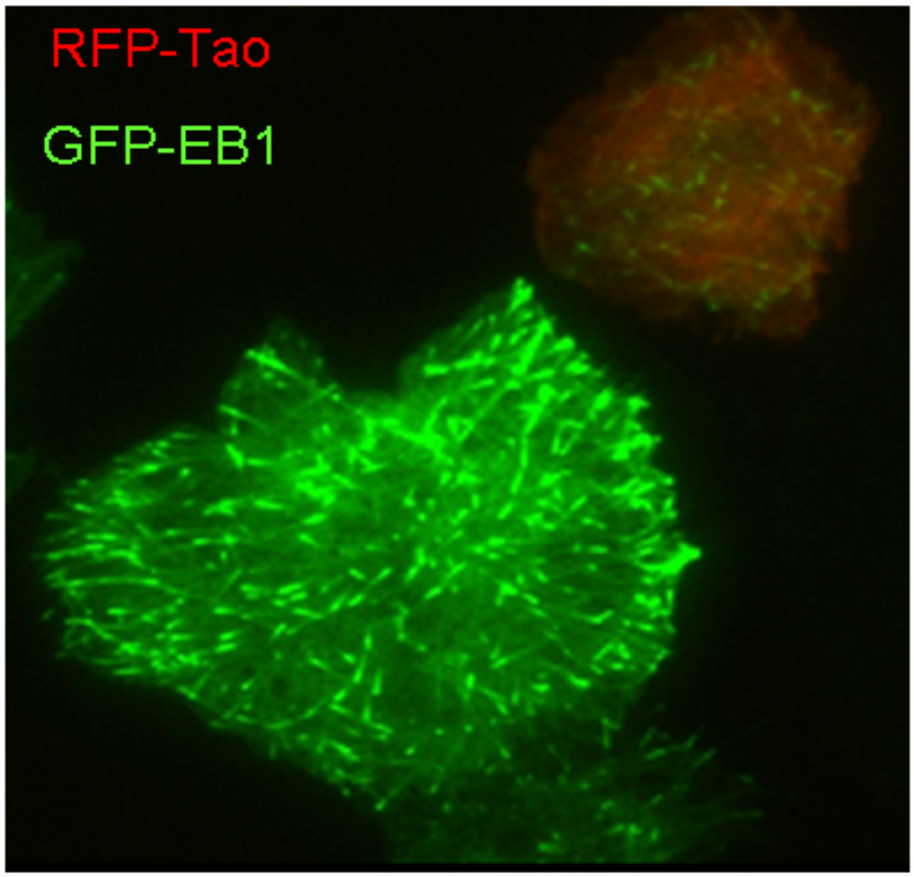

Figure 5-24 OE RFP-Tao-1 inhibits GFP-EB1 binding to microtubules

Seeing RFP-Tao-1 protein directly by TIFR live imaging also supports the idea that Tao-1 is concentrated at the cell cortex.

5.9.3 Overexpression of EB1 can rescue Tao-1 OE phenotypes.

To strengthen this hypothesis I then tried the opposite test. I transfected RFP-Tao-1 expressed from an Act5c promoter into pMT-GFP-EB1 S2 cells, to enable me to co-express both GFP-EB1 and RFP-Tao-1 in parallel, by using $CuSO_4$ to control the expression of EB1.

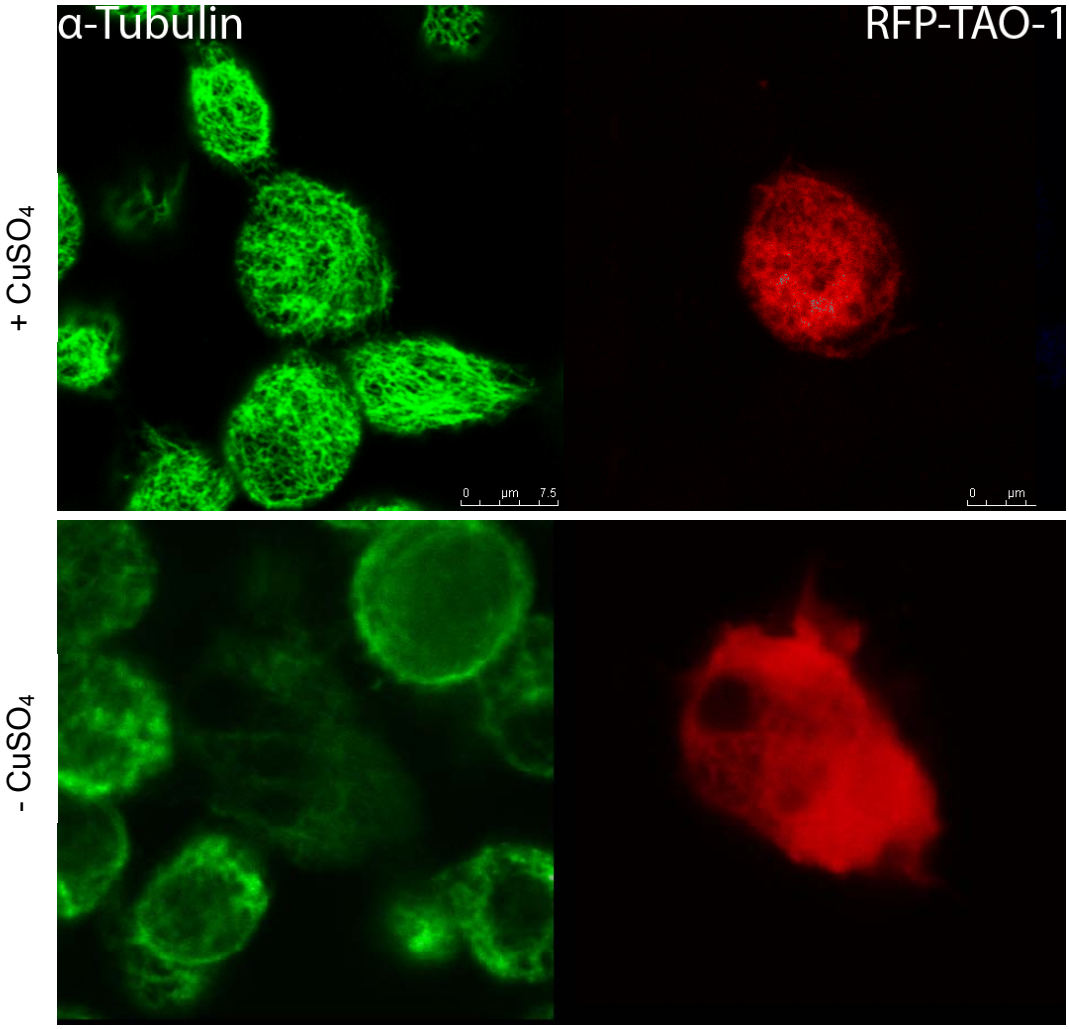

Figure 5-25 EB1 overexpression can rescue Tao-1 overexpression phenotype.
Top panel shows overexpression of GFP-EB1 induced by adding $CuSO_4$ can rescue OE Tao-1 phenotype
Bottom panel shows MTs were destroyed when cells overexpress Tao-1 alone.

The result is shown in Figure 5-25. Cells were in the M3 media +/- 70nm $CuSO_4$ for 24 hours before the fixation. Strikingly, the microtubule network looks denser in cells overexpressing EB1 than in a control experiment without $CuSO_4$ (shown in the bottom panel). Moreover, whereas RPF-Tao-1 overexpression disrupted the microtubule network in S2 cells in the absence of copper, it did not in the EB1-GFP expressing cells, which look

similar to adjacent non-transfected cells.

These data suggest that EB1 could be the effector of Tao-1 or may act in opposition to Tao-1, with Tao-1 inhibiting EB1 directly or indirectly, preventing it binding the plus ends of microtubules. During early mitosis, EB1 is localized to separating centrosomes and associated microtubules, while at metaphase it is associated with the spindle poles and associated microtubules. During cytokinesis EB1 was strongly associated with the midbody microtubules [54]. Interestingly, P-Tao-1 has a similar localization in mitosis (see below), supporting the idea that the two proteins functionally interact. Moreover, EB1 has several potential phosphorylation sites [55, 161], suggesting the possibility that Tao-1 may regulate EB1 by phosphorylation.

5.10 Y2H screens identify potential Tao-1 interactors

In order to find out the mechanism of Tao-1 to destabilize microtubules, a Y2H screen was carried out by sending the full-length *tao-1* construct to a commercial company (Hybrigenics). *Drosophila* Tao-1 (281-1039) has been used as the bait fragment to test the interaction against preys from a *Drosophila* whole embryo cDNA library (0-12+12-24).

	strength of the interaction
CyclinG	a
Khc	a
RNRL	a
S6K	a
MASK	a
Nesprin	a
Tao-1	b
Khc-73	b
CG15087	b
CG6181	b

Table 5-2 Y2H screen results
a means very high confidence in the interaction; b means High confidence in the interaction

In the list of genes identified with a high confidence interaction with *tao-1*, several are microtubule binding proteins. These include Khc. Khc is a kinesin-1 family member that transports proteins from minus end to the plus end of microtubules [162]. However, Khc RNAi did not result in a Tao-1 knock-down phenotype and didn't prevent the Tao-1 overexpression phenotype. Thus, more work is needed to explore the possible relationship between Tao-1 and Khc. But, it is an interesting topic to track down. I will also discuss the perspectives work in chapter 6. Similarly, I would also like to explore possible links between Tao-1 and Khc-73. Alternatively, this could mean that Tao-1 simply binds to regions common to many kinesins.

Finally, the fact that Tao-1 itself was identified in the Y2H screen as a confident hit supports my previous results that overexpression of the kinase domain deletion mutant RFP-delta-51-345 Tao-1 causes the dominant negative phenotype, implying that the Tao-1 coiled-coil domain may interfere with the function of endogenous Tao-1. Again more needs to

be done to explore this further.

5.11 Study of Tao-1 signaling

Tao-1, a STE20 family kinase, seems work on microtubule plus ends to regulate the dynamic instability from the above results. I found microtubule plus end binding protein EB1 could be the downstream effector or cooperator with Tao-1. However, how cells regulate Tao-1 to realize its function is still not clear. To explore the activation of Tao-1, I used a comparison with its human homologues to identify the T-loop phosphorylation site on Tao-1, which should label the active kinase [138, 141], and used it to make a P-Tao-1 antibody. The rabbit P-Tao-1 antibody was made based on the sequence CONH2-RAQRATS[P]NVFAMC+3 and ordered from Eurogentec. A phosphorylation site point mutant Tao-1 GFP-S180E construct was also made to study phosphorylated Tao-1's function and regulation.

5.11.1 Localisation of P-Tao-1

It is important to know the localization of a protein as well as its function. Both P-Tao-1 antibody staining and GFP-S180E show that P-Tao-1 is present in puncta at the cell cortex and is concentrated in the nucleus of interphase S2R+ cells (see Figure 5-26 and figure 5-27).

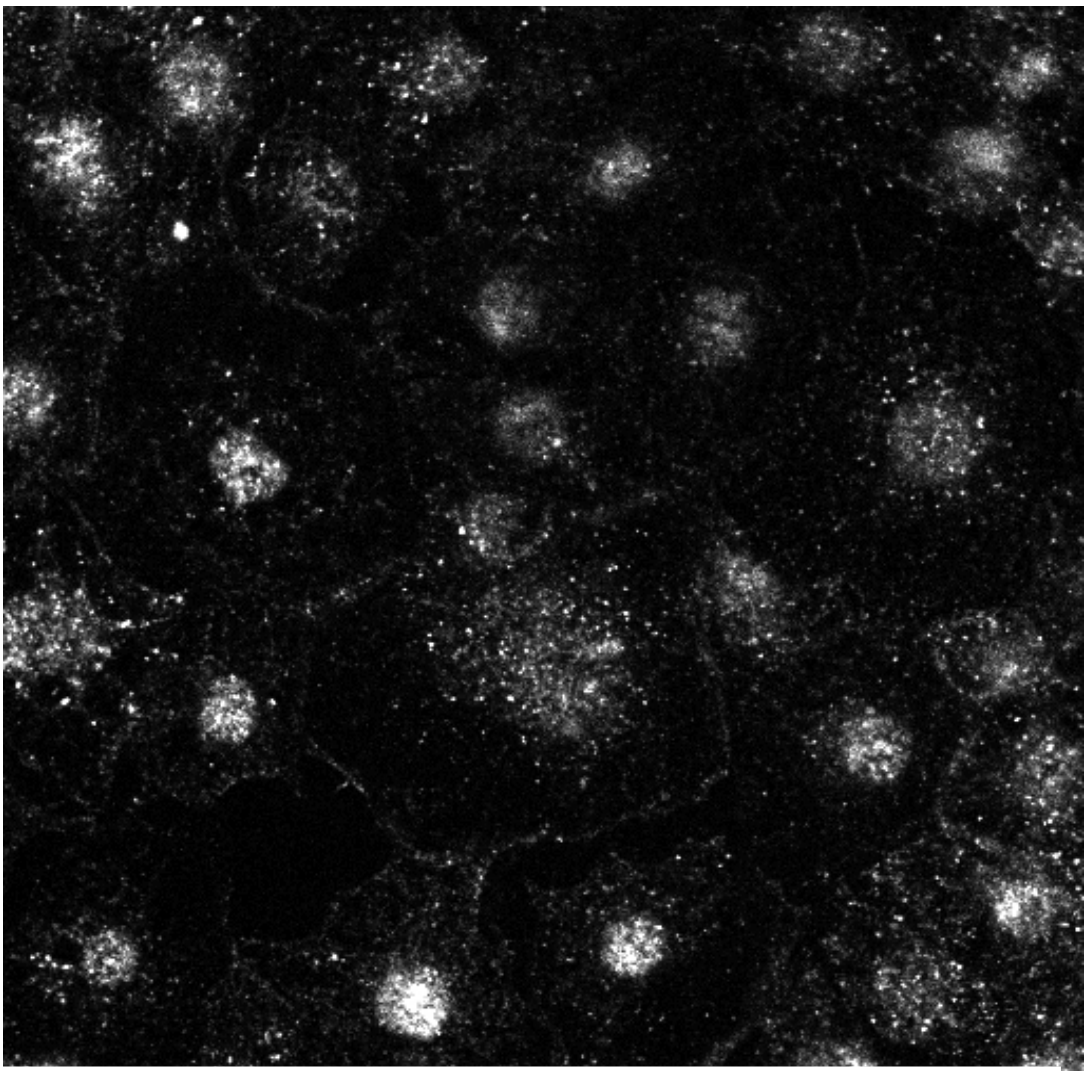

Figure 5-26 P-Tao-1 antibody staining shows P-Tao-1 can be seen as puncta at S2R+ cell cortex and in the nucleus.

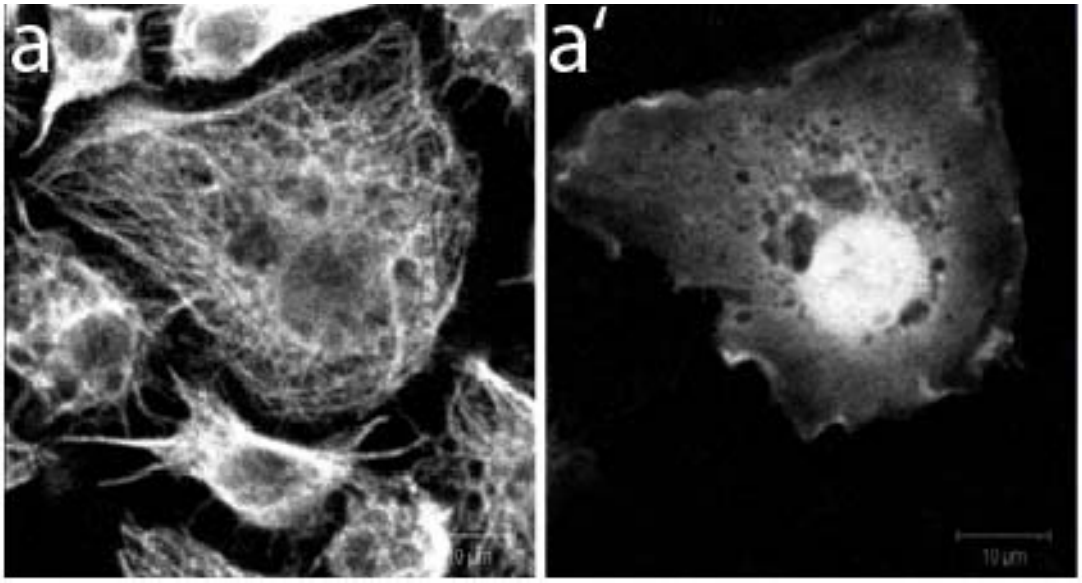

Figure 5-27 GFP tagged phospho-mimic Tao-1 GFP-S180E localizes to the cell cortex and concentrates in the nucleus which is same with P-Tao-1 antibody results.
a shows MTs stained with Dm1α; a' shows GFP-S180E.

This is different to Tao-1 localization, suggesting only a small pool is phosphorylated. I also observed P-Tao-1's localization during mitotic stage (These data were obtained with the help of Pato Kunda to find out enough mitotic stage S2R+ cells). First, in metaphase, P-Tao-1 colocalises with the mitotic spindle and is concentrated at centrosomes as shown in Figure 5-28, as confirmed using a CNN antibody kindly given to me by Jordan Raff's lab. In cytokinesis, Tao-1 was strongly associated with the midbody microtubules (see Figure 5-29). As I mentioned above, the localization of P-Tao-1 is similar to EB1 during mitosis which supports the hypothesis that Tao-1 may work together with EB1 or may directly regulate EB1 by phosphorylation. To test this, I have to do the biochemistry work which will be discussed in chapter 6.

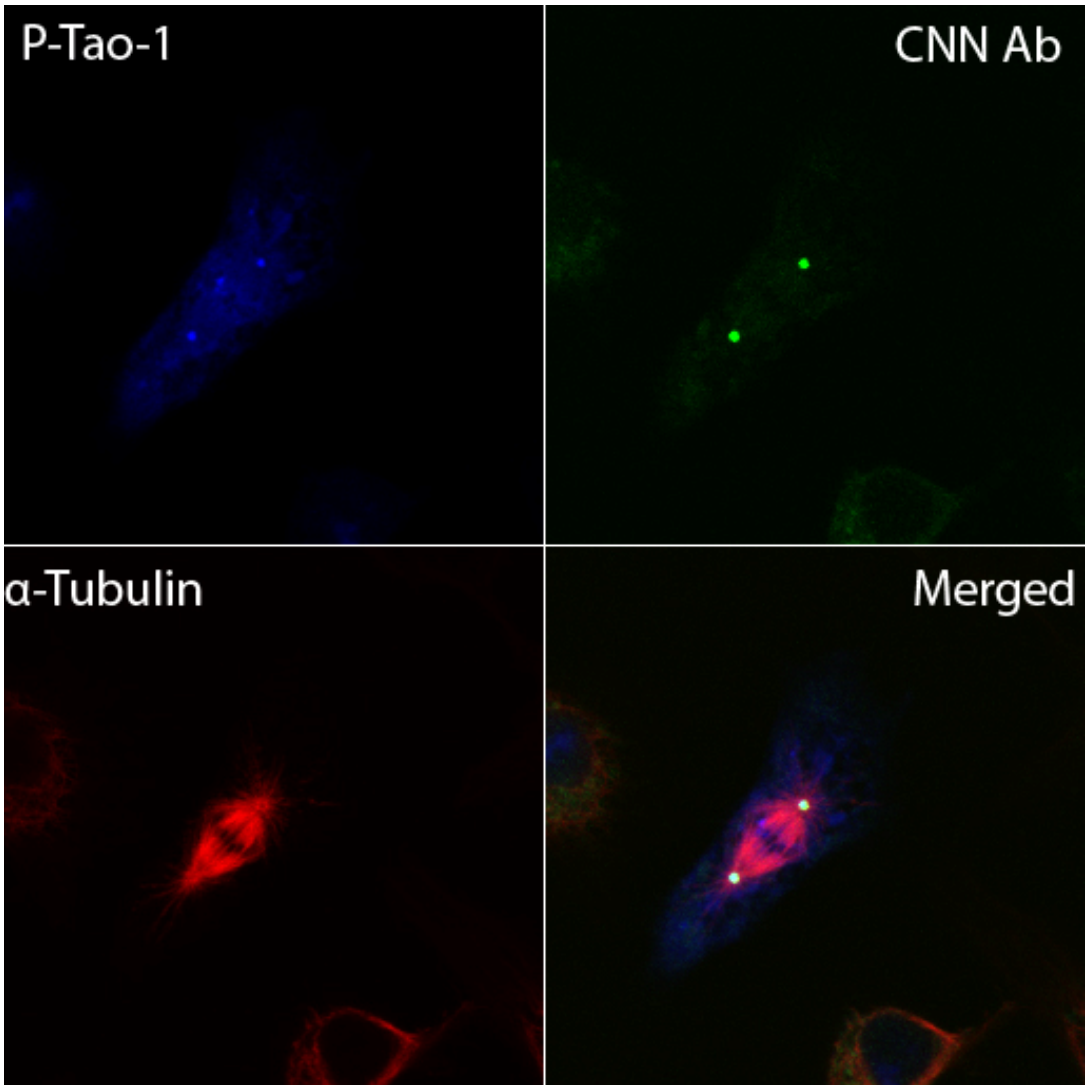

Figure 5-28 P-Tao-1 colocalizes with mitotic spindle and concentrates at centrosomes as confirmed by CNN staining (antibody a gift from Jordan Raff).

Unfortunately, I didn't find any mitotic cells overexpressing GFP-S180E (the phosphorylation mimetic Tao-1) to enable me to visualise the dynamics of P-Tao-1 during the mitotic stage. P-Tao-1 has been shown to be the active Tao-1 [138]. I was also able to show that P-Tao-1 is likely to be the active form of the protein because I stained cells expressing the hyperactive RFP-delta-422-900 ERM-like domain deletion mutant and

found they are full of phosphorylated Tao-1 (data not shown).

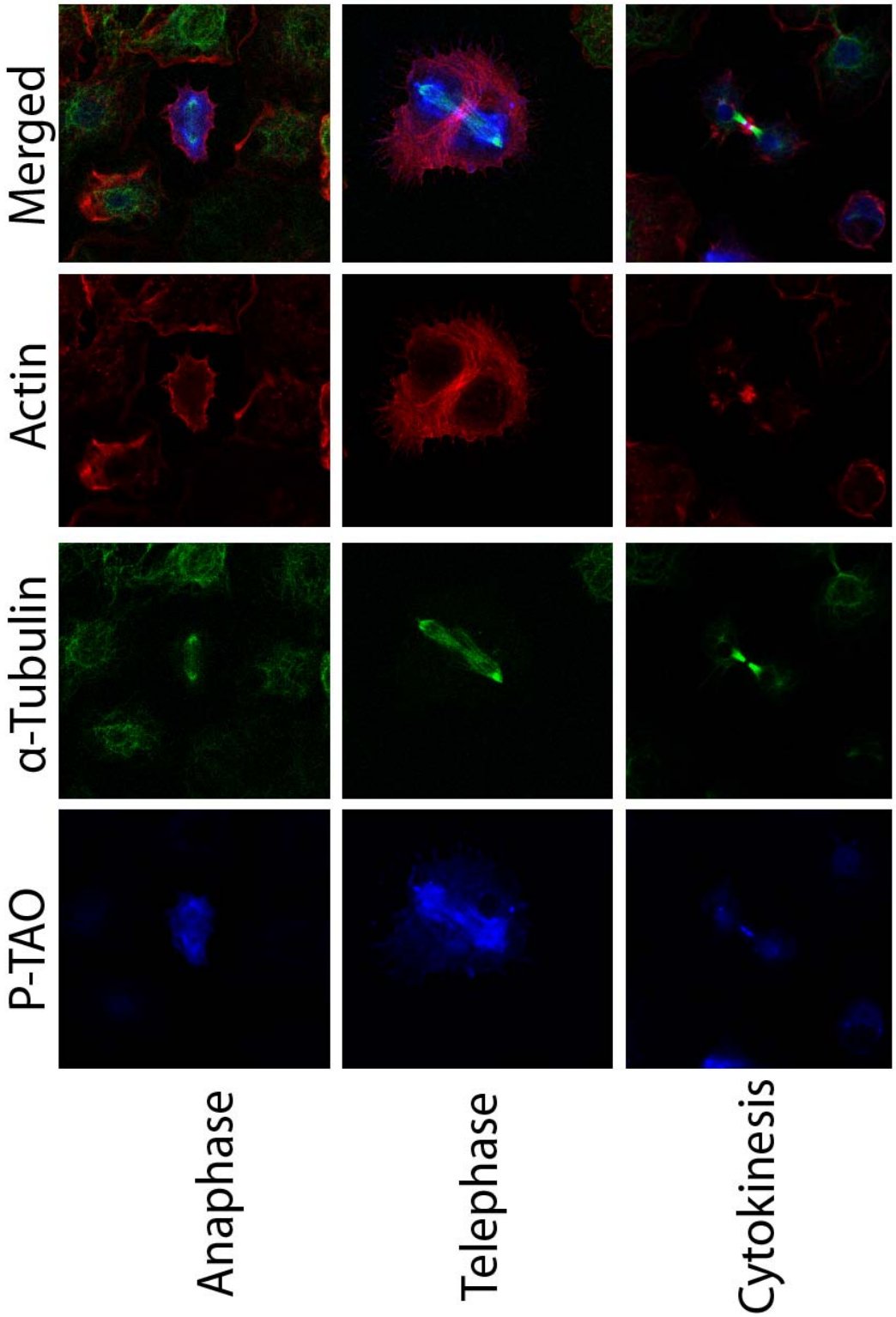

Figure 5-29 P-Tao-1 localisation in mitosis
P-Tao-1's co-localisation with mitotic spindle and centrosome in mitosis (stained with 1:1000 P-Tao-1 rabbit antibody)

5.11.2 P-Tao-1 antibody screen results in the finding of potential regulators of Tao-1

As mentioned above, *Drosophila* Tao-1 is a very high conserved Serine/ Threonine kinase. It has a T-loop phosphorylation site which can be phosphorylated by upstream kinases. The dsRNA kinase library I made for the multiple cell line screens allow me to knock down each different kinase in *Drosophila* to find out which kinase take the responsibility of phosphorylating Tao-1 by detecting the level of P-Tao-1 antibody. In this way, I identified a group of kinases which cause a increase or decrease in P-Tao-1 level (see Table 5-3).

Cell line tested	Gene name	P-Tao-1 antibody level
S2R+	Bsk	decrease
S2R+	Tor	decrease
S2R+	Pp1-87B	increase
S2R+	Gprk1	decrease
S2R+	Caki	decrease
S2R+	Strn-Mlck	decrease
S2R+	Pi3K68D	decrease
S2R+	Ipp	decrease
S2R+	CG3573	decrease
S2R+	Mekk1	decrease
S2R+	Slpr	decrease
S2R+	CG3632	decrease
S2R+	auxillin	decrease

Table 5-3 Potential upstream regulator of Tao-1 kinase from kinase-wide screen using P-Tao-1 antibody

In the hit list, *bsk* and *slpr* have been known involved in JNK pathway, which supports the published data that Tao-1 is involved in JNK signaling pathway, as knocking down these two genes lead to the decrease of P-Tao-1. However, the fact that *bsk* and *slpr* RNAi didn't show a Tao-1 RNAi

phenotype suggests that Tao-1's regulation of microtubules might be independent of JNK pathway.

In cultured mammalian cells, mitogen-activated protein kinase (MAPK) pathway is activated in response to a variety of environmental stresses. *Drosophila* MEKK1 is structurally similar to the mammalian MEKK4/MTK1 MAPKKK. *Drosophila* MEKK1 null mutants are hypersensitive to environmental stresses, including elevated temperature and increased osmolarity [163]. Taken all these results together, it suggests a possible role for Tao-1 in the stress response.

Pi3K68D is one of the subunits of PI3K which is very important cell signaling pathway involved in many cell morphogenesis. Recently, our lab showed that in the context of acute phosphoinositide 3-kinase (PI3K) signalling, dynamic changes in cofilin phosphorylation were found to depend [164] on the Ssh phosphatase and then on changes in lamellipodial F-actin. It gives a hint that Tao-1 could be also involved in the actin regulation in somehow.

PI3K signaling from Akt to FRAP/TOR targets S6K in *Drosophila* [165]. Tor RNAi leads to the decrease of P-Tao-1's level. Combined with the result from Y2H screen which identified S6K as a confident hit, it seems possible that the PI3K-Akt-Tor-S6K pathway is linked to Tao-1's function. All these ideas need be tested further before making firm conclusions

though.

5.11.3 Depolymerization of microtubules causes an increase in P-Tao-1 levels

One more interesting result from my experiments was the finding that Nocodazole treatment dramatically increases levels of P-Tao-1 in S2R+cells (see Figure 5-24 a), even though it only has a mild effect on microtubules. Interestingly the increase of P-Tao-1 is confined to the nucleus. Perhaps destroyed microtubules fail to retain P-Tao-1 in the cytoplasm and cause the accumulation of P-Tao-1 in the nuclear part – as seen with the Tao protein that lacks coiled coil functions. The increase in Tao-1 levels was confirmed by western blotting as shown in Figure 5-24 b. These data suggest the posibility that microtubule depolymerization may activate Tao-1 function while Tao-1 activation may inhibit microtubule depolymerization.

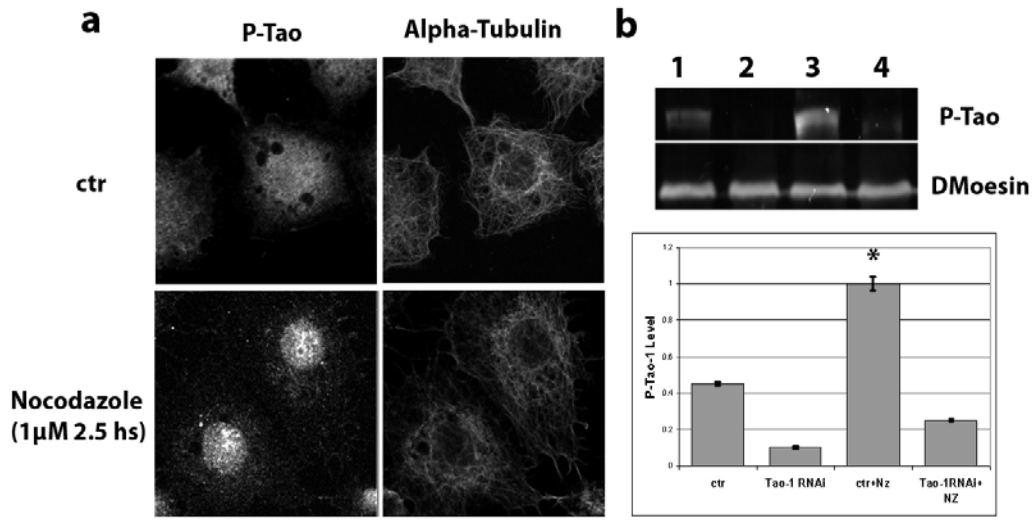

Figure 5-30 MTs depolymerization causes a dramatical increase of P-Tao-1 level in interphase S2R+

5.12 Conclusions

In summary, I have identified *Drosophila* Tao-1 as a novel microtubule regulator that binds weakly to microtubules to inhibit their growth. Tao-1 functions as a microtubule destabilizer independent of the Par-1/Tau pathway. Microtubule dynamic analysis data suggest that Tao-1 has effects on microtubule plus ends especially at the cell cortex, while Tao-1 can bind actin structures at the cell cortex. The loss of an actin filament rich cortex may cause Tao-1 to leave the membrane to induce a Tao-1 RNAi like phenotype in which microtubules fail to stop at the cell cortex. Lack of Tao-1 results in increased dynamics of EB1 at the cell cortex and fewer catastrophes happened when microtubule filaments hit the edge of the cell border. Moreover, P-Tao-1 localization during mitosis is similar to

that of EB1 as presented in published data [166]. Furthermore, Tao-1 seems to inhibit EB1 binding to microtubule plus ends and GFP-EB1 OE can partially rescue the Tao-1 RNAi phenotype. EB1 has been reported to have several potential phosphorylation sites, so could be a substrate of Tao-1. Finally, Y2H screen results and P-Tao-1 kinase screen results suggest a group of candidates that could be involved in the Tao-1 signaling pathway. Taken together, I think it seems likely that Tao-1 is a key regulator of microtubule dynamics in interphase and mitotic stage in fly cells as it is in human cells.

These data suggest a novel mechanism by which cells may regulate microtubule dynamics by using a localised kinase to regulate the cross talk between microtubules and actin structure at the cell cortex.

Chapter 6

Discussion and Future Work

6.1 Introduction

The aims of this thesis were to identify novel generic and cell type specific regulators in the signal-transducing cascades that control cell morphology using high-throughput RNAi screens in different cell lines with different shapes. Through this work, I have identified a core set of kinases required for the normal morphology of all cell lines examined, together with kinases whose requirement is specific to cell lines with a common tissue of origin. This identified a role for *minibrain (mnb)*, a kinase associated with Down's Syndrome (DYRK1A), in the regulation of actin-based protrusions in cell lines derived from neuronal lineages. The specificity of this effect was not due to cell-origin specific differences in cell shape, since it was cell shape independent. In addition, it could not be attributed to differential gene expression, since I was unable to find any correlation between gene expression and function in this analysis. Furthermore, these screens identified an STE20 kinase Tao-1 as a regulator of microtubule plus end instability that controls cell shape in all lines tested. Thus, I believe that this work has contributed to the understanding of the regulation of cell shape in *Drosophila* and will be useful for people studying the signal cascades underlying the cell morphology in the other organisms, since these genes are highly conserved in metazoa.

6.2 Quality control - A key factor in High-throughput RNAi screens

The mechanism of RNAi can generate sequence-specific off-target effects (OTEs), when a siRNA shows significant sequence homology to mRNAs other than its chosen target. Sequence specific off target effects can also result from activation of the miRNA response, leading to the translational repression of off-target mRNAs. Both effects can generate false positives, as has been discussed in many studies. In large scale high-throughput RNAi screens, this can result in a considerable number of false positives. This is thought to be less of a problem when dealing with *Drosophila* cell screens, because the use of long dsRNAs reduces OTEs by summing the non-specific effects of each constituent siRNA present at low levels, while maintaining silencing of the common target. Although a lot of efforts have been made to predict sequence-specific OTEs from sequence data [94], the simplest strategy to minimise this problem is to verify that at least two dsRNAs targeting different regions of the same gene have the same phenotype. If so, then it is likely to be a real phenotype since the chances of generating the same off-target effect are usually negligable. In this study, I used this strategy to design my screens. Although the 2 libraries didn't complement one another for all genes, about 2/3 of the genes in this analysis have been screened at least twice using distinct dsRNAs

generated using different oligos. When analysing the results, I found that the percentage of hits confirmed as positives in screens using both these two libraries was variable, from 79% in BG2 cells to 53% in S2R+ cells, which I considered quite poor. This led me to re-test those genes which failed to be confirmed by both libraries. For the remaining 1/3 of genes that were not covered by the 2 libraries, I estimated a false positive rate between 6.7% and 12.5% based on my analysis of a 3rd dsRNA generated from new oligos. It is also very import to select the appropriate positive and negative controls in the microscope-based cell morphology assays, as a control is needed for each phenotypic class. Multiple negative controls enable the evaluation of experimental false positives and facilitate data normalisation by providing an estimate of the biological and technical variability in the system. This is very important because the data quality depends on the screen reproducibility. In summary, my data suggest that identifying the false positives caused by OTEs in a high-throughput RNAi screen is a key point of quality control which needs to be considered before following up the interesting hits. To avoid the artefacts caused by OTEs in RNAi screen *in vivo* and *in vitro*, it is strongly suggested by my work that two oligos or hairpin RNAi targeting different regions of the gene of interest should be designed at the beginning of the screening work.

6.3 Cell type specific morphological regulator- Mnb

Using parallel RNAi screens in different cell lines I have identified a new CNS-specific cell function for *minibrain*/DYRK1A, a protein previously shown to play a role within both the fly and mammalian CNS, in the regulation of the structure of actin-based protrusions. I have also shown how this functional genomic approach can be used to differentiate between generic and cell type specific gene functions, and to use this functional data to cluster cells into groups of lines that are related by both origin and morphology. Finally, although these groups resemble clusters generated using a gene expression array analysis, my study reveals the dangers of using gene expression data to predict function, and in doing so demonstrates the importance of cell-type specific RNAi screening as an approach for dissecting pathways of cellular control. Moreover, my results also suggest that the screen results from one cell type cannot be extrapolated to all cell types since some genes have cell type specific functions even if they do not have cell type specific expression patterns.

6.4 Drosophila Tao-1 is a regulator of microtubule plus end dynamics at the cell cortex

In this work, I identified Tao-1 in a series of kinome RNAi screens carried out using multiple *Drosophila* cell lines from different tissues. Tao-1 was the kinase with the most pronounced effect on microtubule organisation

across all lines tested. In each case, the silencing of Tao-1 caused cells to accumulate bundled microtubules. These microtubules fail to stop at the edge, pushing on the cell cortex to generate protrusions that give cells a characteristically spiky shape, similar to cells that lack cortical actin filaments, e.g. Scar RNAi cells [129]. Using S2 cells carrying the GFP-EB1 marker I showed that microtubules in Tao-1 RNAi cells have a greatly reduced chance of undergoing catastrophe when they meet the cortex. Significantly, this effect is mimicked by the over-expression of a kinase dead Tao-1 or overexpression of a kinase domain deletion mutant, demonstrating a likely requirement for Tao-1 kinase activity in the destabilization of microtubules. Conversely, Tao-1 overexpression reduces the microtubule density, apparently by increasing the frequency of microtubule catastrophe.

Using a stable S2 cell line expressing GFP-EB1, I was able to record the dynamics of microtubules plus ends *in vivo* in the presence or absence of Tao-1. These data show an absence of microtubule plus end pausing in Tao-1 RNAi cells and in cells expressing the kinase dead mutant variant. An RNAi modifier screen identified proteins that might genetically interact with Tao-1. EB1 RNAi was the only regulator of microtubule dynamics tested that was able to rescue Tao-1 loss-of-function phenotypes. Surprisingly, in the opposite experiment, the overexpression of EB1 was

able to rescue microtubules following Tao-1 overexpression. These data suggest the hypothesis that EB1 and Tao-1 functionally interact.

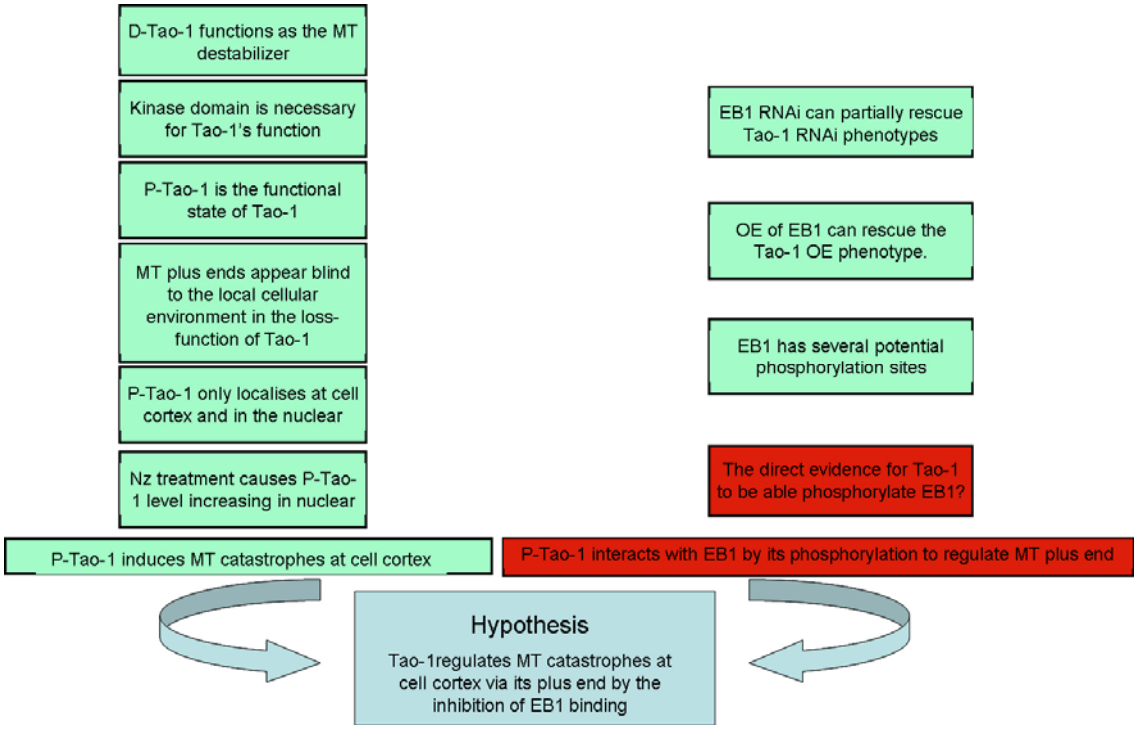

Figure 6-1 A hypothesis based on the data in this study suggests that Tao-1 regulates MT catastrophes at the cell cortex via its plus end by he inhibition of EB1's binding. Green boxes represent the data already generated, while the red boxes indicate the hypothesis that need to be proved; Light blue represents the hypothesis resulting from all of the above.

In summary, as shown in Figure 6-1, I have identified *Drosophila* Tao-1 as a novel microtubule regulator that inhibits the growth of microtubules at the cell cortex via their plus end. The key results can be explained by a simple model that describes how Tao-1 functions as a microtubule destabilizer at the cell cortex to regulator the dynamics of microtubule filaments via their plus ends by the inhibition of EB1's binding (see Figure 6-2).

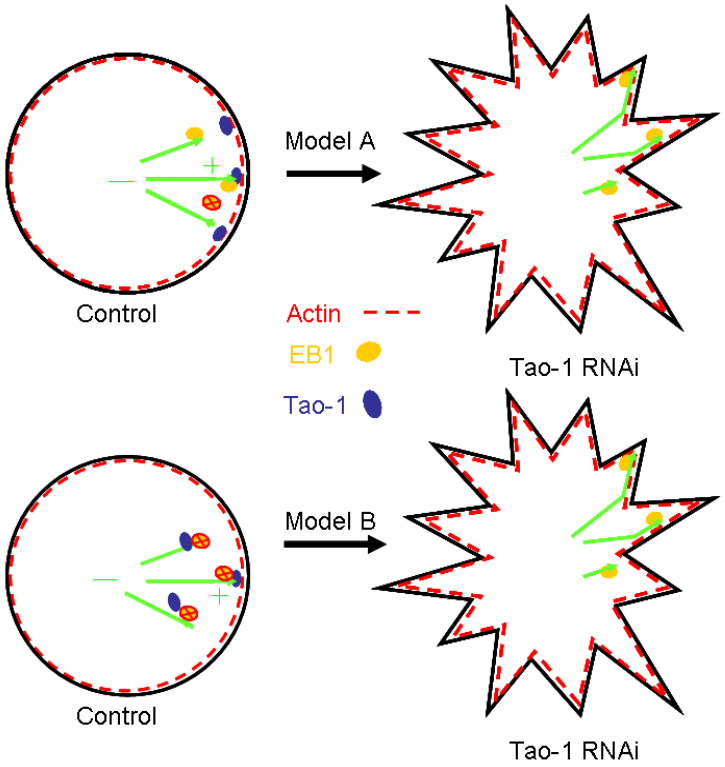

Figure 6-2 Working models for Tao-1's role in the regulation of microtubule dynamic instability in the interphase cells. Model A shows Tao-1 working on the cell cortex to regulate microtubule plus ends via EB1. An alternative model B shows the possible way that Tao-1 could destabilise microtubules directly, leading to reduced growth and reduced EB1 binding.

In this model, inactive, non-phospho Tao-1 in the cytoplasm could be activated by binding actin and/or components of the actin cortex. P-Tao-1 then induces microtubule plus end catastrophe when the growing microtubule filaments hit the cell cortex by inhibiting EB1, perhaps by phosphorylation. Active Tao-1 may then be removed from the cytoplasm because of the destruction of microtubules, and sequestered in the nucleus. Such a mechanism would enable cells to use spatial regulation of Tao-1 activity to inhibit the growth of microtubules when they contact the cell edge, in which case Tao-1 is playing a role in the cross-talk of

microtubules and the actin cortex.

An interesting question raised by the above model is: how could Tao-1/P-Tao-1 change its localization between the nucleus, cytoplasm and the cell cortex? My interest in Khc derives from the Y2H screen for Tao-1 interacters, which identified Khc as a likely Tao-1 partner. Khc is a kinesin-1 family member, which is responsible for the transport of proteins from the minus to the plus end of microtubules [162]. I used Khc RNAi to test for functional interactions between the proteins. However, loss-of-function of Khc did not result in a Tao-1 knock-down phenotype and the Khc knock-down failed to rescue the Tao-1 overexpression phenotype (data not shown). Nevertheless, in S2R+ cells recovering from cold shock, Khc RNAi had a strong microtubule phenotype, causing bundled microtubules to accumulate in circular bundles parallel to the cell cortex after a 10 minute recovery at room temperature (see Figure 6-3). A similar phenotype was reported by the Roger's lab in S2 cells [23]. This suggests the possibility that Khc, like Tao-1, controls microtubule stability. More works needs to be done to explore the relationship between Tao-1 and Khc, for example, by looking at the effects of Khc RNAi on the localisation of Tao-1. This will be an interesting topic to follow up. The other kinesin which shows a confident interaction with Tao-1 in Y2H is Khc-73 which has been reported to localise at astral microtubule plus ends during

mitosis and function in microtubule/Khc-73/Dlg pathway to regulate the cell polarity [167]. Thus, Tao-1 could be involved in this pathway by interacting with Khc-73. However, the fact that Khc-73 RNAi in interphase S2R+ didn't display a similar phenotype of Tao-1 RNAi might suggest that Tao-1 functions at the cell cortex independent of Khc-73 whereas Tao-1 could play a role in the Khc-73 pathway during mitosis.

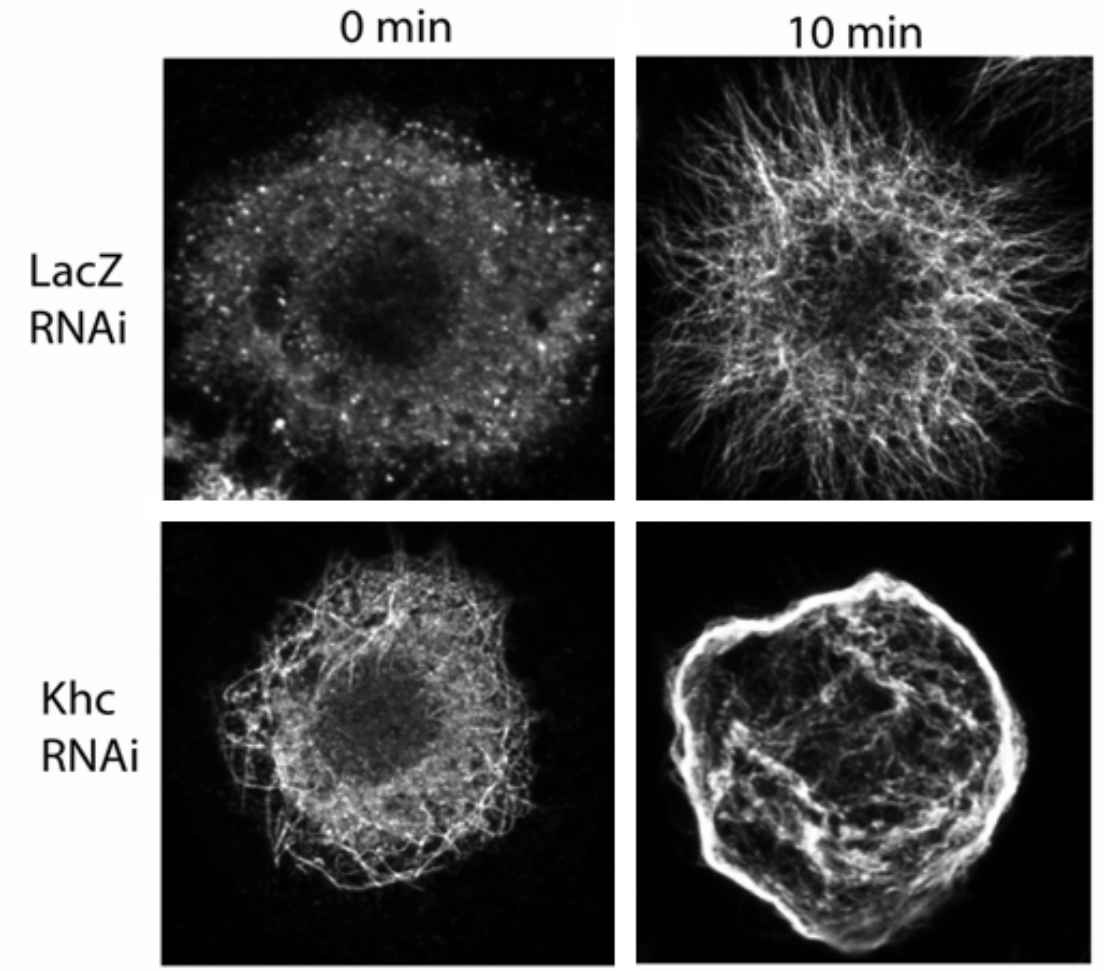

Figure 6-3 Khc RNAi in S2R+ cell causes microtubule phenotypes in cold shock recovery experiment.(MTs were fixed by -20 degree cold MethOH and stained in 1:1000 DM1α.

A weakness of this working model is its reliance on the localisation of Tao-1/P-Tao-1's during interphase at the cell cortex. While a population of Tao-

1 protein appears to be localised to the cortex, Tao-1 is also found in the cytoplasm, on microtubules and in the nucleus. Moreover, the 400-900 deletion mutant appears to be able to remove all MTs regardless of their localisation. These observations suggest a possible alternative working model. In this alternative model, Tao-1 could destabilize microtubules throughout the cytoplasm in interphase cells. Tao-1 could do this by destabilizing microtubules directly, leading to reduced growth and reduced EB1 binding, or by inhibiting EB1's binding to microtubule plus ends. It remains to be tested which of the two models is correct.

This analysis also points to complexities in the regulation of Tao-1. First of all, as I mentioned in the section 5.5.3, the coiled-coil deletion mutation of Tao-1 relocalises to the nucleus. I think there are two possible mechanisms responsible for this change in its localization. 1) The nuclear localisation of Tao-1 is regulated and loss of the coiled-coil domain allows entry into but not export from the nucleus. 2) Tao-1 requires its coiled-coil domain to bind Khc, which keeps Tao-1 bound to microtubules in the cytoplasm and which transports the protein to the cell cortex. To test these two possibilities, I analysed the Tao-1 protein sequence using a database (http://cubic.bioc.columbia.edu/cgi/var/nair/resonline.pl) that predicts Nuclear Localization Signals. This shows that Tao-1 has a typical NLS (*MRKFKRKR)* beginning at amino acid 725 (see Figure 6-4). In addition,

Tao-1 has a Nuclear Export Signal at L881, based on an analysis using the NES prediction tool (http://www.cbs.dtu.dk/services/NetNES/). Although the coiled-coil deletion (delta900-1039-Tao-1) retains both sequences, it is possible that it may affect the activity of the nearby NES, leading to nuclear retention. The presence of an NLS and NES in Tao-1 suggests the hypothesis that Tao-1 may have a function in the nucleus or may be regulated by shuttling between the cytoplasm and nucleus. It is unlikely to function in the nucleus however because overexpression of the coiled-coil mutant has no phenotype.

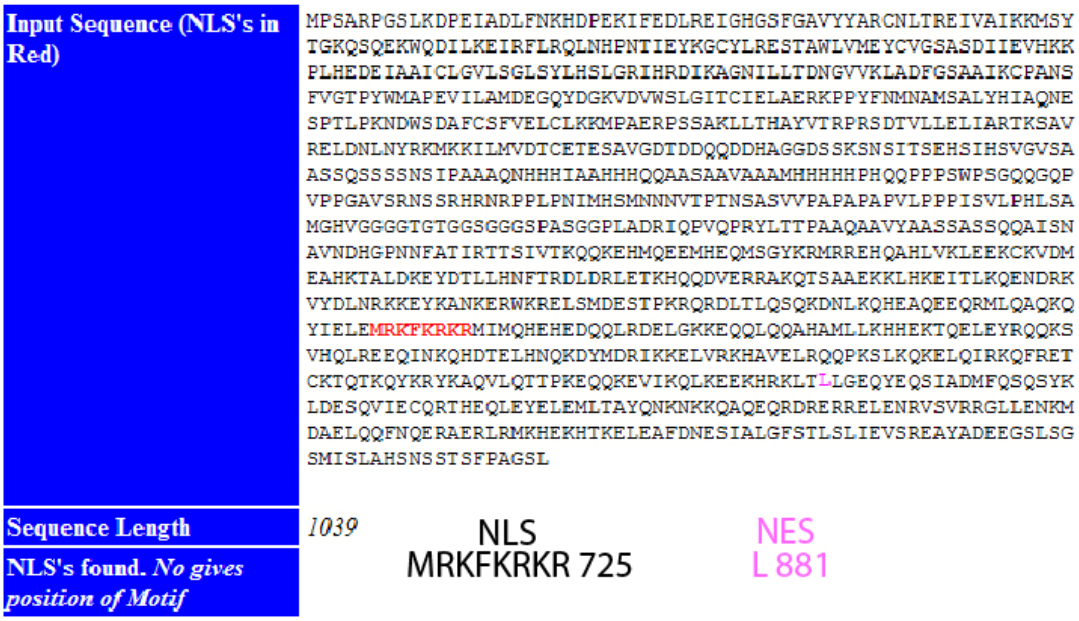

Figure 6-4 *Drosophila* Tao-1 contains a Nuclear Localization Signal *MRKFKRKR* at No.725 amino acid and Nuclear Export Signal at L881 based on the protein sequence prediction.

The other possibility, that Tao-1's localisation is determined by binding to Khc through its coiled coil domain, is supported by the observation that its

human homologues require the coiled-coil domain to bind to microtubules, by the observation that Tao-1 can be seen binding to microtubules in the cytoplasm, and by the fact that depolymerisation of microtubules causes the nuclear accumulation of Tao-1. If this is the case, it is not clear why the NES is not sufficient to maintain Tao-1 in the cytoplasm in the absence of microtubules. It may however be a simply matter of the relative rates of nuclear import and export.

Finally, I have shown Tao-1 is released from the cortex of fly cells in culture and in follicle cells within the *Drosophila* germline following the treatment with the actin monomer binding drug Latrunculin B. This was followed by a reduction in microtubule pausing and the continued growth of microtubules at the cell cortex, mirroring the Tao-1 RNAi phenotype. It is possible however that this phenotype is due to a protein(s) other than Tao-1 binding to the actin cortex to regulate microtubule dynamics because I don't have direct evidence to prove that Tao-1 binds to actin and plays this function at the cell cortex. This hypothesis is important to test. It would be interesting for example to force Tao-1 to bind to the cell membrane to test whether this is sufficient to induce the catastrophe of microtubules reaching the membrane even in the absence of cortical actin, in presence of Latrunculin B. If microtubule filaments still fail to stop at the cell cortex in this case, it is likely that Tao-1 is not sufficient to inhibit the interaction

between microtubules and the cell cortex. The ability of the cortex to induce microtubule catastrophe may require other microtubule regulators and/or actin-dependent forces at the cortex.

6.5 Prospective work and outlook

In order to test for the mechanism by which Tao-1 regulates microtubule dynamics, I plan to carry out a biochemical analysis to test whether Tao-1 alone is able to inhibit microtubule growth and/or induce microtubule catastrophe. To investigate the effects of Tao-1 on the frequency of microtubule growth, pausing and catastrophe, I will use the biochemically defined *in vitro* system that the Howard lab has set up and running to visualize microtubule growth following the addition of recombinant Tao-1 protein [2]. I will use TIRF to test the ability of these proteins to bind labeled microtubules and to measure the effects of Tao-1 on the kinetics of specific steps in the lifetime of a microtubule [1, 2]. By overcoming the effects of background fluorescence from free labeled tubulin, this technology will enable me to focus my attention of a narrow region very close to the coverslip where rhodamine-labeled microtubule seeds are anchored. Using this assay, I should be able to calculate the rate of microtubules plus end growth in the presence or absence of different GFP-Tao-1 variants.

As EB1 genetically interacts with Tao-1, I will also test whether Tao-1

requires EB1 to exert its effects on microtubule dynamics, using a recombinant EB1 generated in the Howard lab. I will then be able to compare these *in vitro* results to the *in vivo* data. If this proves to be the case, I will look for evidence that Tao-1 directly phosphorylates EB1.

Finally, I will generate a myr-tagged full length RFP-Tao-1, which contains a short membrane binding domain sequence. Overexpression of this myr-RFP-Tao-1 will allow me to observe what will happen when Tao-1 is forced to bind to the membrane in the presence or absence of actin filaments. This experiment will tell me whether Tao-1 is sufficient to destabilize microtubules at the cell cortex or whether it requires other factors.

Having worked in the Baum lab using RNAi, *Drosophila* genetics, and cell biology to build up a strong genetic and cell biological argument for a role for the Tao-1 kinase in the regulation of microtubule dynamics in interphase and mitosis, it is important for me to use biochemical assays to test these hypotheses directly. I anticipate that the understanding gained through these studies will be an important step towards a better understanding of microtubule regulation since, when tested using RNAi, Tao-1 has the strongest microtubule phenotype of all kinases in the genome. Since little is known about the regulators that can switch the state of an individual microtubule during the course of its lifetime or the regulators that alter global microtubule dynamics during specific phases of

the cell cycle, this work on the conserved Tao-1 kinase may have important implications for many fields in which cytoskeletal dynamics play a role, e.g. axonal pathfinding, cell polarisation and spindle morphogenesis. Furthermore, Tao-1 was found to associate with two kinesin heavy chains-Khc and Khc-73 in a 2 hybrid screen, suggesting the possibility that Tao-1 kinase may function through interactions with kinesins. Alternatively, kinesins may help to transport Tao-1 along microtubules, which may explain the dramatic effect of Khc on microtubule dynamics [23]. Finally, although direct evidence for phosphorylation of EB1 by Tao-1 hasn't been clearly addressed, this is first time a kinase has been found to function at the cell cortex to regulate microtubule plus end stability, and it also suggests a novel mechanism for cell to regulate the cross-talk between microtubule filaments and the actin cortex.

References

1. Burbank KS, Mitchison TJ: **Microtubule dynamic instability**. *Curr Biol* 2006, **16**(14):R516-517.

2. Mattila PK, Lappalainen P: **Filopodia: molecular architecture and cellular functions**. *Nature reviews* 2008, **9**(6):446-454.

3. Cheeseman IM, Desai A: **Molecular architecture of the kinetochore-microtubule interface**. *Nature reviews* 2008, **9**(1):33-46.

4. Hannon GJ: **RNA interference**. *Nature* 2002, **418**(6894):244-251.

5. Dan I, Watanabe NM, Kusumi A: **The Ste20 group kinases as regulators of MAP kinase cascades**. *Trends in cell biology* 2001, **11**(5):220-230.

6. Small JV, Rottner K, Kaverina I, Anderson KI: **Assembling an actin cytoskeleton for cell attachment and movement**. *Biochimica et biophysica acta* 1998, **1404**(3):271-281.

7. Small JV, Stradal T, Vignal E, Rottner K: **The lamellipodium: where motility begins**. *Trends in cell biology* 2002, **12**(3):112-120.

8. Wang YL: **Exchange of actin subunits at the leading edge of living fibroblasts: possible role of treadmilling**. *The Journal of cell biology* 1985, **101**(2):597-602.

9. Crowther RG, Spinks WL, Leicht AS, Quigley F, Golledge J: **Relationship between temporal-spatial gait parameters, gait kinematics, walking performance, exercise capacity, and physical activity level in peripheral arterial disease**. *J Vasc Surg* 2007, **45**(6):1172-1178.

10. Miki H, Suetsugu S, Takenawa T: **WAVE, a novel WASP-family protein involved in actin reorganization induced by Rac**. *The EMBO journal* 1998, **17**(23):6932-6941.

11. Lewis AK, Bridgman PC: **Nerve growth cone lamellipodia contain two populations of actin filaments that differ in organization and polarity**. *The Journal of cell biology* 1992, **119**(5):1219-1243.

12. Okabe S, Hirokawa N: **Actin dynamics in growth cones**. *J Neurosci* 1991, **11**(7):1918-1929.

13. Svitkina TM, Bulanova EA, Chaga OY, Vignjevic DM, Kojima S, Vasiliev JM, Borisy GG: **Mechanism of filopodia initiation by reorganization of a dendritic network**. *The Journal of cell biology* 2003, **160**(3):409-421.

14. Steffen A, Faix J, Resch GP, Linkner J, Wehland J, Small JV, Rottner K, Stradal TE: **Filopodia formation in the absence of functional WAVE- and Arp2/3-complexes**. *Molecular biology of the cell* 2006, **17**(6):2581-2591.

15. Nobes CD, Hall A: **Rho, rac, and cdc42 GTPases regulate the assembly of multimolecular focal complexes associated with actin stress fibers, lamellipodia, and filopodia**. *Cell* 1995, **81**(1):53-62.

16. Le Clainche C, Carlier MF: **Regulation of actin assembly associated with protrusion and adhesion in cell migration**. *Physiological reviews* 2008, **88**(2):489-513.

17. Wallar BJ, Alberts AS: **The formins: active scaffolds that remodel the cytoskeleton**. *Trends in cell biology* 2003, **13**(8):435-

446.

18. Manton SM: **Developments and science in the Soviet Union**. *Nature* 1952, **169**(4305):729-732.

19. Bruce Alberts AJ, Julian Lewis, Martin Raff, Keith Roberts and Peter Walter: **Molecular Biology of The Cell**. In.: Garland Science; 2002: 915.

20. Moritz M, Zheng Y, Alberts BM, Oegema K: **Recruitment of the gamma-tubulin ring complex to Drosophila salt-stripped centrosome scaffolds**. *The Journal of cell biology* 1998, **142**(3):775-786.

21. Zheng Y, Jung MK, Oakley BR: **Gamma-tubulin is present in Drosophila melanogaster and Homo sapiens and is associated with the centrosome**. *Cell* 1991, **65**(5):817-823.

22. Basto R, Lau J, Vinogradova T, Gardiol A, Woods CG, Khodjakov A, Raff JW: **Flies without centrioles**. *Cell* 2006, **125**(7):1375-1386.

23. Rogers GC, Rusan NM, Peifer M, Rogers SL: **A multicomponent assembly pathway contributes to the formation of acentrosomal microtubule arrays in interphase Drosophila cells**. *Molecular biology of the cell* 2008, **19**(7):3163-3178.

24. Mitchison T, Kirschner M: **Dynamic instability of microtubule growth**. *Nature* 1984, **312**(5991):237-242.

25. Valiron O, Caudron N, Job D: **Microtubule dynamics**. *Cell Mol Life Sci* 2001, **58**(14):2069-2084.

26. Horio T, Hotani H: **Visualization of the dynamic instability of individual microtubules by dark-field microscopy**. *Nature* 1986, **321**(6070):605-607.

27. Mogensen MM, Malik A, Piel M, Bouckson-Castaing V, Bornens M: **Microtubule minus-end anchorage at centrosomal and non-centrosomal sites: the role of ninein**. *Journal of cell science* 2000, **113 (Pt 17)**:3013-3023.

28. Kar S, Fan J, Smith MJ, Goedert M, Amos LA: **Repeat motifs of tau bind to the insides of microtubules in the absence of taxol**. *The EMBO journal* 2003, **22**(1):70-77.

29. Halpain S, Dehmelt L: **The MAP1 family of microtubule-**

associated proteins. *Genome Biol* 2006, **7**(6):224.

30. Megiorni F, Indovina P, Mora B, Mazzilli MC: **Minor expression of fascin-1 gene (FSCN1) in NTera2 cells depleted of CREB-binding protein**. *Neurosci Lett* 2005, **381**(1-2):169-174.

31. Tucker RP: **The roles of microtubule-associated proteins in brain morphogenesis: a review**. *Brain Res Brain Res Rev* 1990, **15**(2):101-120.

32. Mangan ME, Olmsted JB: **The gene for microtubule-associated protein 4 (Mtap4) maps to the distal region of mouse chromosome 9**. *Mamm Genome* 1996, **7**(12):918-919.

33. Mikiciuk-Olasik E, Szymanski P, Zurek E: **Diagnostics and therapy of Alzheimer's disease**. *Indian J Exp Biol* 2007, **45**(4):315-325.

34. Mistry SJ, Atweh GF: **Stathmin inhibition enhances okadaic acid-induced mitotic arrest: a potential role for stathmin in mitotic exit**. *The Journal of biological chemistry* 2001, **276**(33):31209-31215.

35. Wallon G, Rappsilber J, Mann M, Serrano L: **Model for stathmin/OP18 binding to tubulin**. *Embo J* 2000, **19**(2):213-222.

36. Price DK, Ball JR, Bahrani-Mostafavi Z, Vachris JC, Kaufman JS, Naumann RW, Higgins RV, Hall JB: **The phosphoprotein Op18/stathmin is differentially expressed in ovarian cancer**. *Cancer Invest* 2000, **18**(8):722-730.

37. Steinmetz MO, Kammerer RA, Jahnke W, Goldie KN, Lustig A, van Oostrum J: **Op18/stathmin caps a kinked protofilament-like tubulin tetramer**. *Embo J* 2000, **19**(4):572-580.

38. Larsson N, Marklund U, Gradin HM, Brattsand G, Gullberg M: **Control of microtubule dynamics by oncoprotein 18: dissection of the regulatory role of multisite phosphorylation during mitosis**. *Mol Cell Biol* 1997, **17**(9):5530-5539.

39. Vale RD: **Severing of stable microtubules by a mitotically activated protein in Xenopus egg extracts**. *Cell* 1991, **64**(4):827-839.

40. McNally FJ, Vale RD: **Identification of katanin, an ATPase that severs and disassembles stable microtubules**. *Cell* 1993,

75(3):419-429.

41. Roll-Mecak A, Vale RD: **Structural basis of microtubule severing by the hereditary spastic paraplegia protein spastin**. *Nature* 2008, **451**(7176):363-367.

42. Gard DL, Kirschner MW: **A microtubule-associated protein from Xenopus eggs that specifically promotes assembly at the plus-end**. *The Journal of cell biology* 1987, **105**(5):2203-2215.

43. Tournebize R, Popov A, Kinoshita K, Ashford AJ, Rybina S, Pozniakovsky A, Mayer TU, Walczak CE, Karsenti E, Hyman AA: **Control of microtubule dynamics by the antagonistic activities of XMAP215 and XKCM1 in Xenopus egg extracts**. *Nature cell biology* 2000, **2**(1):13-19.

44. van Breugel M, Drechsel D, Hyman A: **Stu2p, the budding yeast member of the conserved Dis1/XMAP215 family of microtubule-associated proteins is a plus end-binding microtubule destabilizer**. *The Journal of cell biology* 2003, **161**(2):359-369.

45. Popov AV, Karsenti E: **Stu2p and XMAP215: turncoat microtubule-associated proteins?** *Trends in cell biology* 2003, **13**(11):547-550.

46. Brittle AL, Ohkura H: **Mini spindles, the XMAP215 homologue, suppresses pausing of interphase microtubules in Drosophila**. *The EMBO journal* 2005, **24**(7):1387-1396.

47. Sharp DJ, Mennella V, Buster DW: **KLP10A and KLP59C: the dynamic duo of microtubule depolymerization**. *Cell Cycle* 2005, **4**(11):1482-1485.

48. Sharp DJ, Rogers GC: **A Kin I-dependent Pacman-flux mechanism for anaphase A**. *Cell Cycle* 2004, **3**(6):707-710.

49. Carvalho P, Tirnauer JS, Pellman D: **Surfing on microtubule ends**. *Trends in cell biology* 2003, **13**(5):229-237.

50. Mennella V, Rogers GC, Rogers SL, Buster DW, Vale RD, Sharp DJ: **Functionally distinct kinesin-13 family members cooperate to regulate microtubule dynamics during interphase**. *Nature cell biology* 2005, **7**(3):235-245.

51. Goshima G, Vale RD: **Cell cycle-dependent dynamics and**

regulation of mitotic kinesins in Drosophila S2 cells. *Mol Biol Cell* 2005, **16**(8):3896-3907.

52. Varga V, Helenius J, Tanaka K, Hyman AA, Tanaka TU, Howard J: **Yeast kinesin-8 depolymerizes microtubules in a length-dependent manner**. *Nature cell biology* 2006, **8**(9):957-962.

53. Su LK, Burrell M, Hill DE, Gyuris J, Brent R, Wiltshire R, Trent J, Vogelstein B, Kinzler KW: **APC binds to the novel protein EB1**. *Cancer Res* 1995, **55**(14):2972-2977.

54. Morrison EE, Wardleworth BN, Askham JM, Markham AF, Meredith DM: **EB1, a protein which interacts with the APC tumour suppressor, is associated with the microtubule cytoskeleton throughout the cell cycle**. *Oncogene* 1998, **17**(26):3471-3477.

55. Askham JM, Moncur P, Markham AF, Morrison EE: **Regulation and function of the interaction between the APC tumour suppressor protein and EB1**. *Oncogene* 2000, **19**(15):1950-1958.

56. Tirnauer JS, Bierer BE: **EB1 proteins regulate microtubule dynamics, cell polarity, and chromosome stability**. *The Journal of cell biology* 2000, **149**(4):761-766.

57. Rogers SL, Rogers GC, Sharp DJ, Vale RD: **Drosophila EB1 is important for proper assembly, dynamics, and positioning of the mitotic spindle**. *The Journal of cell biology* 2002, **158**(5):873-884.

58. Kirschner M, Mitchison T: **Beyond self-assembly: from microtubules to morphogenesis**. *Cell* 1986, **45**(3):329-342.

59. Goshima G, Nedelec F, Vale RD: **Mechanisms for focusing mitotic spindle poles by minus end-directed motor proteins**. *The Journal of cell biology* 2005, **171**(2):229-240.

60. Pierre P, Scheel J, Rickard JE, Kreis TE: **CLIP-170 links endocytic vesicles to microtubules**. *Cell* 1992, **70**(6):887-900.

61. Galjart N: **CLIPs and CLASPs and cellular dynamics**. *Nature reviews* 2005, **6**(6):487-498.

62. Akhmanova A, Hoogenraad CC, Drabek K, Stepanova T, Dortland B, Verkerk T, Vermeulen W, Burgering BM, De Zeeuw CI, Grosveld F *et al*: **Clasps are CLIP-115 and -170 associating proteins involved in the regional regulation of microtubule dynamics in**

motile fibroblasts. *Cell* 2001, **104**(6):923-935.

63. Mimori-Kiyosue Y, Grigoriev I, Lansbergen G, Sasaki H, Matsui C, Severin F, Galjart N, Grosveld F, Vorobjev I, Tsukita S *et al*: **CLASP1 and CLASP2 bind to EB1 and regulate microtubule plus-end dynamics at the cell cortex**. *The Journal of cell biology* 2005, **168**(1):141-153.

64. Bohm M, Schroder HC, Muller IM, Muller WE, Gamulin V: **The mitogen-activated protein kinase p38 pathway is conserved in metazoans: cloning and activation of p38 of the SAPK2 subfamily from the sponge Suberites domuncula**. *Biology of the cell / under the auspices of the European Cell Biology Organization* 2000, **92**(2):95-104.

65. Yao Z, Zhou G, Wang XS, Brown A, Diener K, Gan H, Tan TH: **A novel human STE20-related protein kinase, HGK, that specifically activates the c-Jun N-terminal kinase signaling pathway**. *The Journal of biological chemistry* 1999, **274**(4):2118-2125.

66. Lee KK, Murakawa M, Nishida E, Tsubuki S, Kawashima S, Sakamaki K, Yonehara S: **Proteolytic activation of MST/Krs, STE20-related protein kinase, by caspase during apoptosis**. *Oncogene* 1998, **16**(23):3029-3037.

67. Chen YR, Meyer CF, Ahmed B, Yao Z, Tan TH: **Caspase-mediated cleavage and functional changes of hematopoietic progenitor kinase 1 (HPK1)**. *Oncogene* 1999, **18**(51):7370-7377.

68. Frost JA, Swantek JL, Stippec S, Yin MJ, Gaynor R, Cobb MH: **Stimulation of NFkappa B activity by multiple signaling pathways requires PAK1**. *The Journal of biological chemistry* 2000, **275**(26):19693-19699.

69. Bagrodia S, Cerione RA: **Pak to the future**. *Trends in cell biology* 1999, **9**(9):350-355.

70. Su YC, Treisman JE, Skolnik EY: **The Drosophila Ste20-related kinase misshapen is required for embryonic dorsal closure and acts through a JNK MAPK module on an evolutionarily conserved signaling pathway**. *Genes & development* 1998, **12**(15):2371-2380.

71. Su YC, Maurel-Zaffran C, Treisman JE, Skolnik EY: **The Ste20 kinase misshapen regulates both photoreceptor axon**

targeting and dorsal closure, acting downstream of distinct signals. *Mol Cell Biol* 2000, **20**(13):4736-4744.

72. Baumgartner M, Sillman AL, Blackwood EM, Srivastava J, Madson N, Schilling JW, Wright JH, Barber DL: **The Nck-interacting kinase phosphorylates ERM proteins for formation of lamellipodium by growth factors**. *Proceedings of the National Academy of Sciences of the United States of America* 2006, **103**(36):13391-13396.

73. Napoli C, Lemieux C, Jorgensen R: **Introduction of a Chimeric Chalcone Synthase Gene into Petunia Results in Reversible Co-Suppression of Homologous Genes in trans**. *The Plant cell* 1990, **2**(4):279-289.

74. Craig AW, Haghighat A, Yu AT, Sonenberg N: **Interaction of polyadenylate-binding protein with the eIF4G homologue PAIP enhances translation**. *Nature* 1998, **392**(6675):520-523.

75. Gitlin L, Andino R: **Nucleic acid-based immune system: the antiviral potential of mammalian RNA silencing**. *J Virol* 2003, **77**(13):7159-7165.

76. Winckler T, Dingermann T, Glockner G: **Dictyostelium mobile elements: strategies to amplify in a compact genome**. *Cell Mol Life Sci* 2002, **59**(12):2097-2111.

77. Tuschl T, Zamore PD, Lehmann R, Bartel DP, Sharp PA: **Targeted mRNA degradation by double-stranded RNA in vitro**. *Genes & development* 1999, **13**(24):3191-3197.

78. Schwarz DS, Hutvagner G, Haley B, Zamore PD: **Evidence that siRNAs function as guides, not primers, in the Drosophila and human RNAi pathways**. *Molecular cell* 2002, **10**(3):537-548.

79. Hohjoh H: **RNA interference (RNA(i)) induction with various types of synthetic oligonucleotide duplexes in cultured human cells**. *FEBS letters* 2002, **521**(1-3):195-199.

80. Hohjoh H, Takasu M, Shishikura K, Takahashi Y, Honda Y, Tokunaga K: **Significant association of the arylalkylamine N-acetyltransferase (AA-NAT) gene with delayed sleep phase syndrome**. *Neurogenetics* 2003, **4**(3):151-153.

81. Fire AZ: **Gene silencing by double-stranded RNA**. *Cell death and differentiation* 2007, **14**(12):1998-2012.

82. Pal-Bhadra M, Leibovitch BA, Gandhi SG, Rao M, Bhadra U, Birchler JA, Elgin SC: **Heterochromatic silencing and HP1 localization in Drosophila are dependent on the RNAi machinery**. *Science (New York, NY* 2004, **303**(5658):669-672.

83. Wightman B, Ha I, Ruvkun G: **Posttranscriptional regulation of the heterochronic gene lin-14 by lin-4 mediates temporal pattern formation in C. elegans**. *Cell* 1993, **75**(5):855-862.

84. Biyasheva A, Svitkina T, Kunda P, Baum B, Borisy G: **Cascade pathway of filopodia formation downstream of SCAR**. *Journal of cell science* 2004, **117**(Pt 6):837-848.

85. Worby CA, Simonson-Leff N, Dixon JE: **RNA interference of gene expression (RNAi) in cultured Drosophila cells**. *Sci STKE* 2001, **2001**(95):PL1.

86. Mocellin S, Provenzano M: **RNA interference: learning gene knock-down from cell physiology**. *Journal of translational medicine* 2004, **2**(1):39.

87. Echeverri CJ, Perrimon N: **High-throughput RNAi screening in cultured cells: a user's guide**. *Nat Rev Genet* 2006, **7**(5):373-384.

88. Echeverri CJ, Beachy PA, Baum B, Boutros M, Buchholz F, Chanda SK, Downward J, Ellenberg J, Fraser AG, Hacohen N *et al*: **Minimizing the risk of reporting false positives in large-scale RNAi screens**. *Nature methods* 2006, **3**(10):777-779.

89. Kiger AA, Baum B, Jones S, Jones MR, Coulson A, Echeverri C, Perrimon N: **A functional genomic analysis of cell morphology using RNA interference**. *Journal of biology* 2003, **2**(4):27.

90. Neumann B, Held M, Liebel U, Erfle H, Rogers P, Pepperkok R, Ellenberg J: **High-throughput RNAi screening by time-lapse imaging of live human cells**. *Nature methods* 2006, **3**(5):385-390.

91. Adams MD, Celniker SE, Holt RA, Evans CA, Gocayne JD, Amanatides PG, Scherer SE, Li PW, Hoskins RA, Galle RF *et al*: **The genome sequence of Drosophila melanogaster**. *Science* 2000, **287**(5461):2185-2195.

92. Morrison DK, Murakami MS, Cleghon V: **Protein kinases and phosphatases in the Drosophila genome**. *The Journal of cell biology* 2000, **150**(2):F57-62.

93. Sims D, Bursteinas B, Gao Q, Zvelebil M, Baum B: **FLIGHT: database and tools for the integration and cross-correlation of large-scale RNAi phenotypic datasets**. *Nucleic Acids Res* 2006, **34**(Database issue):D479-483.

94. Arziman Z, Horn T, Boutros M: **E-RNAi: a web application to design optimized RNAi constructs**. *Nucleic Acids Res* 2005, **33**(Web Server issue):W582-588.

95. Reimers M, Carey VJ: **Bioconductor: an open source framework for bioinformatics and computational biology**. *Methods Enzymol* 2006, **411**:119-134.

96. Moore TM, Garg R, Johnson C, Coptcoat MJ, Ridley AJ, Morris JD: **PSK, a novel STE20-like kinase derived from prostatic carcinoma that activates the c-Jun N-terminal kinase mitogen-activated protein kinase pathway and regulates actin cytoskeletal organization**. *The Journal of biological chemistry* 2000, **275**(6):4311-4322.

97. Landy A: **Dynamic, structural, and regulatory aspects of lambda site-specific recombination**. *Annual review of biochemistry* 1989, **58**:913-949.

98. Yu Y, Ge N, Xie M, Sun W, Burlingame S, Pass AK, Nuchtern JG, Zhang D, Fu S, Schneider MD *et al*: **Phosphorylation of Thr-178 and Thr-184 in the TAK1 T-loop is required for interleukin (IL)-1-mediated optimal NFkappaB and AP-1 activation as well as IL-6 gene expression**. *J Biol Chem* 2008, **283**(36):24497-24505.

99. Kunda P, Pelling AE, Liu T, Baum B: **Moesin controls cortical rigidity, cell rounding, and spindle morphogenesis during mitosis**. *Curr Biol* 2008, **18**(2):91-101.

100. Echalier G, Ohanessian A: **[Isolation, in tissue culture, of Drosophila melangaster cell lines]**. *C R Acad Sci Hebd Seances Acad Sci D* 1969, **268**(13):1771-1773.

101. Schneider I: **Cell lines derived from late embryonic stages of Drosophila melanogaster**. *J Embryol Exp Morphol* 1972, **27**(2):353-365.

102. Yanagawa S, Lee JS, Ishimoto A: **Identification and characterization of a novel line of Drosophila Schneider S2 cells that respond to wingless signaling**. *The Journal of biological chemistry* 1998, **273**(48):32353-32359.

103. Ui K, Nishihara S, Sakuma M, Togashi S, Ueda R, Miyata Y, Miyake T: **Newly established cell lines from Drosophila larval CNS express neural specific characteristics**. *In vitro cellular & developmental biology* 1994, **30A**(4):209-216.

104. Peel DJ, Johnson SA, Milner MJ: **The ultrastructure of imaginal disc cells in primary cultures and during cell aggregation in continuous cell lines**. *Tissue Cell* 1990, **22**(5):749-758.

105. Cherbus Ba: **Imaginal discs**. In: *Drosophila: Methods and Protocols (Methods in Molecular Biology).* Edited by Dahmann C, 1 edn: Humana Press; 2008: 456.

106. Drees F, Gertler FB: **Ena/VASP: proteins at the tip of the nervous system**. *Current opinion in neurobiology* 2008.

107. Pires-daSilva A, Sommer RJ: **The evolution of signalling pathways in animal development**. *Nature reviews* 2003, **4**(1):39-49.

108. Menzel N, Schneeberger D, Raabe T: **The Drosophila p21 activated kinase Mbt regulates the actin cytoskeleton and adherens junctions to control photoreceptor cell morphogenesis**. *Mech Dev* 2007, **124**(1):78-90.

109. Winter CG, Wang B, Ballew A, Royou A, Karess R, Axelrod JD, Luo L: **Drosophila Rho-associated kinase (Drok) links Frizzled-mediated planar cell polarity signaling to the actin cytoskeleton**. *Cell* 2001, **105**(1):81-91.

110. Zervas CG, Gregory SL, Brown NH: **Drosophila integrin-linked kinase is required at sites of integrin adhesion to link the cytoskeleton to the plasma membrane**. *J Cell Biol* 2001, **152**(5):1007-1018.

111. Clemens JC, Worby CA, Simonson-Leff N, Muda M, Maehama T, Hemmings BA, Dixon JE: **Use of double-stranded RNA interference in Drosophila cell lines to dissect signal transduction pathways**. *Proceedings of the National Academy of Sciences of the United States of America* 2000, **97**(12):6499-6503.

112. Kulkarni MM, Booker M, Silver SJ, Friedman A, Hong P, Perrimon N, Mathey-Prevot B: **Evidence of off-target effects associated with long dsRNAs in Drosophila melanogaster cell-based assays**. *Nature methods* 2006, **3**(10):833-838.

113. Fabbro D, Ruetz S, Buchdunger E, Cowan-Jacob SW, Fendrich G, Liebetanz J, Mestan J, O'Reilly T, Traxler P, Chaudhuri B *et al*: **Protein kinases as targets for anticancer agents: from inhibitors to useful drugs**. *Pharmacology & therapeutics* 2002, **93**(2-3):79-98.

114. Rufini V, Mirk P, Summaria V, Fileni A, di Giuda D, Troncone L: **Diagnostic imaging of euthyroid goiter**. *Rays* 1999, **24**(2):243-262.

115. Bettencourt-Dias M, Giet R, Sinka R, Mazumdar A, Lock WG, Balloux F, Zafiropoulos PJ, Yamaguchi S, Winter S, Carthew RW *et al*: **Genome-wide survey of protein kinases required for cell cycle progression**. *Nature* 2004, **432**(7020):980-987.

116. Echard A, Hickson GR, Foley E, O'Farrell PH: **Terminal cytokinesis events uncovered after an RNAi screen**. *Curr Biol* 2004, **14**(18):1685-1693.

117. Eggert US, Kiger AA, Richter C, Perlman ZE, Perrimon N, Mitchison TJ, Field CM: **Parallel chemical genetic and genome-wide RNAi screens identify cytokinesis inhibitors and targets**. *PLoS biology* 2004, **2**(12):e379.

118. Huang Y, Chen-Hwang MC, Dolios G, Murakami N, Padovan JC, Wang R, Hwang YW: **Mnb/Dyrk1A phosphorylation regulates the interaction of dynamin 1 with SH3 domain-containing proteins**. *Biochemistry* 2004, **43**(31):10173-10185.

119. Tejedor F, Zhu XR, Kaltenbach E, Ackermann A, Baumann A, Canal I, Heisenberg M, Fischbach KF, Pongs O: **minibrain: a new protein kinase family involved in postembryonic neurogenesis in Drosophila**. *Neuron* 1995, **14**(2):287-301.

120. Guimera J, Casas C, Estivill X, Pritchard M: **Human minibrain homologue (MNBH/DYRK1): characterization, alternative splicing, differential tissue expression, and overexpression in Down syndrome**. *Genomics* 1999, **57**(3):407-418.

121. Marti E, Altafaj X, Dierssen M, de la Luna S, Fotaki V, Alvarez M, Perez-Riba M, Ferrer I, Estivill X: **Dyrk1A expression pattern supports specific roles of this kinase in the adult central nervous system**. *Brain Res* 2003, **964**(2):250-263.

122. Moriya H, Shimizu-Yoshida Y, Omori A, Iwashita S, Katoh M, Sakai A: **Yak1p, a DYRK family kinase, translocates to the nucleus**

and phosphorylates yeast Pop2p in response to a glucose signal. *Genes Dev* 2001, **15**(10):1217-1228.

123. Alvarez M, Altafaj X, Aranda S, de la Luna S: **DYRK1A autophosphorylation on serine residue 520 modulates its kinase activity via 14-3-3 binding**. *Molecular biology of the cell* 2007, **18**(4):1167-1178.

124. Kim D, Won J, Shin DW, Kang J, Kim YJ, Choi SY, Hwang MK, Jeong BW, Kim GS, Joe CO *et al*: **Regulation of Dyrk1A kinase activity by 14-3-3**. *Biochem Biophys Res Commun* 2004, **323**(2):499-504.

125. Sacher F, Moller C, Bone W, Gottwald U, Fritsch M: **The expression of the testis-specific Dyrk4 kinase is highly restricted to step 8 spermatids but is not required for male fertility in mice**. *Mol Cell Endocrinol* 2007, **267**(1-2):80-88.

126. Laguna A, Aranda S, Barallobre MJ, Barhoum R, Fernandez E, Fotaki V, Delabar JM, de la Luna S, de la Villa P, Arbones ML: **The protein kinase DYRK1A regulates caspase-9-mediated apoptosis during retina development**. *Developmental cell* 2008, **15**(6):841-853.

127. Bakal C, Aach J, Church G, Perrimon N: **Quantitative morphological signatures define local signaling networks regulating cell morphology**. *Science (New York, NY* 2007, **316**(5832):1753-1756.

128. Carlier MF, Wiesner S, Le Clainche C, Pantaloni D: **Actin-based motility as a self-organized system: mechanism and reconstitution in vitro**. *Comptes rendus biologies* 2003, **326**(2):161-170.

129. Kunda P, Craig G, Dominguez V, Baum B: **Abi, Sra1, and Kette control the stability and localization of SCAR/WAVE to regulate the formation of actin-based protrusions**. *Curr Biol* 2003, **13**(21):1867-1875.

130. Chodniewicz D, Klemke RL: **Guiding cell migration through directed extension and stabilization of pseudopodia**. *Experimental cell research* 2004, **301**(1):31-37.

131. Euteneuer U, Schliwa M: **Persistent, directional motility of cells and cytoplasmic fragments in the absence of microtubules**. *Nature* 1984, **310**(5972):58-61.

132. Nemethova M, Auinger S, Small JV: **Building the actin cytoskeleton: filopodia contribute to the construction of contractile bundles in the lamella**. *The Journal of cell biology* 2008, **180**(6):1233-1244.

133. Koestler SA, Auinger S, Vinzenz M, Rottner K, Small JV: **Differentially oriented populations of actin filaments generated in lamellipodia collaborate in pushing and pausing at the cell front**. *Nature cell biology* 2008, **10**(3):306-313.

134. Miki H, Sasaki T, Takai Y, Takenawa T: **Induction of filopodium formation by a WASP-related actin-depolymerizing protein N-WASP**. *Nature* 1998, **391**(6662):93-96.

135. Hutchison M, Berman KS, Cobb MH: **Isolation of TAO1, a protein kinase that activates MEKs in stress-activated protein kinase cascades**. *The Journal of biological chemistry* 1998, **273**(44):28625-28632.

136. Chen Z, Hutchison M, Cobb MH: **Isolation of the protein kinase TAO2 and identification of its mitogen-activated protein kinase/extracellular signal-regulated kinase kinase binding domain**. *The Journal of biological chemistry* 1999, **274**(40):28803-28807.

137. Mitsopoulos C, Zihni C, Garg R, Ridley AJ, Morris JD: **The prostate-derived sterile 20-like kinase (PSK) regulates microtubule organization and stability**. *The Journal of biological chemistry* 2003, **278**(20):18085-18091.

138. Zihni C, Mitsopoulos C, Tavares IA, Ridley AJ, Morris JD: **Prostate-derived sterile 20-like kinase 2 (PSK2) regulates apoptotic morphology via C-Jun N-terminal kinase and Rho kinase-1**. *The Journal of biological chemistry* 2006, **281**(11):7317-7323.

139. Draviam VM, Stegmeier F, Nalepa G, Sowa ME, Chen J, Liang A, Hannon GJ, Sorger PK, Harper JW, Elledge SJ: **A functional genomic screen identifies a role for TAO1 kinase in spindle-checkpoint signalling**. *Nature cell biology* 2007, **9**(5):556-564.

140. Raman M, Earnest S, Zhang K, Zhao Y, Cobb MH: **TAO kinases mediate activation of p38 in response to DNA damage**. *The EMBO journal* 2007, **26**(8):2005-2014.

141. Zihni C, Mitsopoulos C, Tavares IA, Baum B, Ridley AJ, Morris JD: **Prostate-derived sterile 20-like kinase 1-alpha induces**

apoptosis. JNK- and caspase-dependent nuclear localization is a requirement for membrane blebbing. *The Journal of biological chemistry* 2007, **282**(9):6484-6493.

142. Berman KS, Hutchison M, Avery L, Cobb MH: **kin-18, a C. elegans protein kinase involved in feeding**. *Gene* 2001, **279**(2):137-147.

143. Nakamura N, Lowe M, Levine TP, Rabouille C, Warren G: **The vesicle docking protein p115 binds GM130, a cis-Golgi matrix protein, in a mitotically regulated manner**. *Cell* 1997, **89**(3):445-455.

144. Timm T, Li XY, Biernat J, Jiao J, Mandelkow E, Vandekerckhove J, Mandelkow EM: **MARKK, a Ste20-like kinase, activates the polarity-inducing kinase MARK/PAR-1**. *The EMBO journal* 2003, **22**(19):5090-5101.

145. Timm T, Matenia D, Li XY, Griesshaber B, Mandelkow EM: **Signaling from MARK to tau: regulation, cytoskeletal crosstalk, and pathological phosphorylation**. *Neurodegener Dis* 2006, **3**(4-5):207-217.

146. Johne C, Matenia D, Li XY, Timm T, Balusamy K, Mandelkow EM: **Spred1 and TESK1--two new interaction partners of the kinase MARKK/TAO1 that link the microtubule and actin cytoskeleton**. *Molecular biology of the cell* 2008, **19**(4):1391-1403.

147. Yonemura S, Tsukita S, Tsukita S: **Direct involvement of ezrin/radixin/moesin (ERM)-binding membrane proteins in the organization of microvilli in collaboration with activated ERM proteins**. *The Journal of cell biology* 1999, **145**(7):1497-1509.

148. Pearson MA, Reczek D, Bretscher A, Karplus PA: **Structure of the ERM protein moesin reveals the FERM domain fold masked by an extended actin binding tail domain**. *Cell* 2000, **101**(3):259-270.

149. Bohm H, Brinkmann V, Drab M, Henske A, Kurzchalia TV: **Mammalian homologues of C. elegans PAR-1 are asymmetrically localized in epithelial cells and may influence their polarity**. *Curr Biol* 1997, **7**(8):603-606.

150. Tomancak P, Piano F, Riechmann V, Gunsalus KC, Kemphues KJ, Ephrussi A: **A Drosophila melanogaster homologue of Caenorhabditis elegans par-1 acts at an early step in embryonic-axis formation**. *Nature cell biology* 2000, **2**(7):458-460.

151. Shulman JM, Benton R, St Johnston D: **The Drosophila homolog of C. elegans PAR-1 organizes the oocyte cytoskeleton and directs oskar mRNA localization to the posterior pole**. *Cell* 2000, **101**(4):377-388.

152. Doerflinger H, Benton R, Shulman JM, St Johnston D: **The role of PAR-1 in regulating the polarised microtubule cytoskeleton in the Drosophila follicular epithelium**. *Development* 2003, **130**(17):3965-3975.

153. Shelden E, Wadsworth P: **Observation and quantification of individual microtubule behavior in vivo: microtubule dynamics are cell-type specific**. *The Journal of cell biology* 1993, **120**(4):935-945.

154. Tirnauer JS, O'Toole E, Berrueta L, Bierer BE, Pellman D: **Yeast Bim1p promotes the G1-specific dynamics of microtubules**. *The Journal of cell biology* 1999, **145**(5):993-1007.

155. Rusan NM, Fagerstrom CJ, Yvon AM, Wadsworth P: **Cell cycle-dependent changes in microtubule dynamics in living cells expressing green fluorescent protein-alpha tubulin**. *Molecular biology of the cell* 2001, **12**(4):971-980.

156. Sproul LR, Anderson DJ, Mackey AT, Saunders WS, Gilbert SP: **Cik1 targets the minus-end kinesin depolymerase kar3 to microtubule plus ends**. *Curr Biol* 2005, **15**(15):1420-1427.

157. Wu X, Xiang X, Hammer JA, 3rd: **Motor proteins at the microtubule plus-end**. *Trends in cell biology* 2006, **16**(3):135-143.

158. Schwartz K, Richards K, Botstein D: **BIM1 encodes a microtubule-binding protein in yeast**. *Molecular biology of the cell* 1997, **8**(12):2677-2691.

159. Brunner D, Nurse P: **CLIP170-like tip1p spatially organizes microtubular dynamics in fission yeast**. *Cell* 2000, **102**(5):695-704.

160. Brunner D, Nurse P: **New concepts in fission yeast morphogenesis**. *Philosophical transactions of the Royal Society of London* 2000, **355**(1399):873-877.

161. Wei RR, Al-Bassam J, Harrison SC: **The Ndc80/HEC1 complex is a contact point for kinetochore-microtubule attachment**. *Nature structural & molecular biology* 2007, **14**(1):54-59.

162. Kanai Y, Okada Y, Tanaka Y, Harada A, Terada S, Hirokawa N: **KIF5C, a novel neuronal kinesin enriched in motor neurons**. *J Neurosci* 2000, **20**(17):6374-6384.

163. Inoue H, Tateno M, Fujimura-Kamada K, Takaesu G, Adachi-Yamada T, Ninomiya-Tsuji J, Irie K, Nishida Y, Matsumoto K: **A Drosophila MAPKKK, D-MEKK1, mediates stress responses through activation of p38 MAPK**. *The EMBO journal* 2001, **20**(19):5421-5430.

164. Jovceva E, Larsen MR, Waterfield MD, Baum B, Timms JF: **Dynamic cofilin phosphorylation in the control of lamellipodial actin homeostasis**. *Journal of cell science* 2007, **120**(Pt 11):1888-1897.

165. Miron M, Lasko P, Sonenberg N: **Signaling from Akt to FRAP/TOR targets both 4E-BP and S6K in Drosophila melanogaster**. *Mol Cell Biol* 2003, **23**(24):9117-9126.

166. Morrison EE: **Action and interactions at microtubule ends**. *Cell Mol Life Sci* 2007, **64**(3):307-317.

167. Siegrist SE, Doe CQ: **Microtubule-induced Pins/Galphai cortical polarity in Drosophila neuroblasts**. *Cell* 2005, **123**(7):1323-1335.